# Dissertation

**submitted to the**

**Combined Faculty of Natural Sciences and Mathematics**

**of the Ruperto Carola University Heidelberg, Germany**

**for the degree of**

**Doctor of Natural Sciences**

**presented by**

**Chih-Yeh Chen, M.Sc.**

**born in Taipei, Taiwan**

**Oral examination:**

**.....**

# Induction of autoreactive regulatory T cells through promiscuous gene expression by bone marrow-resident plasma cells

**Referees:**

**Prof. Dr. Philipp Beckhove**

**Prof. Dr. Viktor Umansky**

The work described in this thesis was performed from 2013 to 2015 in the Department of Translational Immunology at the National Center for Tumor Diseases – NCT of the German Cancer Research Center - DKFZ in Heidelberg, Germany and from 2016 to 2018 in the Department of Interventional Immunology at the Regensburg Center for Interventional Immunology – RCI in Regensburg under the supervision of Prof. Dr. Philipp Beckhove.

**Declaration**

I herewith declare that I have completed this thesis single-handedly without any unauthorized help of a second party. Any help that I have received in my research work or in the preparation of this thesis has been duly acknowledged.

Heidelberg, 02.07.2018

_____

Chih-Yeh Chen

“It matters if you just don’t give up.”

Stephen William Hawking

# Summary

Bone marrow (BM) serves as a site for T cell priming against blood-derived antigens but also harbors a diverse repertoire of regulatory T (Treg) cells. BM Treg cells are essential in hematopoiesis as they provide immune-privileged niches for hematopoietic stem cells, and are required for peripheral tolerance towards self-antigens. Treg cell accumulation in the BM has been hitherto viewed as a consequence of preferential immigration of thymus-derived Treg (tTreg) cells. However, it remains unknown whether Treg cells are also induced *in situ* in the BM, and to which degree these peripherally induced Treg (pTreg) cells contribute to the diversity of Treg cells in this lymphoid organ.

Previously in our lab, a novel cell subset which expresses autoimmune regulator (Aire) has been identified in both murine and human BM. The BM Aire-expressing cells (BMACs) are characterized by the expression of major histocompatibility complex class II (MHC-II) and epithelial cell adhesion molecule (EpCAM). Moreover, they ectopically express a highly diverse repertoire of peripheral tissue-restricted self-antigens. The aim of this study is to characterize the cellular origin of BMACs, and evaluate their immunological function to induce peripheral tolerance, especially their role in the conversion of naïve T cells into Treg cells.

In this study, I demonstrate that BMACs show features of $CD19^{low}CD138^{+}B220^{-}Blimp\text{-}1^{+}IgM^{+}$ plasma cells. They reside in proximity to $CD4^{+}$ T cell clusters, express CD80, CD86, and PD-L1 and are able to present Aire-regulated antigens to $CD4^{+}$ T cells. Furthermore, BMACs over-express genes associated with Treg induction, such as genes for retinoic acid production, the TIGIT ligand CD155 and IL-10. After encountering BMACs, which express the cognate antigen in BM, naïve $CD4^{+}$ T cells specific for Aire-regulated antigens are converted to $CD25^{+}Foxp3^{+}$ Treg cells *in vitro* and *in vivo*. Treg cells induced by BMACs express high levels of CTLA-4 and LAP, and can suppress cytotoxic T cell responses *in vivo*. In conclusion, we

have identified a plasma cell subset that expresses Aire and tissue-restricted self-antigens ectopically, and is capable to promote peripheral tolerance by inducing a repertoire of autoreactive Treg cells in the BM.

# Zusammenfassung

Das Knochenmark (KM) dient als Standort für das Priming von T-Zellen gegen Antigene, die über das Blut transportiert werden, beherbergt aber auch ein diverses Repertoire an regulatorischen T-Zellen (Treg). KM Treg Zellen sind essentiell für die Hämatopoese, da sie immunprivilegierte Nischen für hämatopoetische Stammzellen bieten, und daher für die periphere Toleranz gegenüber Selbst-Antigene notwendig sind. Die Anreicherung von Treg Zellen im KM wurde bisher als Konsequenz präferentieller Immigration von Thymus-stämmigen Treg (tTreg) Zellen angesehen. Es ist jedoch ungewiss, ob Treg Zellen auch in situ im KM indusziert werden, und diese peripher induzierten Treg (pTreg) Zellen zur Diversität des Treg Zellen Repertoires in diesem lymphoiden Organ beitragen.

In unserem Labor wurde eine neuartige Zellpopulation, welche den Autoimmun- Regulator (Aire) exprimiert, sowohl in murinem, als auch humanem KM identifiziert. Die Aire-exprimierenden Zellen im Knochenmark (BMACs) exprimieren den MHC-Klasse-II-Komplex (MHC-II) und das epitheliale Zelladhäsionsmolekül (EpCAM). Außerdem exprimieren sie ektopisch ein diverses Repertoire von peripheren, Gewebe-restringierten, Selbst-Antigenen. In der vorliegenden Arbeit habe ich BMACs phänotypisch, molekular und funktionell charakterisiert. Dies geschah insbesondere im Hinblick auf ihre Fähigkeit zur Induktion peripherer Immuntoleranz, vor allem durch eine Konvertierung naïver T Zellen in Treg Zellen.

In dieser Studie zeige ich, dass BMACs Eigenschaften von $CD19^{low}CD138^{+}B220^{-}Blimp\text{-}1^{+}IgM^{+}$ Plasmazellen aufzeigen. Sie sind in der Nähe des $CD4^{+}$ T-Zell Clusters angesiedelt, exprimieren CD80, CD86, und PD-L1 und sind in der Lage, Aire-regulierte Antigene $CD4^{+}$ T-Zellen zu präsentieren. Desweiteren überexprimieren BMACs Gene, die mit Treg Induktion assoziiert sind, wie z.B. Gene für die Retinsäureproduktion, den TIGIT Liganden CD155 und IL-10. Nach der Interaktion mit BMACs, die das verwandte Antigen im KM exprimieren,

werden naïve $CD4^+$ T Zellen, die spezifisch für Aire-regulierte Antigen sind, *in vitro* und *in vivo*, zu $CD25^+Foxp3^+$ Treg Zellen konvertiert. Treg Zellen, die durch BMACs induziert wurden, exprimieren hohe Level an CTLA-4 und LAP, und können zytotoxische T-Zell Antworten *in vivo* unterdrücken. Zusammenfassend demonstriert meine Arbeit somit, dass ein Plasmazell-Subset Aire und Gewebe-beschränkte Selbst-Antigene ektopisch exprimiert, und in der Lage ist, periphere Immuntoleranz, durch Induktion eines Repertoires autoreaktiver Treg Zellen, im KM, zu induzieren.

# Table of Contents

# 1. Introduction

## 1.1 T cell central tolerance

In healthy individuals, the immune system is exquisitely balanced between tolerance towards self-antigens and inflammatory responses against pathogens or neo-antigens. Tip of this balance either leads to immunopathology (such as autoimmune diseases) due to inadequate tolerance, or results in immunodeficiency due to insufficient immune responses. The maintenance of such balance largely depends on the fine regulation by $CD4^+$ T cells. They express T-cell receptors (TCRs) with highly diverse specificities, which enable accurate activation upon engagement to specific antigens. Activated $CD4^+$ T cells further promote the responses of effector cells such as cognate $CD8^+$ T cells and B cells[1, 2], and thus are pivotal to the control of adaptive immunity. The diversity of TCR specificity arises from stochastic V(D)J recombination of *Tcra* (TCR α chain) and *Tcrb* (β chain) genes[3], and TCRs with specificities against self-antigens can also occur. It is therefore crucial to remove T cells with autoreactivity in order to avoid autoimmune diseases. In thymus, the specificities of TCRs on immature thymocytes are examined in order to generate a repertoire of T cells that can distinguish "self" and "non-self". This process of self-testing is termed T cell central tolerance[4].

T cell progenitors enter the cortex of the thymus as $CD4^-CD8^-$ (double negative, DN) cells and undergo TCR rearrangement (**Figure I**), and become double positive (DP) cells after successful production of functional TCR β-chain (β-selection)[5]. After generating a complete TCR, the DP cells then interact with cortical thymic epithelial cells (cTECs) to test if their TCRs have sufficient affinity to thymo-proteosome (β5t)-processed peptide presented on major histocompatibility complex (MHC) class I or class II of cTECs[6]. Those thymocytes with

insufficient affinity to MHC are subject to programmed cell death by neglect. After positive selection, the surviving thymocytes become single positive (SP) cells.

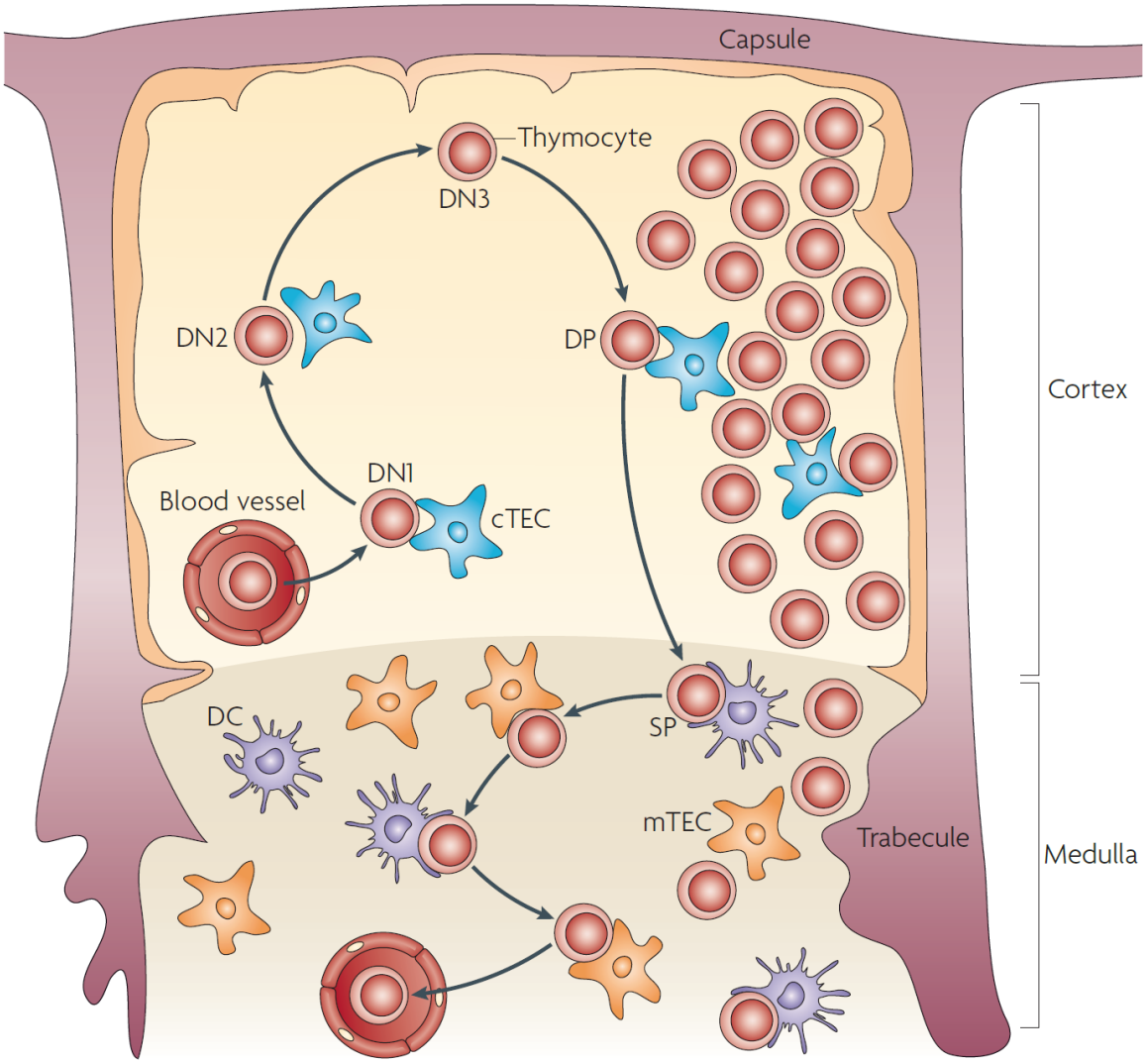


**Figure I**. **Thymocyte development in the thymus.** Immature T cells migrate from the circulation into the cortex of thymus where they go through positive selection by cTECs and commit to $CD4^+$ or $CD8^+$ SP thymocytes. The SP cells then migrate to the medulla and undergo negative selection, in which their autoreactivity of TCRs is examined by mTECs and hematopoietic cells in the medulla. Figure credit: Klein *et al.* (2009) Nat. Rev. Immunol.[5]

These positive-selected $CD4^+$ or $CD8^+$ SP thymocytes then enter the medulla of thymus for negative selection, in which their TCR specificities are examined against self-antigens presented by the antigen presenting cells (APCs) in the thymic medulla, including medullary thymic epithelial cells (mTECs), thymic B cells (BCs) and dendritic cells (DCs)[5]. The mTECs are able to ectopically express tissue-restricted self-antigens (TRAs), which are normally expressed exclusively in peripheral tissues, such as insulin in pancreatic β cells[7, 8]. The ectopic expression of TRAs is essential for T cell central tolerance and thus the prevention of autoimmunity. The epitopes of TRAs are processed and presented by mTECs to SP thymocytes, and those SP cells with high affinity to self-antigens are subjected to apoptosis and thus eliminated (clonal deletion, **Figure II**)[6]. Thymic B cells are also able to express TRAs ectopically and promote clonal deletion of autoreactive thymocytes[9, 10]. Thymic DCs also contribute to the deletion of autoreactive thymocytes. However, they do not express TRAs themselves; instead they acquire TRAs transferred from mTECs and subsequently present the TRA epitopes to SP thymocytes to facilitate clonal deletion of autoreactive thymocytes[5, 6, 11].

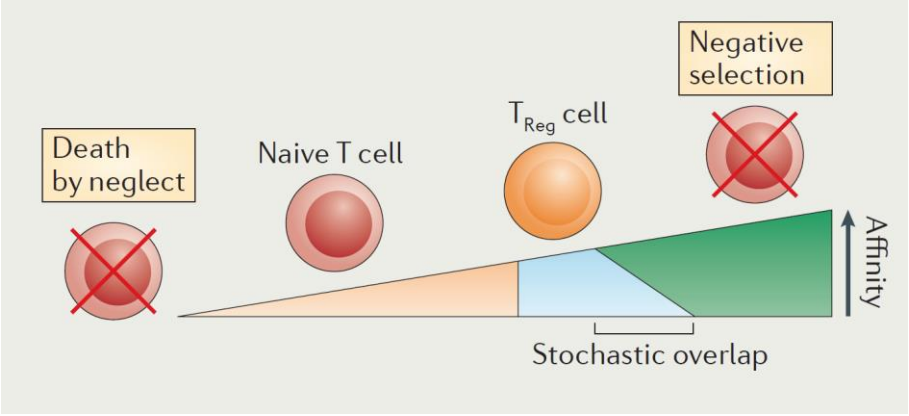


**Figure II. The affinity model of thymocyte selection.** Low to intermediate affinities of TCRs to self-peptides allow thymocytes to pass the negative selection and become mature naïve T cells, whereas strong interaction between TCR and peptide:MHC complex often leads to clonal deletion. A broad range of affinities in between positive and negative selection is permissive for Treg differentiation. Figure credit: Klein *et al.* (2014) Nat. Rev. Immunol.[6]

In addition to negative selection through clonal deletion, an alternative fate of autoreactive $CD4^+$ thymocytes after encountering self-antigens presented by APCs in the thymic medulla is their differentiation to regulatory T (Treg) cells (**Figure II**)[12-14]. No single APC subset is exclusively responsible for clonal deletion or Treg differentiation[6]. Both mTECs and hematopoietic cells (such as thymic DCs) can promote Treg induction in the thymus (**Figure III**)[13-16], however, evidences suggest that different types of APCs, although playing redundant roles in clonal deletion and Treg differentiation, are responsible for the induction of distinct Treg cell repertoires[11, 17].

Clonal deletion and Treg differentiation are both critical features in T cell central tolerance: the former results in a passive tolerance towards self-antigens, whereas the latter creates a dominant tolerance through the establishment of a repertoire of thymus-derived Treg (tTreg) cells, which can actively suppress autoimmune responses.

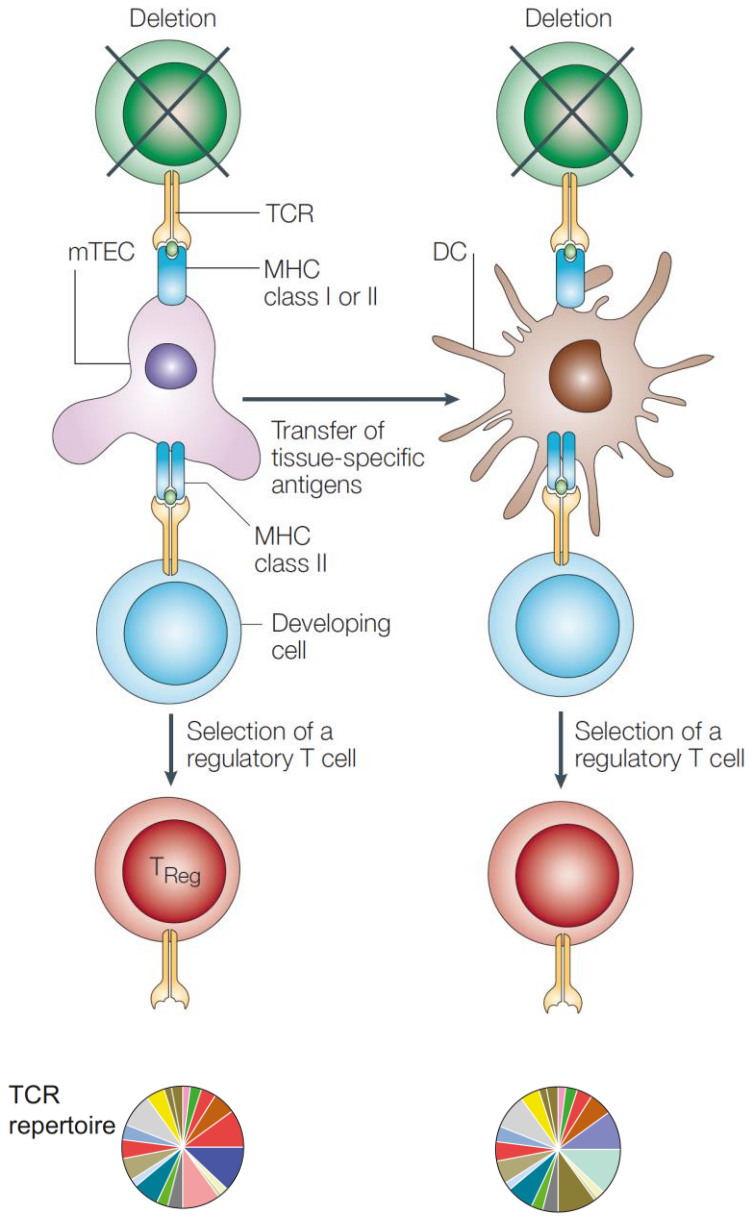


**Figure III. Clonal deletion and Treg differentiation cooperatively mediate T cell tolerance towards tissue specific self-antigens**. Both mTECs and thymic DCs contribute to clonal deletion and Treg differentiation. While mTECs test the autoreactivity of thymocytes through autonomous TRA expression and direct presentation, thymic DCs mediate T cell tolerance via cross-presentation of TRAs derived from mTECs. Thymic DCs and mTECs are responsible for generating distinct repertoires of naïve T cells and tTreg cells in terms of TCR clones. Figure adapted from Kyewski *et al.* (2004) Nat. Rev. Immunol. and Kyewski *et al.* (2014) Immunity[8, 18]

## 1.2 Autoimmune regulator (Aire) mediates promiscuous gene expression

The expression of TRAs ectopically in thymic medulla – referred to as promiscuous gene expression (pGE) – is the fundament of T cell central tolerance. The genetic regulation of pGE is predominantly controlled by the transcription factor, autoimmune regulator (Aire)[19, 20]. Mutations of Aire are associated with autoimmune diseases, such as autoimmune polyglandular syndrome type 1 (APS1)[21, 22]. Independent studies with animal models of *Aire*-deficiency have demonstrated that Aire is indispensable for both clonal deletion[19] and Treg differentiation[23, 24] in T cell central tolerance.

In mTECs, Aire controls the ectopic expression of TRAs with ordered stochasticity[25]. One particular TRA is expressed by only 1-3% of mTECs, and therefore whether a given individual mTEC expresses one particular TRA gene is stochastic[26, 27]. On the other hand, certain sets of TRAs are frequently found to be co-expressed in the same individual mTEC, suggesting that the expression of TRA genes is not completely random, but rather governed by a hitherto unknown mechanism[25, 28, 29]. This expression pattern assures that the whole spectrum of self-antigens are expressed by mTECs and can be "seen" by thymocytes[30].

Aire does not promote gene expression by targeting specific DNA sequences, as no clear DNA binding motif has been identified within the protein. Instead, it targets transcriptional repressive complexes (where gene expression is silenced) of the genome, and subsequently activates the transcription of the downstream genes. Aire protein consists of four domains: CARD (caspase activation and recruitment domain), SAND domain (SP100, AIRE-1, NucP41/P75, DEAF1), PHD1 (plant homeodomain 1) and PHD2[20, 30]. CARD is essential for the homologous multimerization of Aire[31], and therefore genetic defects on other domains of Aire often lead to dominant mutations due to the formation of multimer protein containing malfunctioning monomers[32, 33]. The PHD1 and SAND domains are critical for "directing" the protein to transcriptional repressive loci of the genome: PHD1 directly recognizes unmethylated histone

H3 lysine 4 (H3K4)[34, 35], which is a repressive epigenetic mark; SAND interacts with proteins that are associated with repressive chromatin states, such as the protein complex of activating transcription factor 7-interacting protein (ATF7IP), methyl-CpG-binding domain protein 1 (MBD1), and methyltransferase ESET (**Figure IV**)[36]. Furthermore, DNA-dependent protein kinase (DNA-PK) recruits Aire via the PHD domains to double-strand breaks near transcription initiation sites[37], where RNA polymerase II stalls after starting the transcription for 50-100 base pairs in the absence of Aire[38]. After Aire is recruited to the stalled RNA polymerase II, it promotes the RNA elongation by recruiting positive transcription elongation factor b (P-TEFb)[39], heterogeneous nuclear ribonucleoprotein L (hnRNPL)[40] and bromodomain-containing 4 (BRD4)[41], which release the stalled RNA polymerase II and enable the transcription to proceed.

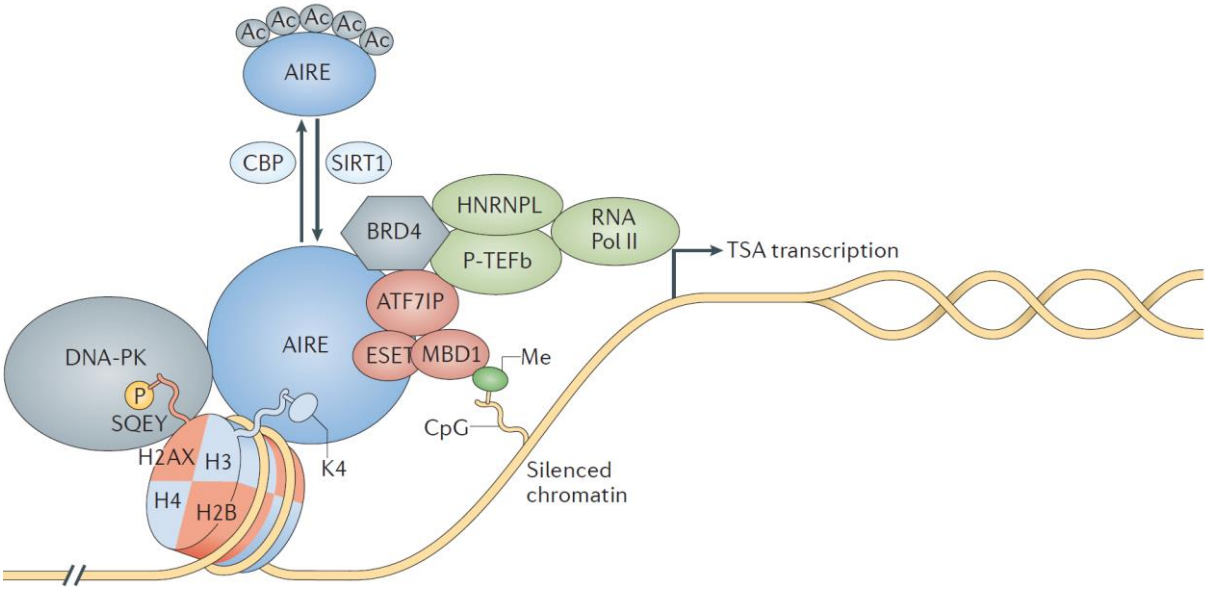


**Figure IV. Mechanisms of pGE by Aire and binding partners.** Aire directly interacts with the repressed chromatin via recognizing unmethylated histone H3 lysine 4 (H3K4) of the silenced chromatin, or indirectly through the interaction with ATF7IP-MBD1-ESET complex and DNA-PK, which are associated with methylated DNA and double-strand breaks at transcription initiation sites, respectively. The recruitment of P-TEFb, hnRNPL and BRD4 by Aire facilitates the release of stalled

RNA polymerase II. SIRT1 and CBP control the acetylation of Aire, which regulates its transcriptional activity. Figure adapted from Anderson *et al.* (2016) Nat. Rev. Immunol.[30]

The receptor activator of nuclear factor-κB (RANK) signaling induces the maturation of mTECs and concomitantly promotes Aire expression[42]. The expression of Aire is regulated transcriptionally, whereas the functional efficiency of Aire is regulated at both post-transcriptional and post-translational levels. The enhancer elements upstream of *Aire* locus are essential for its transcription. These enhancer elements consist of conserved noncoding sequences which are responsive to nuclear factor-κB (NF-κB)[43, 44]. After *A*ire is transcribed, the splicing of the *Aire* transcript is regulated by lysyl-hydroxylase and arginine demethylase JMJD6. The deficiency of *JMJD6* does not affect the expression of *Aire*, but significantly reduces the expression levels of Aire-regulated TRA genes[45]. At the protein level, deacetylation of lysine residues of Aire by deacetylase sirtulin 1 (SIRT1) increases Aire transcriptional activity[46], while acetylation by CREB-binding protein (CBP) results in reduction of Aire-mediated TRA expression[47]. In addition, phosphorylation of Aire by DNA-PK also promotes the transcriptional activity of Aire[48, 49].

Due to the essence of pGE for T cell central tolerance, the expression and functional regulation of Aire has been deeply investigated in mTECs. However, its impact on the peripheral tolerance of T cells still remains poorly understood.

## 1.3 Ectopic expression of TRAs in periphery

After maturation in the thymus, naïve T cells emigrate from the thymus and recirculate into blood and lymphatic vessels patroling the vascular system to identify their cognate antigens[50]. During pathogen infection, naïve T cells recognize antigens presented by APCs that are preconditioned by inflammatory signals such as pathogen-associated molecular patterns (PAMPs). Consequently, these T cells become activated and differentiate into conventional

effector and memory T cells[51]. In steady state, however, activation and differentiation of T cells are exquisitely regulated to avoid unnecessary immune responses[52]. Self-antigen specific T cells are detectable in healthy humans, despite successful negative selection in the thymus. Various mechanisms of peripheral tolerance are essential to keep these autoreactive T cells in check[53]. Importantly, ectopic TRA expression is not only a hallmark of mTECs for the initiation of T cell central tolerance in the thymus, but also plays an important role in maintaining peripheral tolerance for T cells.

Lymph node stromal cells including fibroblastic reticular cells (FRCs, $gp38^{+}CD31^{-}$), lymphatic endothelial cells (LECs, $gp38^{+}CD31^{+}$) and blood endothelial cells (BECs, $gp38^{-}CD31^{+}$) ectopically express TRAs[54-56]. After encountering FRCs, naïve TRA-specific $CD8^{+}$ T cells are activated and consequently deleted via direct presentation of TRA antigen by FRCs[57, 58]. Although *Aire* transcript is expressed in FRCs, Aire protein is undetectable. Moreover, after treated with polyinosinic:polycytidylic acid (poly I:C), a ligand of toll-like receptor 3 (TLR3), FRCs downregulate the expression of TRAs, and exhibit reduced ability to induce apoptosis of autoreactive $CD8^{+}$ T cells[58], showing that the tolerogenic characteristics of FRCs is present only in steady state, but not under inflammatory conditions. Of note, after poly I:C treatment, TRA genes and Aire are upregulated in $gp38^{-}CD31^{-}$ cell subset in the lymph nodes, which includes hematopoietic-derived cells[58], suggesting that hematopoietic cells respond to inflammation differently in terms of peripheral tolerance induction, compared to lymph node stroma cells. LECs also have the ability to directly present TRAs to autoreactive $CD8^{+}$ T cells via MHC-I and induce their deletion[59-61]. The authors have shown that the ectopic expression of TRAs in LECs is Aire-independent, while in $CD45^{+}$ hematopoietic cells it is Aire-dependent[59].

In addition to regulating autoreactive $CD8^{+}$ T cells, lymph node stromal cells are also involved in the maintenance of peripheral tolerance of $CD4^{+}$ T cells. FRCs, LECs and BECs express

MHC-II in a class II transactivator (CIITA)-dependent manner[61, 62]. These lymph node stromal cells can induce anergy and apoptosis of autoreactive $CD4^+$ T cells in cooperation with DCs. However, it is still controversial whether these stromal cells can directly present TRAs via MHC-II to $CD4^+$ T cells, or their tolerogenic effect depends on the DCs in lymph nodes that can receive antigens from stromal cells and present them to $CD4^+$ T cells[56, 61, 62]. Furthermore, Baptista *et al.* have demonstrated that the transplantation of MHC-II-deficient lymph nodes (and thus MHC-II-deficient lymph node stromal cells) to WT mice leads to reduction of Treg cell frequencies[63], indicating that lymph node stromal cells are important for Treg homeostasis. However, it is not known if the stromal cells can induce the conversion of peripherally derived Treg (pTreg) cells, or only maintain the survival of tTreg cells.

Intriguingly, Aire protein expression has also been found in peripheral lymphoid organs, such as spleen and lymph nodes. These extra-thymic Aire-expressing cells (eTACs) are able to express Aire-dependent TRAs and present the self-antigens to autoreactive $CD8^+$ and $CD4^+$ T cells. It has been shown that eTACs can prevent the onset of diabetes by inducing apoptosis of pancreatic β cell-specific $CD8^+$ T cells[64]. Moreover, presentation of pancreatic antigens to cognate naïve $CD4^+$ T cells induces their anergy/hyporesponsiveness, resulting from strong TCR signaling and lack of co-stimulatory signals from eTACs[65]. An additional study has revealed that eTACs are hematopoietic-derived cells, and show characteristics of DCs, such as expression of CD11c as well as Zbtb46, the master transcription factor of DCs[65]. Of note, after recognizing the self-antigens presented by eTACs, naïve autoreactive $CD4^+$ T cells are partially converted to $CD25^+Foxp3^+$ Treg cells. However, these eTAC-induced Treg cells do not exert suppressive function to actively prevent diabetes[65]. Therefore the peripheral tolerance induced by eTACs is passive rather than active.

To date, there is no study showing a direct presentation of ectopically expressed TRAs which leads to the conversion of naïve autoreactive $CD4^+$ T cells into Treg cells in the spleen, lymph nodes, or bone marrow (BM), which are the reservoirs of circulating Treg cells.

## 1.4 T cell immunity in the bone marrow

As an indispensable primary and secondary lymphoid organ for hematopoietic homeostasis, BM harbors various types of cellular compartments for the development of hematopoietic stem cells and progenitor cells, as well as for the modulation of adaptive immune responses under physiological and inflammatory circumstances[66, 67]. This lymphoid organ is vascularized by blood vessels, which span through the endosteum and central marrow in the form of sinusoids. All the immune cells migrate in and out of the BM through the sinusoids, as this organ is not connected to lymphatic system[68]. For T cell homeostasis, BM niches provide survival signals including cytokines and cell adhesion molecules to antigen-specific memory T cells for their self-renewal and maintenance[69, 70]. Memory T cells specific to tumor-associated antigens reside in the BM of cancer patients[71, 72], and these tumor-specific memory T cells can be utilized for cancer immunotherapy such as adoptive T cell transfer therapy[73-76].

Apart from accommodating memory T cells, BM also serves as a T-cell priming site, as BM-resident DCs can activate both $CD4^+$ and $CD8^+$ naïve T cells in the absence of other secondary lymphoid organs[77-79]. Moreover, Treg cells are also enriched in BM with a higher frequency than those in spleen and lymph nodes[67], and their immigration into the BM depends on the balance between CXCL12 and G-CSF[80, 81]. As key regulators of both local and systemic immunity, Treg cells in BM play crucial roles in different types of diseases and manifest great value for clinical application. BM Treg cells are essential for immune hematopoiesis as they provide immune-privileged niches of hematopoietic stem cells[82], control IL-7 expression of BM stromal cells[83], regulate hematopoiesis[84], and are required for maintaining tolerance after stem cell transplantation[85]. In addition to their local impact in the BM, Treg cells migrate from the

BM to the periphery and regulate immune responses under inflammatory conditions. In cancer patients, tumor-specific Treg cells reside in their BM and upon selective activation upregulate the expression of chemokine receptors S1P1, which leads to the emigration of tumor-specific Treg cells to peripheral tumor sites[86, 87]. The origin of the tumor-specific Treg cells, as well as the mechanisms underlying the activation of those Treg cells is hitherto unknown.

## 1.5 Aims of this study

BM Treg cells comprise diverse functional clones which cover a broad spectrum of self-antigens. However, how the diverse repertoire of Treg cells is generated in the BM remains largely elusive. To date, BM has been viewed as a preferential site for the recirculation of tTreg cells[81], while little is known about its role in the generation of pTreg cells. Here, I seek to investigate whether ectopic TRA expression takes place in the BM, and if the presentation of these self-antigens leads to generation of functional pTreg cells which help maintaining peripheral tolerance.

## 1.6 Preliminary data

### 1.6.1 Aire is expressed by BM-resident MHC-II$^+$EpCAM$^+$CD45$^+$ cells

The working hypothesis is that self-antigens are expressed locally in the BM and serve to generate or maintain peripherally-induced Treg cells. Since Aire is the key transcription factor that controls the ectopic expression of TRAs, Dr. Felix Klug in our group first assessed Aire expression in murine BM. He harnessed Adig transgenic mice, in which the GFP reporter protein is driven by a murine Aire locus[64]. Immunofluorescence demonstrated that Aire-GFP reporter protein was expressed in both the thymus and BM (**Figure V-A**).

Immunocytochemistry was performed on sorted Aire-GFP+ cells to assess Aire protein expression. The pattern of Aire expression exhibited puncta-like structure in the nuclei (**Figure V-B**), which was also observed in the BM tissue of WT Balb/c mice (**Figure V-C**), resembling the Aire expression pattern in mTECs[32]. BMACs and mTECs also shared other common features, such as the expression of MHC-II and epithelial cell adhesion molecule (EpCAM) (**Figure V-C, D**). However, hematopoietic marker CD45 was also expressed by BMACs, and hence the developmental origin of BMACs remains unclear.

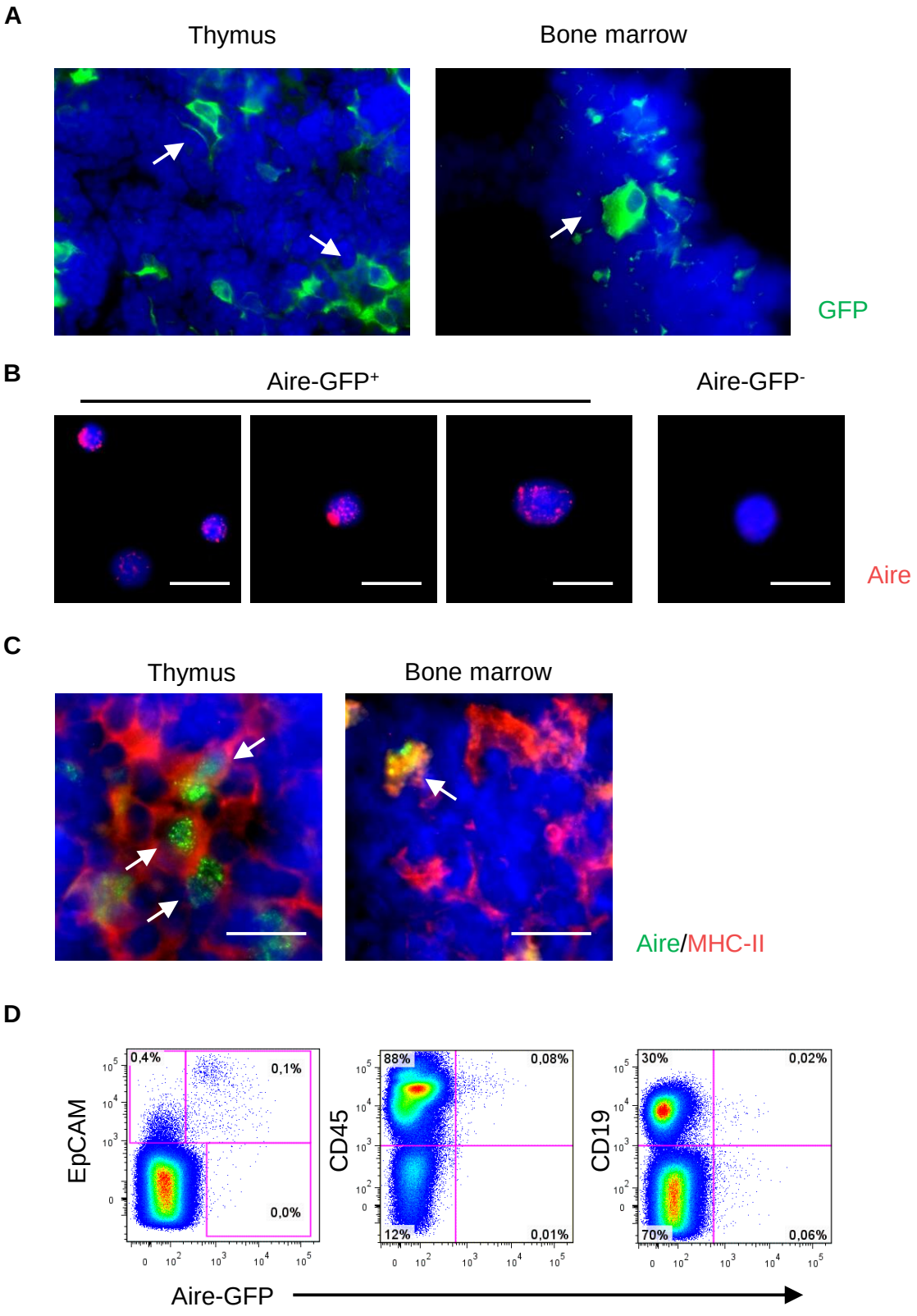


**Figure V. BM-resident Aire-expressing cells are MHC-II$^+$EpCAM$^+$CD45$^+$. (A)** Immunofluorescence of GFP on thymus and BM tissue of Adig mice. Arrows indicate Aire-GFP expressing cells. **(B)** Immunocytochemistry of Aire on Adig BM cells sorted by GFP expression. **(C)** Immunofluorescence of Aire and MHC-II on thymus and BM tissue of WT Balb/c mice. Arrows indicate

Aire-expressing cells. **(D)** Flow cytometric analysis of surface marker expression on total BM cells of Adig mice.

### 1.6.2 AIRE is detected in human BM but not in blood

To assess the presence of BMACs in human BM, Dr. Klug further isolated mononuclear cells from human blood and BM donors and conducted flow cytometric analysis after intracellular staining for AIRE protein. As depicted in **Figure VI**, AIRE protein was detected in human BM, and in agreement with the findings in murine models, human BM AIRE-expressing cells also expressed EpCAM and HLA-DR. Among $EpCAM^+HLA\text{-}DR^+$ cells, 5.5±4.7% (mean±SEM) expressed AIRE (**Figure VI-B**), and 0.13±0.05% of total BM mononuclear cells were $AIRE^+EpCAM^+HLA\text{-}DR^+$ (**Figure VI-C**). In blood derived mononuclear cells, however, AIRE was undetectable, demonstrating that human AIRE-expressing cells are significantly enriched in BM compared to peripheral blood (**Figure VI**). Thus, AIRE is also expressed in human BM, and AIRE expression is restricted to $MHC\text{-}II^+EpCAM^+$ BM cells.

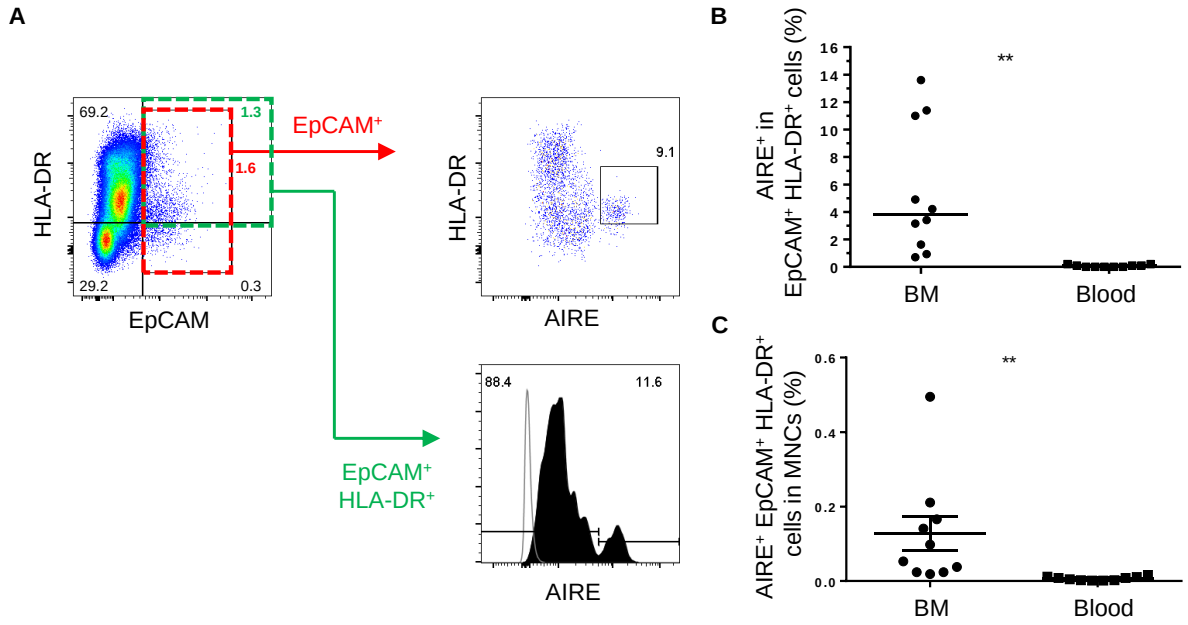


**Figure VI. AIRE is expressed in human BM. (A)** Representative data of AIRE expressing cells in human BM. **(B)** Frequencies of AIRE-expressing cells in human BM cells and peripheral blood

mononuclear cells. Unshaded grey curve indicates isotype control. **(C)** Frequencies of $AIRE^{+}EpCAM^{+}HLA\text{-}DR^{+}$ cells in mononuclear cells (MNCs) in the BM and blood (mean ± SEM), evaluated according to the gating strategy shown in (**A**), upper panel. **, $P < 0.01$ (paired Student's *t*-test).

### 1.6.3 Aire regulates the expression of TRA genes in BMACs

Next, Dr. Klug examined the function of Aire as a transcription factor to promote ectopic TRAs expression in the BM. BMACs and mTECs of Adig mice were sorted according to Aire-GFP expression and subjected to gene expression array analysis. This revealed that BMACs expressed 721 genes which are classified as TRAs according to previously described criteria[8, 88], and 634 genes (88%) of these TRAs were commonly expressed by both mTECs and BMACs, whereas 87 of them were exclusively expressed in BMACs (**Figure VII-A**). Of note, among the TRAs expressed by BMACs, Dr. Klug found numerous self-antigens associated to various autoimmune diseases, such as *CNP* for multiple sclerosis and *Col5a1* for rheumatoid arthritis, as well as tumor-associated testis antigens such as *Mage-e1*. The TRA genes expressed by BMACs represented highly diverse tissue types (**Figure VII-B**). To delineate which of these TRAs were controlled by Aire, we compared gene expression profiles in BMACs of Adig × $Aire^{-/-}$ to the ones of Adig × $Aire^{+/+}$ mice. As shown in **Figure VII-C**, 268 genes showed significant differential expression in the presence of Aire. Among the Aire-regulated genes, 80 genes were Aire-induced and 188 were repressed by Aire. Of note, the overlap between Aire-regulated genes in BMACs and mTECs was limited to 4 genes[28], and only one gene was shared between BMACs and previously reported Aire-regulated genes in eTACs[64] (**Figure VII-C**). This demonstrates the presence of complementary sets of TRAs expressed by Aire-expressing cells in different organs.

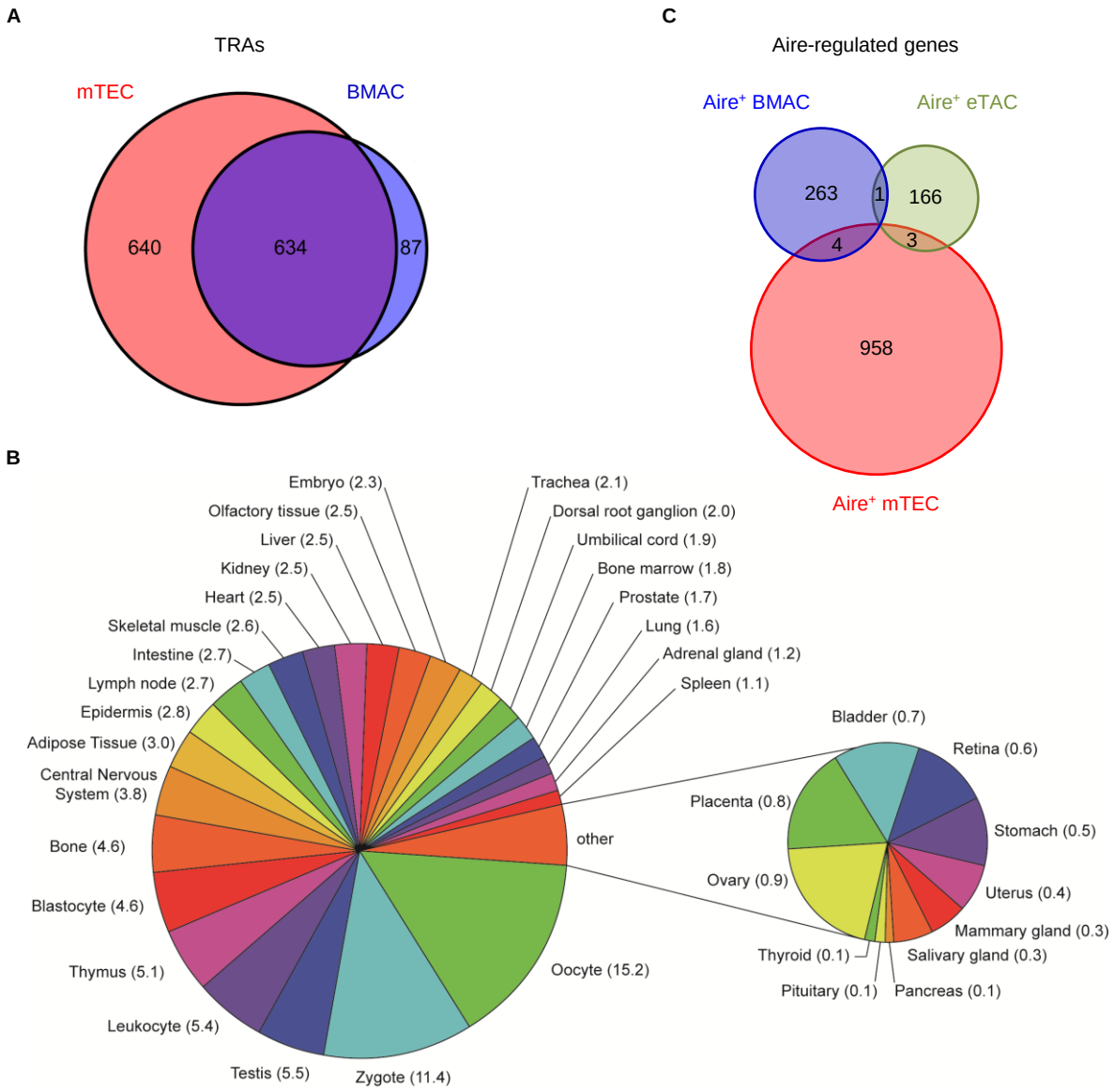


**Figure VII. Aire regulated the expression of TRA genes in BMACs. (A)** Venn diagram of the numbers of TRA genes expressed exclusively in either mTECs or BMACs, or commonly expressed in both. **(B)** Distribution of the tissue types represented by the TRAs expressed by BMACs. Numbers in brackets indicate percentages of each tissue type. **(C)** Venn diagram of the numbers of Aire-regulated genes which were commonly or exclusively expressed in Aire-GFP+ BMACs, splenic eTACs and mTECs sorted from Adig × Aire$^{+/-}$ mice, compared to the Aire-GFP$^{+}$ cells in Adig × Aire$^{-/-}$ mice.

# 2. Materials and Methods

## 2.1 Materials

### 2.1.1 Mice

Adig[64], Aire-HCO[9], 6.5 TCR-HA[12] and Aire$^{-/-}$ mice[89] have been described previously. Both Adig and Aire$^{-/-}$ mice were backcrossed onto Balb/c background for more than 10 generations, and all mice were maintained on Balb/c background under specific pathogen-free condition. Animal experiments were approved and regularly controlled by the authorities of the local states (Regierungspräsidium Karlsruhe and Regierung von Unterfranken), in compliance with EU Directive 2010/63/EU.

### 2.1.2 Human samples

Collection of peripheral blood and BM samples from donors was performed in compliance with the ethics committee (approval reference number 70/99) of the University of Heidelberg upon signed consent.

### 2.1.3 Reagents for cell preparation and *in vitro* culture

| Reagent | Vendor | Catalog number |
|---|---|---|
| PBS | Sigma-Aldrich | D8537 |
| FBS | Sigma-Aldrich | F7524 |
| RPMI-1640 | Sigma-Aldrich | R8758 |
| DMEM | Sigma-Aldrich | D6429 |
| Biocoll | Biochrom GmbH | L6715 |
| Cell strainer | Greiner | 542000 |

### 2.1.4 Buffer

| **FACS buffer** | **Vendor** | **Amount for 500 ml** |
|---|---|---|
| FBS | Sigma-Aldrich | 10 ml |
| $ddH_2O$ | - | 490 ml |

| **ACK buffer, pH 7.2-7.4** | **Vendor** | **Amount for 1 l** |
|---|---|---|
| $NH_4Cl$ | Sigma-Aldrich | 8.29 g |
| $KHCO_3$ | Sigma-Aldrich | 1 g |
| $Na_2EDTA$ | Sigma-Aldrich | 37.2 mg |
| $ddH_2O$ | - | up to 1 l |

| **MACS buffer** | **Vendor** | **Amount for 500 ml** |
|---|---|---|
| FBS | Sigma-Aldrich | 2.5 ml |
| EDTA (1%) | Biochrom GmbH | 25 ml |
| $ddH_2O$ | - | 472.5 ml |

### 2.1.5 Antibodies against mouse antigens used in flow cytometric analyses

| **Antigen** | **Clone** | **Isotype** | **Conjugated fluorochrome** | **Vendor** | **Dilution fold** |
|---|---|---|---|---|---|
| CD16/32 | 2.4G2 | Rat IgG2b, κ | None (Fc Block) | BD Biosciences | 100 |
| CD16/32 | 93 | Rat IgG2a, λ | None (Fc Block) | BioLegend | 100 |
| B220 | RA3-6B2 | Rat IgG2a, κ | APC-Fire750 | BioLegend | 100 |
| Blimp-1 | 5E7 | Rat IgG2b, κ | PE | BioLegend | 100 |
| CD3 | 17A2 | Rat IgG2b, κ | AlexaFluor700 | BD Biosciences | 100 |
| CD4 | RM4-5 | Rat IgG2a, κ | V500 | BD Biosciences | 100 |
| CD11b | M1/70 | Rat IgG2b, κ | PerCP-Cy5.5 | eBioscience | 100 |
| CD11c | N418 | Hamster IgG | PerCP | BioLegend | 100 |
| CD19 | 1D3 | Rat IgG2a, κ | PE-Cy7 | BD Biosciences | 100 |
| CD19 | 6D5 | Rat IgG2a, κ | AlexaFluor700 | BioLegend | 100 |

| | | | | | |
|---|---|---|---|---|---|
| CD25 | PC61 | Rat IgG1, λ | Brilliant Violet421 | BioLegend | 200 |
| CD44 | IM7 | Rat IgG2b, κ | FITC | BD Biosciences | 100 |
| CD45 | 30-F11 | Rat IgG2b, κ | APC-eFluor780 | eBioscience | 400 |
| CD45.1 | A20 | Mouse IgG2a, κ | APC | BD Biosciences | 200 |
| CD45.1 | A20 | Mouse IgG2a, κ | AlexaFluor700 | BD Biosciences | 100 |
| CD45.2 | 104 | Mouse IgG2a, κ | PE-CF594 | BD Biosciences | 200 |
| CD45.2 | 104 | Mouse IgG2a, κ | Brilliant Violet605 | BD Biosciences | 100 |
| CD62L | MEL-14 | Rat IgG2a, κ | PerCP-Cy5.5 | BD Biosciences | 100 |
| CD80 | 16-10A1 | Hamster IgG | Pacific Blue | BioLegend | 200 |
| CD86 | GL1 | Rat IgG2a, κ | PE | BioLegend | 100 |
| CD138 | 281-2 | Rat IgG2a, κ | PE | BioLegend | 200 |
| CD138 | 281-2 | Rat IgG2a, κ | APC | BioLegend | 100 |
| CD200 | OX110 | Rat IgG2a, κ | PerCP-eFluor710 | eBioscience | 200 |
| CTLA-4 | UC10-4B9 | Hamster IgG | PE | BioLegend | 100 |
| EpCAM | G8.8 | Rat IgG2a, κ | AlexaFluor647 | BioLegend | 100 |
| F4/80 | BM8 | Rat IgG2a, κ | AlexaFluor700 | BioLegend | 100 |
| Foxp3 | MF23 | Rat IgG2b, κ | AlexaFluor647 | BD Biosciences | 100 |
| IgD | 11-26c.2a | Rat IgG2a, κ | PerCP-Cy5.5 | BioLegend | 100 |
| IgG1 | A85-1 | Rat IgG1, κ | Brilliant Violet421 | BD Biosciences | 100 |
| IgG2a/2b | R2-40 | Rat IgG1, κ | Brilliant Violet605 | BD Biosciences | 100 |
| IgM | RMM-1 | Rat IgG2a, κ | AlexaFluor647 | BioLegend | 100 |
| IgM | RMM-1 | Rat IgG2a, κ | Brilliant Violet605 | BioLegend | 100 |
| I-A/I-E | M5/11.15.2 | Rat IgG2b, κ | PE-Cy7 | BioLegend | 200 |
| I-A/I-E | M5/11.15.2 | Rat IgG2b, κ | APC-eFluor780 | eBioscience | 100 |
| LAG-3 | C9B7W | Rat IgG1, κ | PE-Cy7 | eBioscience | 100 |
| LAP | TW7-16B4 | Mouse IgG1, κ | PerCP-Cy5.5 | eBioscience | 200 |
| Ly-51 | BP-1 | Mouse IgG2a, κ | PE | BD Biosciences | 100 |

| | | | | | |
|---|---|---|---|---|---|
| Ly-6D | 49-H4 | Rat IgG2c, κ | eFluor450 | eBioscience | 200 |
| PD-L1 | MIH5 | Rat IgG2a, λ | PE-Cy7 | eBioscience | 100 |
| PD-L2 | TY25 | Rat IgG2a, κ | PE | BD Biosciences | 100 |
| TACI | 8F10 | Rat IgG2a, κ | PE | BioLegend | 100 |

### 2.1.6 Antibodies against human antigens used in flow cytometric analyses

| **Antigen** | **Clone** | **Isotype** | **Conjugated fluorochrome** | **Vendor** | **Dilution factor** |
|---|---|---|---|---|---|
| AIRE | 6.1 | Rabbit | AlexaFluor647 | Kindly provided by P. Peterson[48] | 500 |
| CD2 | RPA-2.10 | Mouse IgG1, κ | Brilliant Blue515 | BD Biosciences | 200 |
| CD200 | OX-104 | Mouse IgG1, κ | PE-Cy7 | eBioscience | 20 |
| EpCAM | 9C4 | Mouse IgG2b, κ | AlexaFluor488 | BioLegend | 20 |
| HLA-DR | L243 | Mouse IgG2a, κ | PerCP-eFluor710 | eBioscience | 20 |
| PD-L1 | MIH1 | Mouse IgG1, κ | Brilliant Violet421 | BD Biosciences | 20 |
| TACI | 1A1-K21-M22 | Rat IgG2a, κ | PE | BD Biosciences | 100 |

### 2.1.7 Viability dyes used in flow cytometric analyses

| **Viability dye** | **Vendor** | **Dilution factor** |
|---|---|---|
| 7-AAD | BioLegend | 50 |
| Yellow LIVE/DEAD Fixable Dead Cell Stain Kit | Molecular Probes | 1000 |
| Zombie Aqua Fixable Viability Kit | BioLegend | 1000 |
| Zombie NIR Fixable Viability Kit | BioLegend | 1000 |

### 2.1.8 Reagent used in flow cytometric analyses

| Reagent | Vendor | Working concentration |
|---|---|---|
| CFSE Cell Division Tracker Kit | BioLegend | 5 μM or 0.5 μM |
| Foxp3/Transcription Factor Fixation/Permeabilization Concentrate and Diluent | eBioscience | - |

### 2.1.9 Enzymes and reagents for thymus digestion

| Reagent | Vendor | Working concentration |
|---|---|---|
| Collagenase IV | Worthington | 0.2 mg/ml |
| Neutral Protease (Dispase) | Worthington | 0.2 mg/ml |
| DNase I | Sigma-Aldrich | 25 μg/ml |
| HEPES | Sigma-Aldrich | 20 mM |

### 2.1.10 Reagent for cell isolation

| Reagent | Vendor |
|---|---|
| CD45 magnetic microbeads | Miltenyi Biotech |
| MojoSort Mouse CD4 Naïve T Cell Isolation Kit | BioLegend |
| EasySep Mouse Memory CD4+ T Cell Isolation Kit | STEMCELL Technologies |

### 2.1.11 Primary antibodies for immunofluorescence

| Antigen | Clone | Isotype | Conjugated fluorochrome | Vendor | Dilution factor |
|---|---|---|---|---|---|
| Aire | 5H12 | Rat IgG2c, κ | AlexaFluor488 | eBioscience | 50 |
| Aire | 5H12 | Rat IgG2c, κ | AlexaFluor660 | eBioscience | 20 |
| CD4 | H129.19 | Rat IgG2a, κ | None | BD Biosciences | 50 |
| CD8 | 53-6.7 | Rat IgG2a, κ | None | BD Biosciences | 50 |
| CD19 | 1D3 | Rat IgG2a, κ | None | BD Biosciences | 25 |

### 2.1.12 Secondary antibodies for immunofluorescence

| Antigen | Conjugated fluorochrome | Vendor | Dilution factor |
|---|---|---|---|
| Goat-anti-rat IgG | AlexaFluor488 | Molecular Probes | 200 |
| Goat-anti-rat IgG | AlexaFluor647 | Molecular Probes | 200 |

### 2.1.13 Reagents used in immunofluorescence

| Reagent | Vendor |
|---|---|
| Tissue-Tek | Sakura |
| DAPI-containing Fluoromount-G mounting medium | eBioscience |
| Acetone | Sigma-Aldrich |
| Tween-20 | AppliChem |

### 2.1.14 Reagents for RNA isolation and Real-Time PCR

| Reagent | Vendor |
|---|---|
| RNeasy Mini Kit | Qiagen |
| QuantiTect Reverse Transcription Kit | Qiagen |
| QuantiFast SYBR Green PCR Kit | Qiagen |

### 2.1.15 Primers used in Real-Time PCR

| Gene | Position | Sequence |
|---|---|---|
| *Aire* | forward | 5’-TGCAGGAGATCCCCAGTG-3’ |
| | reverse | 5’-TGGGACAGGTTCTGTTGGAC-3’ |
| *Actb* | forward | 5’-ACGGCCAGGTCATCACTATTG-3’ |
| | reverse | 5’-AGGATTCCATACCCAAGAAGGAA-3’ |

### 2.1.16 Reagents for whole transcriptome amplification, single cell end-point PCR, and gene expression array

| Reagent | Vendor |
|---|---|
| mTRAP™ Lysis buffer | Active Motif |
| tRNA | Sigma-Aldrich |
| SuperAmp Kit | Miltenyi Biotec |
| Klenow Fragment | Fermentas |
| Random Octamer | Enzo Life Sciences GmbH |
| MouseRef-8 v2.0 Expression BeadChip | Illumina |
| MyTaq HS Red Mix | Bioline |
| Agarose | Carl Roth |
| GelRed Nucleic Acid Gel Stain | Biotium |

### 2.1.17 Primers for quality control in single cell end-point PCR

| Gene | Position | Sequence |
|---|---|---|
| *Actb* | forward | 5’-CAGCTTCTTTGCAGCTCCTT-3’ |
| | reverse | 5’-CTCGTCACCCACATAGGAGTC-3’ |
| *B2m* | forward | 5’-TGGTGCTTGTCTCACTGACC-3’ |
| | reverse | 5’-CCGTTCTTCAGCATTTGGAT-3’ |
| *Gapdh* | forward | 5’-GAAGGGCATCTTGGGCTAC-3’ |
| | reverse | 5’- GCCTCTCTTGCTCAGTGTCC-3’ |

### 2.1.18 Primers for detecting gene expression in single cell end-point PCR

| Gene | Position | Sequence |
|---|---|---|
| *Aire* | forward | 5’-TGCAGGAGATCCCCAGTG-3’ |
| | reverse | 5’-TGGGACAGGTTCTGTTGGAC-3’ |
| *Csna* | forward | 5’-CCTATGAGTGTAGTGGATCAGGCA-3’ |
| | reverse | 5’-AGGCATCATACTGGAAGATTTGTG-3’ |
| *Csnb* | forward | 5’-TGTGCTCCAGGCTAAAGTTCACT-3’ |
| | reverse | 5’-GGTTTGAGCCTGAGCATATGG-3’ |

| | | |
|---|---|---|
| *Csng* | forward | 5'-ATGTTGCACACCTCTTCACCAG-3' |
| | reverse | 5'-GGCGTGTTATGGATGGCATT-3' |
| *Crp* | forward | 5'-GGATTGTAGAGTTCTGGATTGATGG-3' |
| | reverse | 5'-TGCTCCTGCCCCAAGATG-3' |
| *Expi* | forward | 5'-AACCTGGCGCTTGTCCTAAG-3' |
| | reverse | 5'-GTTGCCAGAGCACGATCCAT-3' |
| *Gad67* | forward | 5'-GGTTCGCACAGGTCACCC-3' |
| | reverse | 5'-GCCATTCACCAGCTAAACCAA-3' |
| *Ins2* | forward | 5'-GAAGTGGAGGACCCACAAGT-3' |
| | reverse | 5'-AGTGCCAAGGTCTGAAGGTC-3' |
| *Tlbp* | forward | 5'-ACATCCAAGCAGGAAGTGCAT-3' |
| | reverse | 5'-TCTGCAGTGGTCTCTTCAAACTCT-3' |

### 2.1.19 Reagents for *in vitro* BMAC stimulation

| **Reagent** | **Clone** | **Isotype** | **Vendor** |
|---|---|---|---|
| Polyinosinic-polycytidylic acid (poly I:C) | - | - | Sigma-Aldrich |
| Lipopolysaccharide (LPS) | - | - | Sigma-Aldrich |
| CpG oligodeoxynucleotide (ODN) 2395 | - | - | Invivogen |
| Anti-mouse CD40 antibody | FGK45 | Rat IgG2a, κ | Biomol |
| Anti-mouse RANK antibody | polyclonal | Goat IgG | R&D |

### 2.1.20 Immunogen and adjuvant for immunization

| **Reagent** | **Vendor** |
|---|---|
| HA peptide (SVSSFERFEIFPK) | thinkpeptides |
| Polyinosinic-polycytidylic acid (poly I:C) | Sigma-Aldrich |
| Lipopolysaccharide (LPS) | Sigma-Aldrich |

### 2.1.21 Instruments and software

| **Instrument** | **Vendor** |
|---|---|
| FACSCanto II | BD Biosciences |

| | |
|---|---|
| LSR II | BD Biosciences |
| FACSLyric | BD Biosciences |
| FACSAria II | BD Biosciences |
| LSM 710 confocal microscopy | Carl Zeiss |
| 7300 Real-Time PCR System | Applied Biosystems |
| myECL Imager | ThermoFisher |
| Gammacell 40 Exactor | Best Theratronics |

| **Software** | **Developer** |
|---|---|
| FlowJo | Tree Star |
| ImageJ | National Institutes of Health |

## 2.2 Methods

### 2.2.1 Preparation of mouse BM cells and splenocytes

After Adig or WT Balb/c mice were euthanized, femurs and tibias were dislocated and the attached muscle was removed. Bones were crushed with mortars and pestles in PBS. Cells in suspension were collected and filtered with 100-μm cell strainers. Spleens were mashed through a 100-μm cell strainer, and cells in suspension were collected. After centrifugation at 300×*g* for 5 min at 4°C, cell pellets were resuspended in 1 ml ACK buffer for 1 min (BM cells) or 2 min (splenocytes) to remove the erythrocytes. After wash with 10 ml PBS and centrifugation, cells were counted and subjected for further analyses.

### 2.2.2 Preparation of human BM and blood sample

PBMCs and BM mononuclear cells were isolated from peripheral blood and bone marrow aspirates, respectively, using gradient centrifugation with Biocoll according to manufacturer's protocol. Blood or bone marrow aspirate (40 to 45 ml) were suitably diluted and gently overlaid on top of 15 ml of Biocoll solution, and then centrifuged for 20 min at 2,000 rpm at room

temperature without forced deceleration. The interface containing mononuclear cells was carefully collected, washed with RPMI-1640 medium twice, and subjected to antibody staining for flow cytometric analysis.

### 2.2.3 Flow cytometric analysis and fluorescence-activated cell sorting

Single cell suspension (1-2×$10^6$ cells/100 µl) was incubated with anti-mouse CD16/32 antibody (Fc Block) for 15 min on ice, followed by incubation with the antibodies against surface markers for 30 min on ice. Anti-human AIRE antibody (clone 6.1)[48] was kindly provided by Prof. Pärt Peterson. After subsequent wash, cells were stained with viability dye, and all cells analyzed were gated on viable cells (viability dye-negative). Viability dyes used for excluding dead cells were 7-AAD, Yellow LIVE/DEAD Fixable Dead Cell Stain Kit, Zombie Aqua Fixable Viability Kit, and Zombie NIR Fixable Viability Kit. For intracellular staining, after viability staining, cells were fixed and permeablized using Foxp3/Transcription Factor Fixation/Permeabilization Concentrate and Diluent according to manufacturer's protocol, and then incubated with antibodies against intracellular antigens for 30 min on ice. FACSCanto II, LSR II or FACSLyric flow cytometry were used for fluorescence measurement, and FACSAria II was used for cell sorting. The analysis was performed using FlowJo software.

### 2.2.4 Immunofluorescence

After Adig or WT Balb/c mice were euthanized, thymi were dissected and embedded in Tissue-Tek and frozen at -20°C. Femurs and tibias were dislocated and the attached muscle was removed. Epiphyses of the bones were gently removed, and marrow tissue was carefully pushed out from the bones with PBS by 27-gauge needle, without disrupting the marrow tissue. The intact marrow tissue was then embedded and frozen in the same way as the thymi tissue. Cryo-sections (5 µm) of thymus and BM tissue were fixed with cold acetone for 10 min, and then blocked with 10% goat serum for 30 min at room temperature. Tissue was incubated with unconjugated primary antibodies for 1 h at room temperature. After washed with Tween-

20/PBS and PBS, tissue was incubated with goat anti-rat or goat anti-rabbit secondary antibodies. After being washed with Tween-20/PBS and PBS, tissue was incubated with anti-Aire antibody for 1 h at room temperature. Stained slides were mounted in DAPI-containing Fluoromount-G mounting medium after wash with Tween-20/PBS and PBS, and visualized by LSM 710 confocal microscopy. Merging and contrast-adjustment were applied equivalently to experimental and control groups using ImageJ software.

### 2.2.5 Isolation of mTECs and thymic B cells

The mTECs from WT, Adig or Aire-HCO mice were isolated as previously described[29]. In brief, thymi of Aire-HCO mice were digested by Collagenase IV and Dispase, and $CD45^+$ cells were depleted using CD45 magnetic microbeads. $CD45^-EpCAM^+Ly\text{-}51^-MHC\text{-}II^+$ mTECs (from pre-enriched thymic stromal cell fraction) and $CD19^+$ B cells (from $CD45^+$ cell fraction) were stained and sorted using FACSAria II.

### 2.2.6 Real-Time PCR

Aire-$GFP^+$ BM cells were isolated and sorted from Adig mice by FACS according to GFP expression, and Adig mTECs were isolated and sorted as described above. In addition, $MHC\text{-}II^+EpCAM^+TACI^+CD200^+Ly\text{-}6D^+PD\text{-}L1^+$ BM cells were sorted from WT mice. RNA from the sorted cells was extracted using RNeasy Mini Kit. After quantification, RNA was reverse transcribed using QuantiTect Reverse Transcription Kit according to manufacturer's protocol. *Aire* and *Actb* gene expression was detected by 7300 Real-Time PCR System using QuantiFast SYBR Green PCR Kit according to manufacturer's protocol. ΔΔCt values was calculated for relative expression.

### 2.2.7 Single cell end-point PCR

WT mTECs and BM cells from femurs and tibias were isolated as described above. $CD45^-EpCAM^+Ly\text{-}51^-MHC\text{-}II^+$ mTECs and $MHC\text{-}II^+EpCAM^+TACI^+CD200^+Ly\text{-}6D^+PD\text{-}L1^+$ BM

single cells were sorted by FACSAria II into arrays of 96 PCR tubes containing 6.4 µl of lysis buffer with 10 ng of tRNA. Whole transcriptome amplification was performed as previously described[90]. The quality of the amplified cDNA samples was evaluated by end-point PCR for expression of housekeeping genes (*Actb*, *B2m* and *Gapdh*). Amplified cDNA samples, which failed to show more than two of the housekeeping genes were discarded and not further analyzed. After quality control, cDNA samples from BM cells (110 single cell samples, 7 pools of 10 cells, and 8 pools of 100 cells) and mTECs (20 single cells, 4 pools of 10 cells, and 4 pools of 100 cells) were subjected to end-point PCR using MyTaq HS Red Mix. The PCR program was set as follows: 95°C, 3 min; 35 (*Aire*) or 40 (TRA genes) cycles of repetitive denaturation (95°C, 15 s), anneal (60°C, 20 s), and elongation (72°C, 20 s); 72°C, 7 min. PCR products were subjected to 2% agarose gel electrophoresis with GelRed Nucleic Acid Gel Stain and visualized by myECL Imager. Color inversion was applied equivalently to all pictures using ImageJ for better visualization.

### 2.2.8 *In vitro* TLR, CD40, and RANK stimulation

For TLR stimulation, $4\times10^6$ BM cells from Adig or WT mice were cultured on 6-well plates in RPMI-1640 with poly I:C (2.5 µg/ml), LPS (2 µg/ml) or CpG ODN (2 µM) for 20 h. For agonistic CD40 and RANK stimulation, $4\times10^6$ BM cells from Adig or WT mice were cultured on 6-well plates with 10 µg/ml anti-CD40, anti-RANK or corresponding isotype antibody for 72 h. Cells were washed and subjected to antibody staining for flow cytometric analysis.

### 2.2.9 Antigen presentation assay

Aire-expressing cells from BM (femurs and tibias) and spleens were sorted from Aire-HCO or Adig mice by FACS according to human CD2 or GFP expression, respectively, and mTECs form Aire-HCO mice were isolated and sorted according to the method described above. The sorted APC subsets were co-cultured in DMEM with $2\times10^4$ A5 T-hybridoma cells at designated

APC:TC ratio for 17 h, and $CD4^+$ A5 cells were analyzed for GFP expression as previously described[12].

### 2.2.10 *In vitro* Treg induction

CD25-depleted $CD4^+$ T cells were isolated by negative selection using MojoSort Mouse CD4 Naïve T Cell Isolation Kit from the spleens of $CD45.2^+$ 6.5 TCR-HA or $CD45.1^+$ WT Balb/c mice, pooled together at 1:1 ratio, and labeled with 5 μM CFSE for 5 min at room temperature[91]. Aire-$GFP^+$ cells or Aire-human $CD2^+$ cells from BM (femurs and tibias) were sorted from Adig or Aire-HCO mice, respectively. Sorted APCs ($2\times10^4$) were co-cultured in RPMI-1640 with $2\times10^4$ pooled naïve $CD4^+$ T cells for 5 days, and $CD45.2^+$ HA-specific $CD4^+$ T cells and $CD45.1^+$ polyclonal $CD4^+$ T cells were analyzed by flow cytometry.

### 2.2.11 Gene expression array

To compare the function of BMACs and plasma cells, Aire-$GFP^+$ cells and $CD138^+IgM^+$ plasma cells were isolated and sorted from femurs and tibias of Adig mice by FACS. RNA of sorted cells was isolated and amplified using μMACS SuperAmp Kit followed by Klenow labeling with random octamer according to manufacturer's protocol, and subjected to MouseRef-8 v2.0 Expression BeadChip. The corresponding chip annotation file was obtained from Illumina website. Raw data were processed with R using limma package. First, normalization was performed locally and globally. Using normexp background correction method, spots within each sample were corrected by local background. A subsequent quantile normalization was performed for global normalization across all samples. Second, preprocessing was applied based on whether a gene is expressed in the cohort. Based on the spot detection *p*-value returned from detectionPValues function, genes not expressed in any sample ($p$-value < 0.05) were excluded from further analysis. Lastly, differential expression analysis was performed. Expression of each gene was fitted with a linear model using lmFit function, then eBayes function applied empirical Bayes method to stabilize standard deviations

between genes. Benjamini, Hochberg multiple correction method was used to correct differential expression *p*-values. The significantly differentially expressed genes were then subject to functional enrichment analysis with R package EGSEA.

### 2.2.12 BM chimera

For the generation of reciprocal BM chimeras, CD45.1$^+$ WT congenic Balb/c or CD45.2$^+$ Adig recipient mice were irradiated twice in Gammacell 40 Exactor at 450 rad with an interval of 3h, and i.v. injected with $1\times10^7$ BM mononuclear cells from CD45.2$^+$ Adig or CD45.1$^+$ WT congenic Balb/c mice, respectively. After at least 8 weeks of reconstitution of hematopoietic system, recipient mice were euthanized, and BM mononuclear cells from femurs and tibias were isolated. The chimerism was confirmed using CD45 congenic marker expression by flow cytometric analysis, showing that more than 98.9% of CD45$^+$ cells had the congenic CD45 phenotype of the donor mice. For the preparation of recipient mice with HA-expressing hematopoietic cells, CD45.1$^+$CD45.2$^+$ WT Balb/c mice were irradiated twice at 450 rad with an interval of 3h, and intravenously injected with $1\times10^7$ BM mononuclear cells from CD45.1$^+$CD45.2$^+$ Aire-HCO or CD45.1$^+$CD45.2$^+$ WT Balb/c mice. Further manipulations were performed at least 8 weeks after the BM transplantation.

### 2.2.13 Adoptive T cell transfer

CD25-depleted CD4$^+$ T cells were isolated by negative selection using MojoSort Mouse CD4 Naïve T Cell Isolation Kit from the spleens of CD45.2$^+$ 6.5 TCR-HA or CD45.1$^+$ WT Balb/c mice, pooled together at 1:1 ratio, and labeled with 5 μM CFSE for 5 min at room temperature[91]. The labeled cells ($1\times10^7$ per recipient mouse) were i.v. injected into CD45.1$^+$CD45.2$^+$ host mice, which were reconstituted with Aire-HCO or WT BM cells at least 8 weeks before the transfer of naïve CD4$^+$ T cells. On day 3 and day 14 post transfer, BM cells from femurs and tibias and splenocytes were isolated and analyzed by flow cytometry.

### 2.2.14 *In vivo* cytotoxicity

$CD45.1^+CD45.2^+$ 6.5 TCR-HA mice were immunized twice (2-week interval) with 100 µg HA-peptide (SVSSFERFEIFPK) with 10 µg LPS and 10 µg poly I:C via intraperitoneal (i.p.) injection. One week after the second immunization, effector T cells were isolated from the spleens, femurs and tibias of the immunized mice using EasySep Mouse Memory $CD4^+$ T Cell Isolation Kit. Recipient mice (previously reconstituted with WT or Aire-HCO BM, and transferred with naïve HA-specific $CD4^+$ T cells, as described above) received $3\times10^6$ effector T cells via i.v. injection at 14 days post naïve T cell transfer. One day later, BM cells and splenocytes isolated from $CD45.1^+$ WT Balb/c mice were pooled together at 1:1 ratio and labeled with 5 or 0.5 µM of CFSE for 5 min at room temperature. The $CFSE^{high}$ cells were pulsed with 20 µM (31.5 µg) HA-peptide for 2 h at 37°C, and the $CFSE^{low}$ cells were incubated without peptide. After 2 washes with PBS, the peptide-loaded $CFSE^{high}$ and unloaded $CFSE^{low}$ target cells were mixed at 1:1 ratio and transferred into the recipient mice ($5\times10^5$ cells/mouse). Eighteen hours later, recipient mice were sacrificed, and BM cells from femurs and tibias and splenocytes were isolated for flow cytometric analysis. $CD45.1^+CD45.2^-B220^+$ cells were gated for analyzing the percentages of $CFSE^{high}$ and $CFSE^{low}$ target cells. Cytotoxicity was calculated as follows:

$$\% \text{ specific cytotoxicity} = 100\% \times (1-(CFSE^{low} / CFSE^{high})_{control} / (CFSE^{low} / CFSE^{high})_{experimental}).$$

### 2.2.15 Statistics

Except for gene expression array analyses, statistical significance was assessed using two-tailed Student's *t* test with unequal variance. Data were shown in mean ± SEM.

# 3. Results

## 3.1 Lineage mapping of bone marrow Aire-expressing cells (BMACs)

### 3.1.1 Phenotypic analyses of BMACs reveal plasma cell characteristics

As described in the preliminary data, our group identified a novel Aire-expressing cell subset in the bone marrow (BM) by harnessing Adig transgenic mice, in which the GFP reporter protein is driven by Aire promoter[64]. These BM Aire-expressing cells (henceforth termed BMACs) were MHC-II$^+$, ectopically expressed a diverse repertoire of tissue-restricted antigens (TRAs), and showed a potential capacity to present these TRAs to CD4$^+$ T cells. Surface marker screening of BMACs using BD Lyoplate Screening Panel in the preliminary data has revealed that they expressed epithelial cell adhesion molecule (EpCAM) and CD45, showing mixed features of both epithelial cells and hematopoietic cells, respectively. To validate these findings, I used individual antibodies to detect EpCAM, CD45, and MHC-II on BMACs from Adig mice by flow cytometric analysis. In addition, as BMACs are potential antigen presenting cells (APCs), surface markers for B cell lineage (CD19, B220 and CD138) and myeloid APCs (CD11b and CD11c) were also included to elucidate the cell type of BMACs. In agreement with the preliminary data, the EpCAM$^+$CD45$^+$MHC-II$^+$ phenotype of BMACs was further validated (**Figure 1A** and **1B**). The majority of Aire-GFP$^+$ cells did not express CD11b and CD11c, suggesting the major population of BMACs is not derived from myeloid lineage. Approximately half of BMACs showed low level of CD19 expression, which is reminiscent of the phenotype of plasma cells. In line with this plasma cell feature, BMACs express CD138, while no expression of B220 was detected (**Figure 1B**), resembling the CD138$^+$B220$^-$ plasma cell phenotype. Importantly, as shown in **Figure 1C**, BMACs also expressed B lymphocyte-induced maturation protein (Blimp-1), the master transcription factor of plasma cells that controls their differentiation and suppress transcriptional activities of mature B cells[92, 93]. These

data demonstrated that BMACs displayed characteristics of plasma cells ($CD19^{low}B220^{-}CD138^{+}Blimp\text{-}1^{+}$), albeit expressing EpCAM.

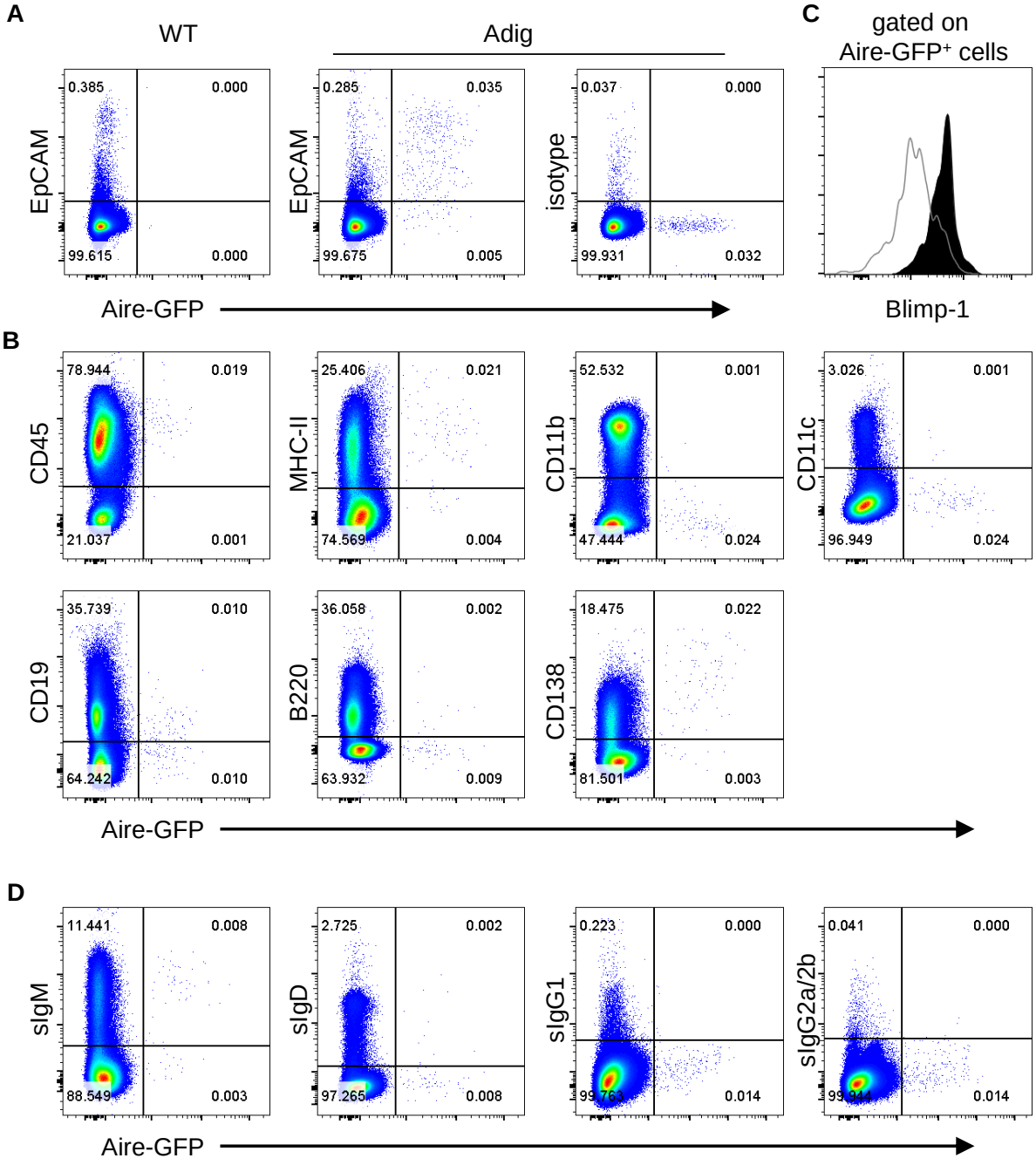


**Figure 1. Phenotypical analysis of BMACs revealed plasma cell features. (A)** EpCAM surface expression on total BM cells of WT and Adig mice. Representative data are shown (n = 6). **(%TB)** Lineage surface marker expression on total BM cell of Adig mice. Representative data are shown (n = 4). **(C)** Intracellular Blimp-1 staining on Aire-GFP$^{+}$ BM cells. Unshaded grey curve indicates isotype control. Representative data are shown (n = 3). **(D)** Surface immunoglobulin (Ig) isotype expression on total BM cells of Adig mice. Representative data are shown (n = 3).

In the classical B cell terminal differentiation, most of activated follicular B cells undergo immunoglobulin (Ig) class-switch recombination, rearranging the loci of constant region of Ig from IgM/IgD to other isotypes, before they further differentiate into plasma cells[92]. Interestingly, BMACs expressed surface IgM (sIgM), but not sIgD, sIgG1, sIgG2a and sIgG2b (**Figure 1D**), reminiscent of recently identified cytokine-secreting regulatory plasma cells that express membrane-bound IgM and MHC-II[94, 95]. These findings showed that BMACs manifested features of a subset of plasma cells which do not undergo class-switch and express IgM on cellular membrane.

### 3.1.2 Reciprocal BM chimera show that BMACs are transferable and irradiation-resistant

In order to further confirm the hematopoietic origin of BMACs, I performed reciprocal BM chimeras, in which the BM cells from Adig mice were transplanted via intravenous injection into lethally irradiated recipient WT mice (Adig →WT), and WT BM cells into lethally irradiated Adig mice (WT → Adig), as depicted in **Figure 2**. BM chimera is a well-established method to confirm if a cell population of interest is derived from hematopoietic system. The hematopoietic stem cells of the recipient mice are abolished by lethal irradiation, and reconstituted by the donor BM cells, thus creating a new hematopoietic system with the genetic and phenotypic features of the BM donor mice. The Adig and WT mice had different congenic CD45 markers (CD45.2 for Adig mice and CD45.1 for WT mice), and in this way, the efficiency of chimerism could be assessed.

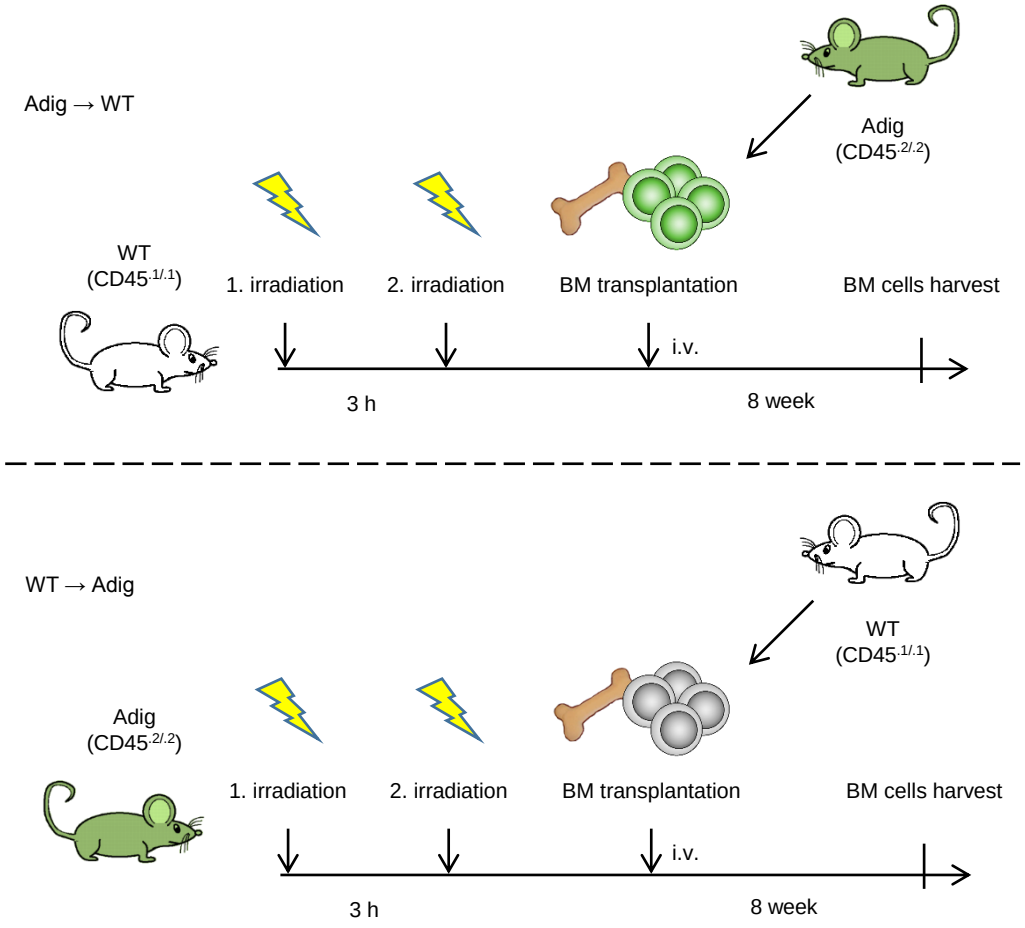


**Figure 2. BM chimera experimental scheme.** WT or Adig recipient mice were irradiated (4.5 Gy) twice with a 3-hour interval, and transplanted intravenously (i.v.) with BM cells from Adig or WT donor mice, respectively. BM cells were analyzed 8 weeks after transplantation.

After 8 weeks of reconstitution, the remaining hematopoietic cells from the recipient mice constituted less than 1% of total BM cells in both groups (**Figure 3A**), showing a successful replacement of the hematopoietic system. In WT recipient mice receiving Adig BM cells (Adig → WT), Aire-GFP$^+$ cells were detected, indicating that BMACs are derived from hematopoietic stem cells, instead of stromal cells which cannot migrate from the circulation to the BM (**Figure 3B** and **3C**). Intriguingly, Aire-GFP$^+$ cells were also observed in Adig recipient mice receiving WT BM cells (WT → Adig), suggesting that BMACs are resistant to irradiation, which falls in line with the terminal differentiation characteristics of plasma cells[96]. Of note, although the frequencies of MHC-II$^+$ BMACs in these two groups were comparable, the expression levels

of MHC-II were different (**Figure 3D** and **3E**). The frequency of MHC-II$^{hi}$ Aire-GFP$^{+}$ cells in Adig → WT group was significantly higher than in WT → Adig group, while BMACs in WT → Adig group expressed intermediate levels of MHC-II.

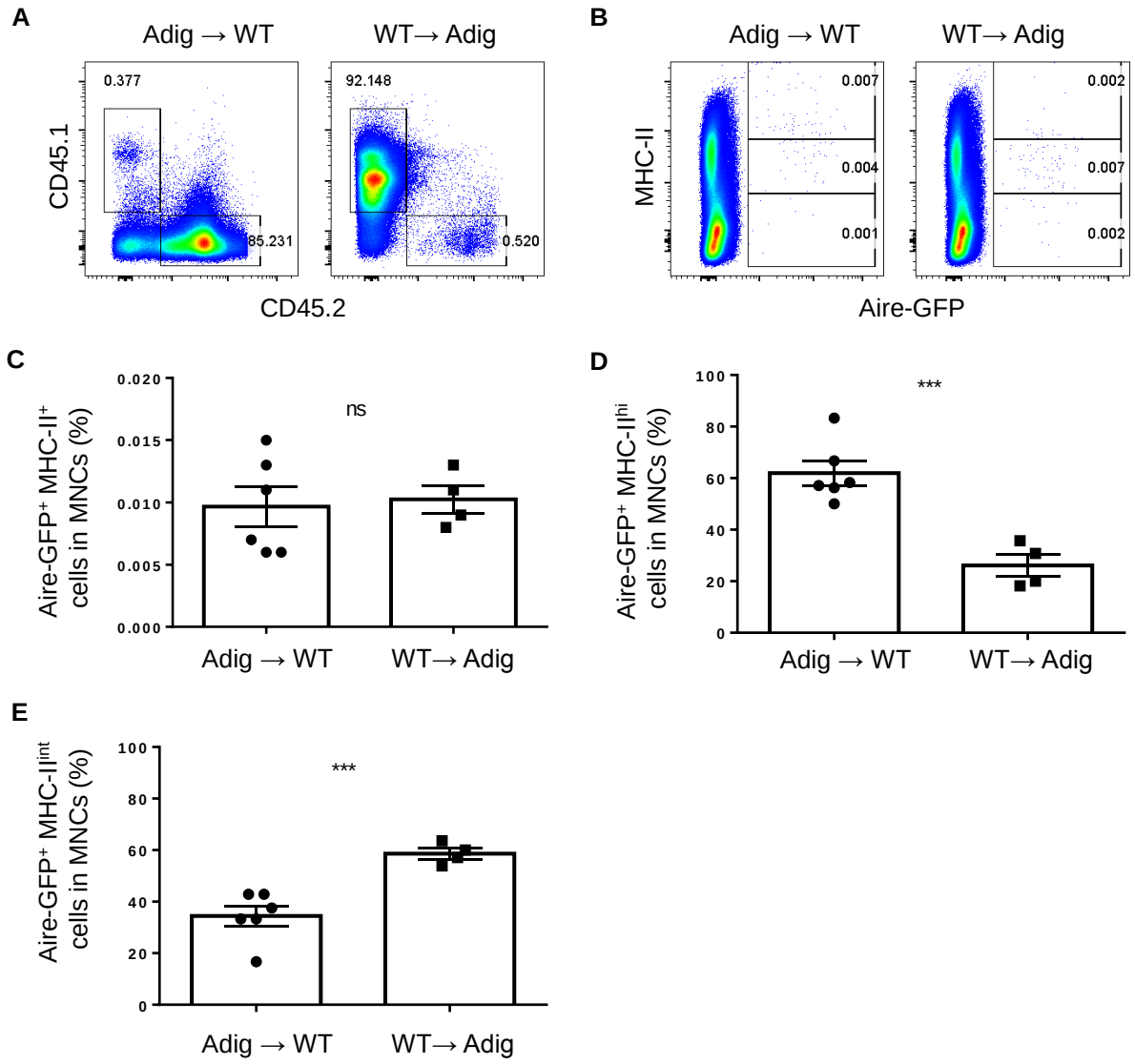


**Figure 3. Reciprocal BM chimera demonstrated that BMACs are transferable and irradiation-resistant. (A)** Analysis of CD45 congenic marker on total BM cells of reciprocal BM chimera mice. Representative data are shown. **(B and C)** Frequencies of Aire-GFP$^{+}$ cells among total BM mononuclear cells of reciprocal BM chimera mice (Adig→WT, n = 6, and WT→Adig, n = 4). Representative data are shown in **B**. **(D and E)** Frequencies of Aire-GFP$^{+}$MHC-II$^{hi}$ or Aire-GFP$^{+}$MHC-II$^{int}$ cells among total BM mononuclear cells of reciprocal BM chimera mice. MNCs, mononuclear cells. ***, $P < 0.001$; ns, $P > 0.05$ (Student's *t*-test). Error bars indicate SEM.

It merits further investigation to determine whether irradiation induces downregulation of MHC-II expression, or BMACs comprise (at least) two cell subsets, which express different levels of MHC-II and have different sensitivities to irradiation. In conclusion, these data demonstrated that BMACs are transferrable hematopoietic cells and irradiation-resistant, which is consistent with the features of plasma cells.

### 3.1.3 BMACs substantially diminish in the absence of B cells

In order to confirm that BMACs are plasma cells that derived from B cell lineage, I crossed Adig mice with *RAG2*-deficient mice, in which T-cell and B-cell development is blocked and no mature T cells and B cells are present[97]. As shown in **Figure 4A** and **4B**, BMACs diminished significantly in the BM of *RAG2*-deficient Adig mice compared to *RAG2*-proficient ones, supporting the notion of BMACs' plasma cell identity. It is noteworthy that a residual population of Aire-GFP$^+$ cells was still detectable in a fraction of the *RAG2*-deficient Adig mice. Interestingly, these residual Aire-GFP$^+$ cells expressed high level of MHC-II (**Figure 4A**), and only the frequencies of MHC-II$^{int}$ Aire-GFP$^+$ cells were significantly lower in *RAG2*-deficient Adig mice, while no significant difference of MHC-II$^{hi}$ Aire-GFP$^+$ cells frequencies was observed between these two groups (**Figure 4C** and **4D**).

Further investigation on the surface markers expressed by MHC-II$^{hi}$ and MHC-II$^{int}$ Aire-GFP$^+$ cells in *RAG2*-deficient and *RAG2*-proficient Adig mice revealed that, MHC-II$^{int}$ Aire-GFP$^+$ cells were EpCAM$^{hi}$CD11b$^-$CD11c$^-$CD19$^{low}$CD138$^+$IgM$^+$. They were the major population of BMACs, and were absent in *RAG2*-deficient Adig mice (**Figure 5**), showing the characteristics of plasma cells. In contrast, MHC-II$^{hi}$ Aire-GFP$^+$ cells were still detectable in *RAG2*-deficient Adig mice, and showed EpCAM$^{int}$CD19$^-$CD138$^-$IgM$^-$ phenotype, with negative to low expression levels of CD11b and CD11c. MHC-II$^{hi}$ Aire-GFP$^+$ cells are a relatively minor

fraction, which composes less than one third of total BMACs. These data fall in line with the BM chimera results, and demonstrate that the major population of BMACs show plasma cell markers and is *RAG2*-dependent, while a minor fraction of BMACs is *RAG2*-independent. In this study, we further focused on the major population of BMACs.

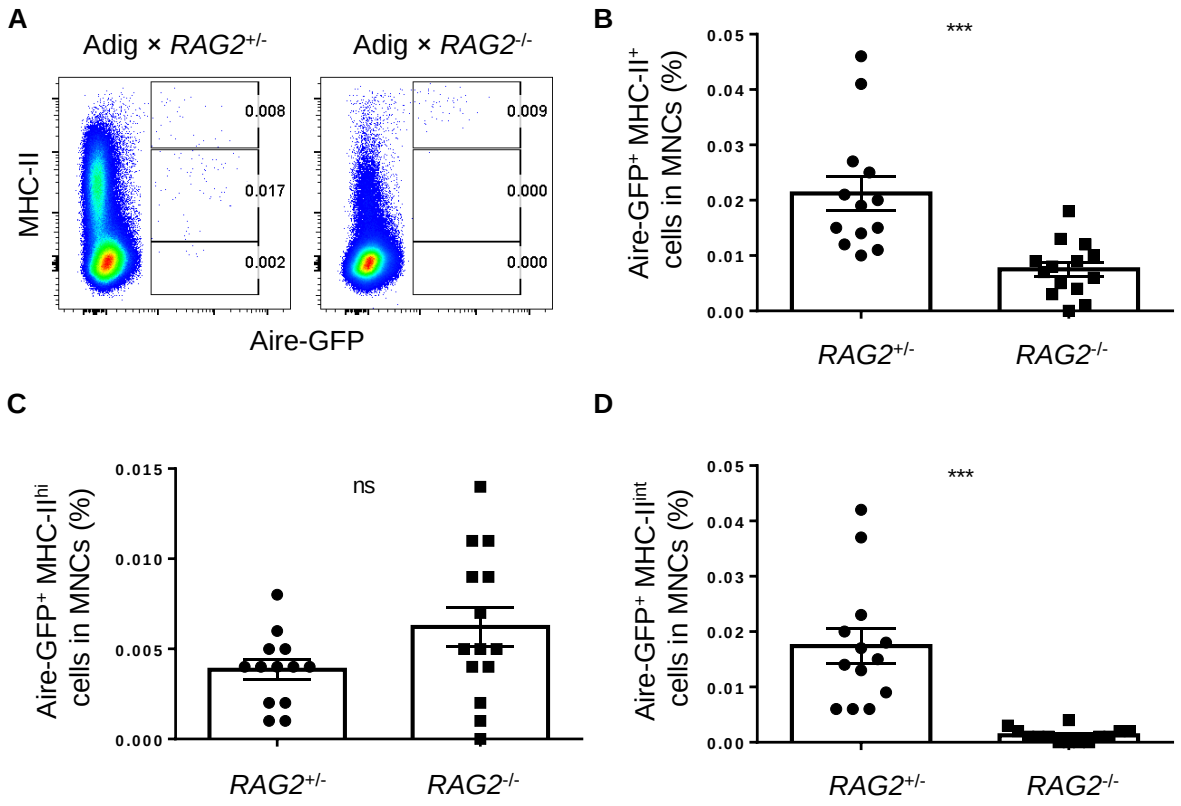


**Figure 4. BMACs substantially diminished in RAG2-deficient mice. (A and B)** Frequencies of Aire-GFP$^{+}$ cells among total BM mononuclear cells of RAG2$^{+/-}$ (n = 13) and RAG2$^{-/-}$ (n = 14) Adig mice. Representative data are shown in **A**. **(C and D)** Frequencies of Aire-GFP$^{+}$MHC-II$^{hi}$ or Aire-GFP$^{+}$MHC-II$^{int}$ cells among total BM mononuclear cells of RAG2$^{+/-}$ and RAG2$^{-/-}$ Adig mice. MNCs, mononuclear cells. ***, $P < 0.001$; ns, $P > 0.05$ (Student's *t*-test). Error bars indicate SEM.

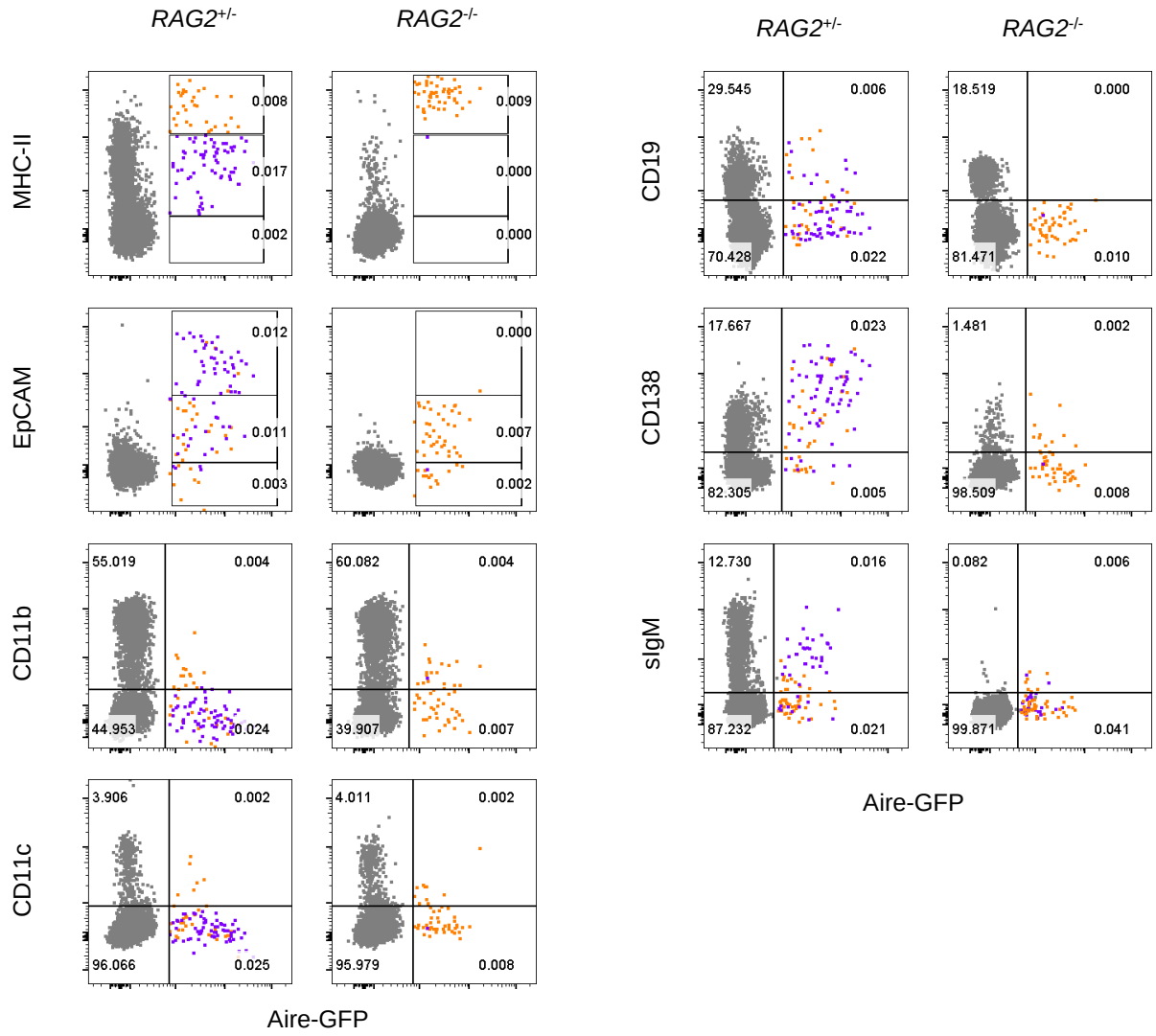


**Figure 5. The majority of BMACs expressed plasma cell markers and diminished in RAG2-deficient mice.** Surface marker expression of Aire-GFP$^{+}$MHC-II$^{hi}$ (orange) or Aire-GFP$^{+}$MHC-II$^{int}$ (purple) cells among total BM mononuclear cells of RAG2$^{+/-}$ and RAG2$^{-/-}$ Adig mice. Representative data are shown.

### 3.1.4 BMACs are derived from B cell lineage

There are two potential explanations which might account for the significant reduction of BMACs in *RAG2*-deficient mice. The first scenario is that BMACs belong to one of the cell types whose development directly depends on *RAG2*, namely T cells and B cells. The other possibility is that Aire-expression in BMACs requires the presence of T cells or B cells,

meaning the reduction of BMACs in *RAG2*-deficient mice is an indirect effect of the absence of T cells or B cells. To unravel if the impact of *RAG2*-deficiency on the frequency of BMACs is direct or indirect, I replenished the hematopoietic system of Adig$^{+}$×*RAG2*$^{-/-}$ mice with BM cells from Adig$^{-}$×*RAG2*$^{+/-}$ mice by performing BM chimera in which donor BM cells from Adig$^{+}$×*RAG2*$^{-/-}$ mice were mixed 1:1 with Adig$^{-}$×*RAG2*$^{+/-}$ BM cells (**Figure 6**), so that WT T cells and B cells were present in Adig$^{+}$×*RAG2*$^{-/-}$ mice after the reconstitution.

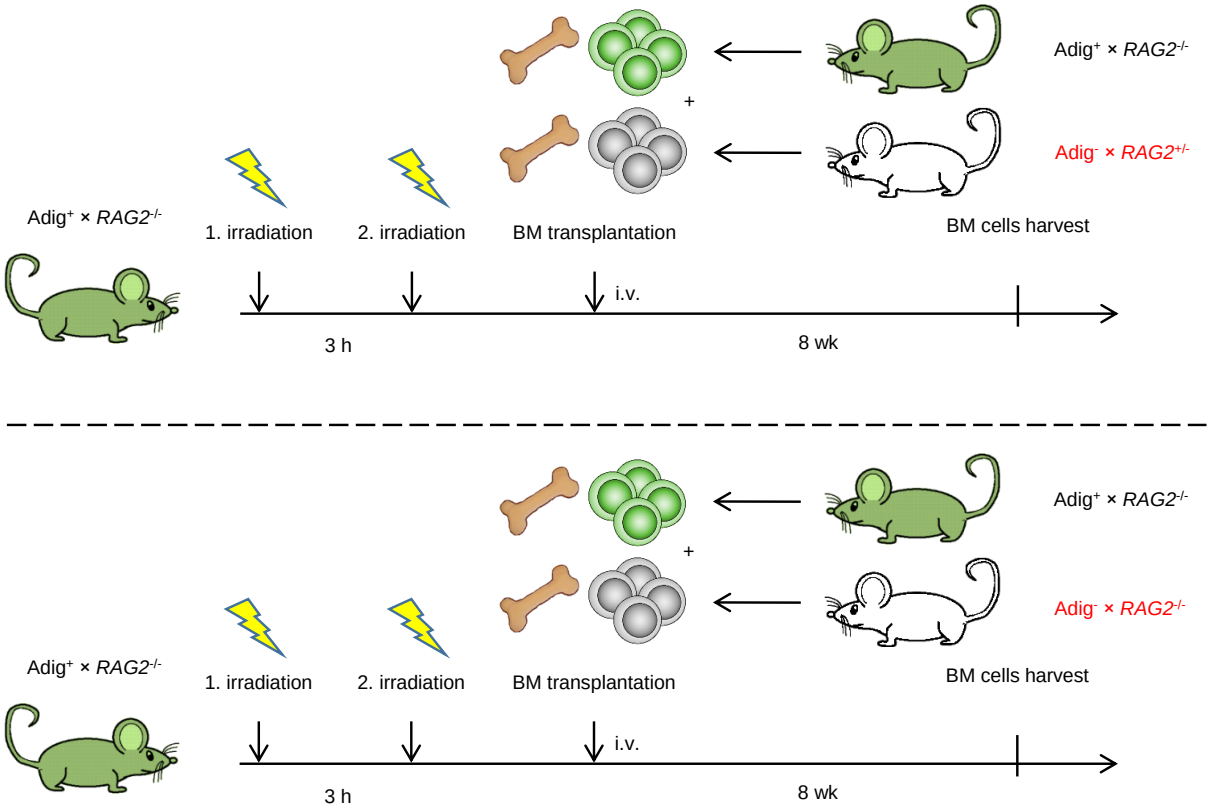


**Figure 6. Experimental scheme of replenishment of RAG2-proficient cells.** Adig$^{+}$ × *RAG2*$^{-/-}$ recipient mice were irradiated (4.5 Gy) twice with a 3-hour interval, and transplanted i.v. with Adig$^{+}$ × *RAG2*$^{-/-}$ donor BM cells mixed with Adig$^{-}$ × *RAG2*$^{+/-}$ or Adig$^{-}$ × *RAG2*$^{-/-}$ donor BM cells. After reconstitution for 8 weeks, mice were sacrificed for analysis of BM cells.

As shown in **Figure 7A** and **7B**, the replenishment of T cells and B cells did not rescue the reduction of Aire-GFP$^{+}$ cells in Adig$^{+}$×*RAG2*$^{-/-}$ mice, as the percentages of Aire-GFP$^{+}$ cells in

the mice which received Adig$^{-}$×*RAG2*$^{+/-}$ donor BM cells (**Figure 7A**, where T cells and B cells were present) were comparable to those in the mice receiving Adig$^{-}$×*RAG2*$^{-/-}$ BM cells (**Figure 7B**, where T cells and B cells were absent). In mice receiving Adig$^{+}$×*RAG2*$^{+/-}$ BM cells (**Figure 7C**), the frequency of Aire-GFP$^{+}$ cells was substantially higher than in mice receiving Adig$^{+}$×*RAG2*$^{-/-}$ BM cells (**Figure 7A** and **7B**), regardless of whether T cells and B cells were present (from Adig$^{-}$×*RAG2*$^{+/-}$ BM cells, **Figure 7A**) or not **(Figure 7B**). These data demonstrated that the impact of *RAG2*-deficiency on the reduction of BMACs is cell intrinsic (that is, BMACs themselves require *RAG2*), and thus indicated that BMACs are derived from T cells or B cells. Neither T cell receptor nor CD3 was detectable on BMACs (preliminary data), suggesting that BMACs are not derived from T cell lineage. Taken together, these data indicate that BMACs largely consist of CD19$^{low}$B220$^{-}$CD138$^{+}$Blimp-1$^{+}$MHC-II$^{+}$IgM$^{+}$ plasma cells, which are irradiation-resistant and *RAG2*-dependent.

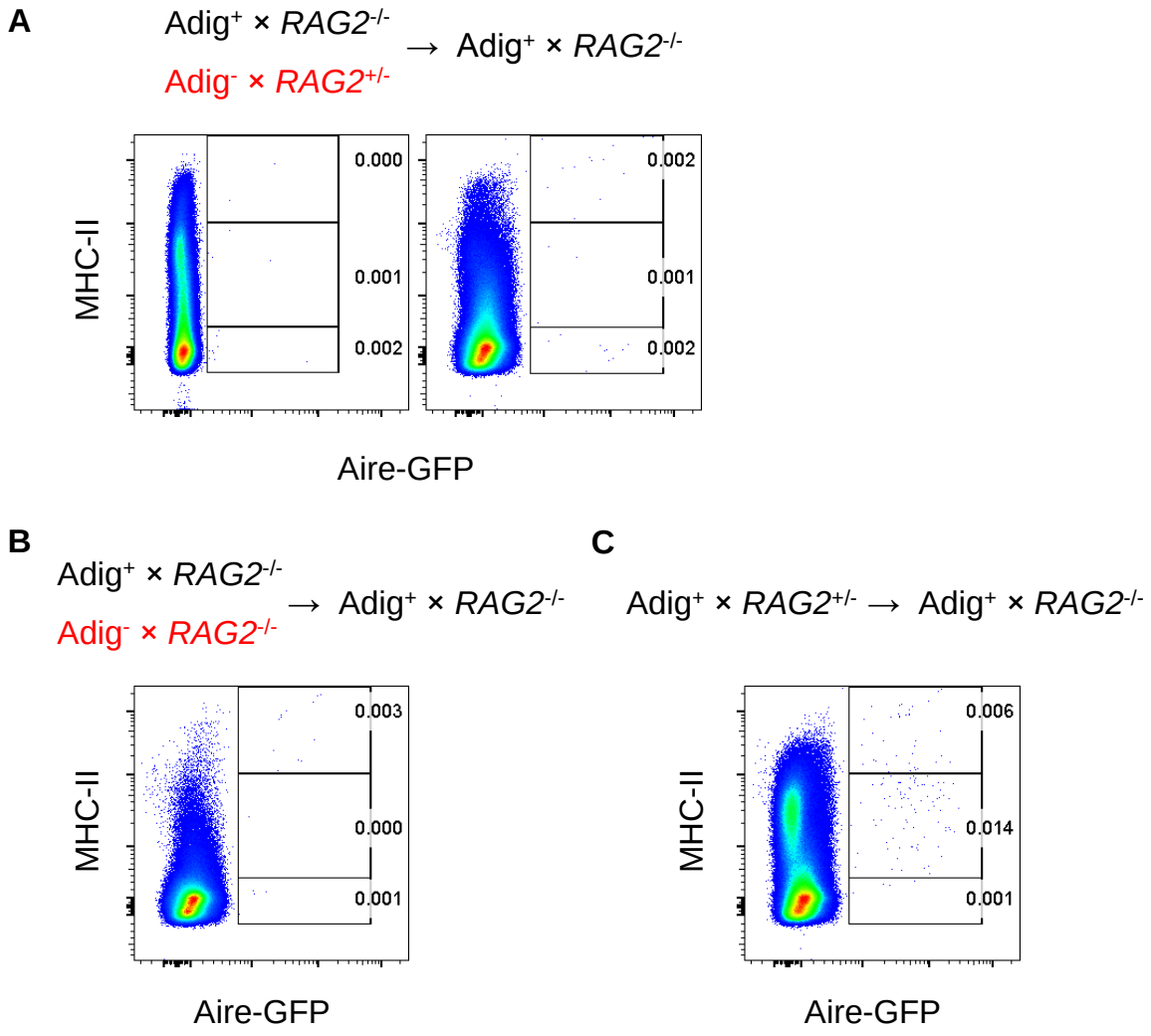


**Figure 7. BMACs were derived from B cell lineage.** Frequencies of Aire-GFP$^+$ cells among total BM cells in BM chimera mice with or without replenishment of *RAG2*-proficient BM cells. Representative data are shown (n = 3).

## 3.2 Cell-extrinsic signals induce Aire expression in BMACs

### 3.2.1 Toll-like receptor (TLR) agonists induce Aire expression in BMACs

Promiscuous gene expression (pGE) in the periphery contributes to the maintenance of local T cell tolerance. However, the mechanisms underlying the induction of TRAs and Aire in peripheral APCs remain unknown. In mTECs, Aire expression is activated by Nuclear Factor-κB (NF-κB)[30, 43, 44]. TLR stimulation is one of the potential factors which activate NF-κB and

regulate the ectopic expression of TRAs and Aire. Fletcher and colleagues demonstrated that stimulation with polyinosinic-polycytidylic acid (polyI:C), a TLR3 agonist, increases *Aire* and TRA expression in $CD31^{-}gp38^{-}$ stromal cells, albeit the capacity of fibroblastic reticulum cells (FRCs) to express TRAs reduces. This finding indicates that different subsets of ectopic TRA-expressing cells respond differently to inflammatory signaling such as TLR stimulation in terms of Aire and TRA expression. In order to evaluate whether BMACs upregulate Aire expression upon TLR stimulation, total BM cells from Adig mice were isolated and incubated *in vitro* with polyI:C, lipopolysaccharide (LPS) and CpG oligodeoxynucleotide (CpG ODN), which are the agonists of TLR3, TLR4 and TLR9, respectively. Signal transduction of TLR is MyD88-dependent, while TLR3 signaling is governed by TRIF[98]. Both MyD88 and TRIF are involved in TLR4 signaling[98]. The pathways downstream both MyD88 and TRIF leads to NF-κB signaling. As shown in **Figure 8**, frequencies of Aire-$GFP^{+}$ cells substantially increased after polyI:C and LPS treatment, compared to untreated (4.9-fold and 8.6-fold, respectively), whereas stimulation with CpG ODN resulted in a modest increase of Aire-$GFP^{+}$ cells (1.7-fold). Interestingly, the expression levels of MHC-II and EpCAM varied in between the groups treated with different TLR agonists. While the majority of polyI:C-induced Aire-$GFP^{+}$ cells express both MHC-II and EpCAM, only 50% of LPS-induced Aire-$GFP^{+}$ cells showed MHC-II expression, and none of LPS-induced Aire-$GFP^{+}$ cells expressed EpCAM. The expression level of MHC-II was higher in polyI:C-induced Aire-$GFP^{+}$ cells compared to LPS-induced ones. These data indicate that stimulation of TLR3 and TLR4 signaling pathways can lead to strong upregulation of Aire expression. The different phenotypes of the newly induced Aire-expressing cells suggest that distinct mechanisms may govern Aire expression in response to different extrinsic signals.

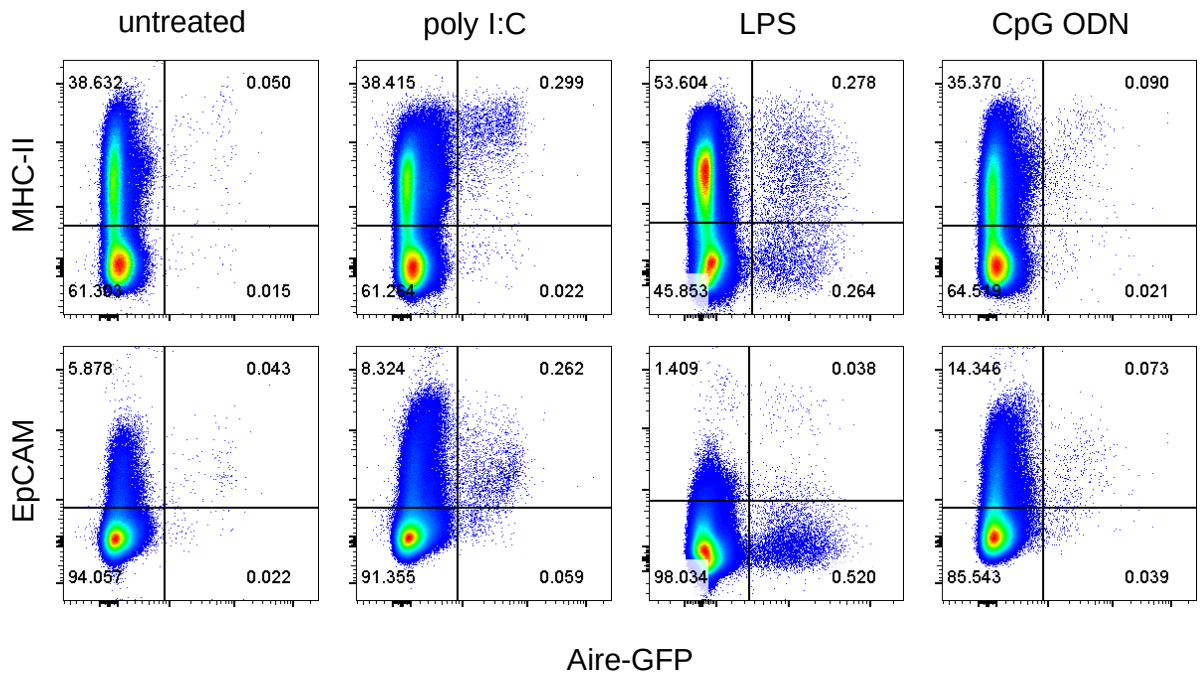


**Figure 8. Toll-like receptor (TLR) agonists induced Aire expression in BMACs.** Flow cytometric analysis of MHC-II and EpCAM expression on Aire-GFP$^{+}$ cells in BM of Adig mice after *in vitro* stimulation with poly I:C (2.5 μg/ml), LPS (2 μg/ml) or CpG ODN (2 μM) for 20 h. Representative data are shown (n = 3).

### 3.2.2 Aire expression in BMACs is substantially induced by CD40, but not RANK signaling

In the thymus, the extrinsic signals that induce Aire expression in mTECs and thymic B cells are well-studied. RANK signaling provided by CD4$^{+}$CD3$^{-}$ thymic inducer cells promotes the maturation of mTECs from CD80$^{-}$MHCII$^{lo}$Aire$^{-}$ progenitors to a CD80$^{+}$MHCII$^{hi}$ mature state[99], leading to Aire expression. On the contrary, RANK signaling does not induce Aire expression of thymic B cells. Instead, they require CD40 signals from the thymocytes that express CD40L and subsequently upregulate expression of Aire, MHC-II, and TRAs[9, 10]. In order to examine whether these signals can induce Aire expression in BMACs, agonistic anti-RANK and anti-CD40 antibodies were used to stimulate Adig BM cells *in vitro*. As depicted in **Figure 9**, RANK stimulation showed modest effect in Aire-GFP induction (1.8-fold compared to isotype

antibody control). Strikingly, CD40 signal robustly induced Aire-GFP expression (179.5-fold compared to isotype antibody control), leading to a substantial Aire-GFP$^{+}$ fraction (more than 34%) of stimulated BM cells. These data indicate that the mechanism underlying Aire expression in BMACs is similar to thymic B cells, not to mTECs, reflecting the findings that BMACs are derived from B cell lineage. Of note, the Aire-GFP$^{+}$ cells induced by CD40 signal were CD19$^{+}$CD138$^{-}$, and showed high level of MHC-II expression, suggesting the newly induced Aire-expressing cells are at earlier stage of B cell development than that of BMACs (CD19$^{low}$CD138$^{+}$) under physiological condition. It merits further investigation to determine the role of CD40 in Aire induction in BM *in vivo*.

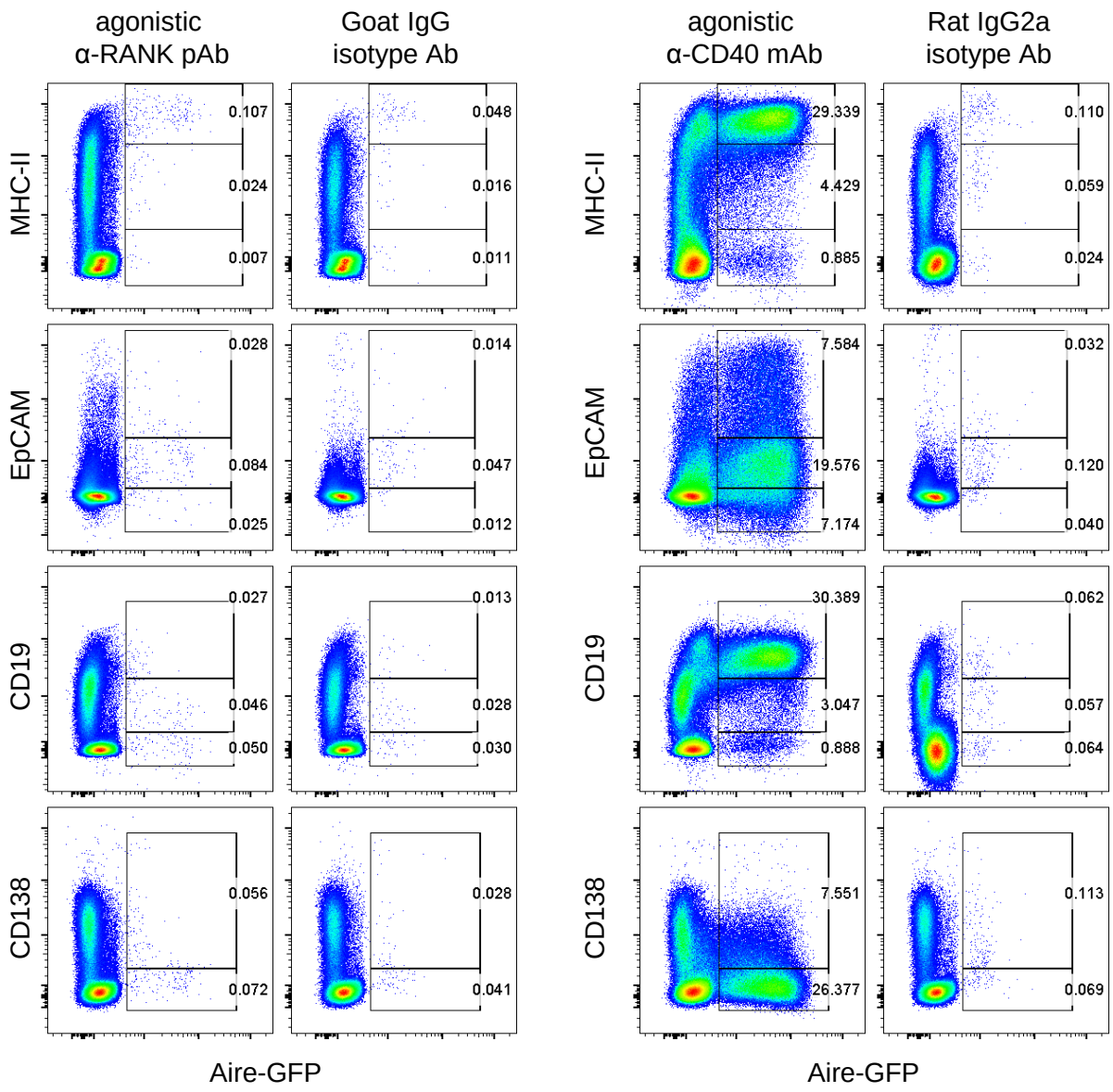


**Figure 9. Aire expression in BMACs was substantially induced by CD40.** Flow cytometric analysis of surface marker expression on Aire-GFP$^+$ cells in BM of Adig mice after *in vitro* stimulation with agonistic 10 µg/ml anti-RANK or anti-CD40 antibodies for 72 h. Representative data are shown (n = 3).

## 3.3 Identifying surrogate BMAC surface markers for precise isolation from WT mouse and human

### 3.3.1 Validation of surrogate BMAC markers by Adig reporter system

In the preliminary data, gene expression microarray analyses revealed that BMACs in Adig mice express a highly diverse repertoire of TRAs that comprise 721 genes representing more than 25 types of peripheral tissue. It is unknown if TRAs are also expressed by BMACs of WT mice. In addition, the AIRE-expressing cells were also identified in human BM through intracellular AIRE staining and flow cytometric analysis. It is still unclear whether human BMACs are also able to express TRAs ectopically, and if yes, whether the diversity of the TRAs expressed by human BMACs covers the same scope of tissue types as their murine counterparts. In order to address these questions, human BMACs have to be sorted and subjected to transcriptome analysis without fixation and permeabilization for intracellular AIRE staining, as this experimental procedure damages RNA quality. To identify BMACs without intracellular Aire staining, I first exploited Adig mice for surface markers that are expressed on BMACs and can best distinguish them from other BM cell subsets. The following surface markers were identified on BMACs, but largely not expressed by non-Aire-expressing BM cells: EpCAM, MHC-II, Ly-6D, CD200, TACI and PD-L1 (**Figure 1A**, **1B** and **10A**). Gating on BM cells of Adig mice using these surface markers (henceforth termed BMAC surrogate markers) revealed a large overlap (higher than 96%) with Aire-GFP$^+$ cells (**Figure 10B**), thus allowing sorting BMACs with high purity for gene expression analysis without abrogating RNA quality. Of note, in terms of absolute cell numbers, the gating strategy using BMAC surrogate markers covered 35% of Aire-GFP$^+$ cells (149 out of 420 cells). Although this gating strategy did not cover the majority of BMACs, since the aim is to sort BMACs with high purity, these identified surrogate markers were used to isolate BMACs from WT mice, and further on to identify BMACs in human BM aspirate.

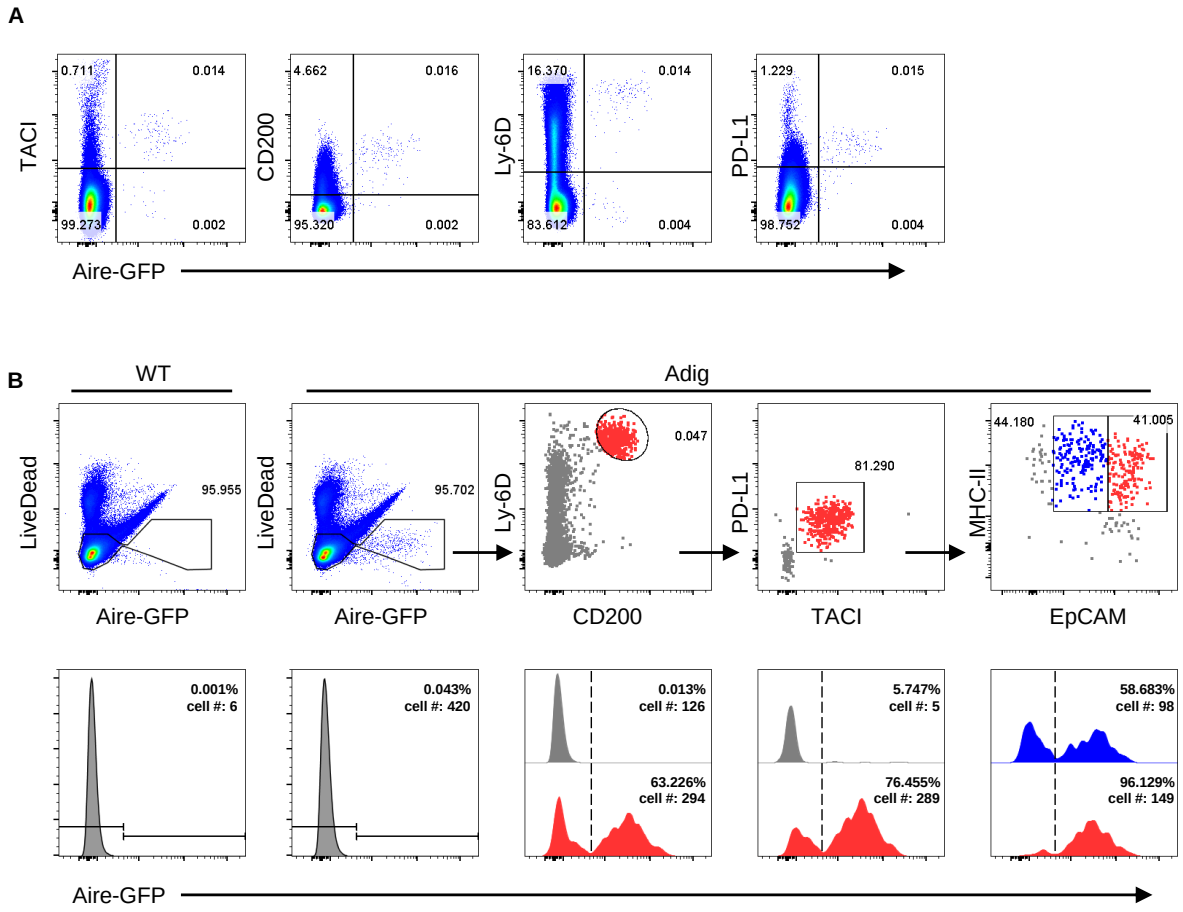


**Figure 10. Identifying BMACs using surface marker expression in the absence of Aire-GFP reporter. (A)** Surface markers expressed by BMACs of Adig mice. Frequencies of each quadrant among total BM cells are depicted in percentage. Representative data are shown (n= 4). **(B)** Gating strategy using the surrogate BMAC markers (Ly-6D, CD200, PD-L1, TACI, MHC-II and EpCAM) and percentages of Aire-GFP$^{+}$ cells. Numbers indicate percentages of gated populations. Representative data are shown (n = 3).

### 3.3.2 *Aire* and TRA expression in WT BMACs gated by surrogate BMAC markers

To confirm the validity of representation of BMACs by surrogate surface markers in WT mice, I sorted WT BM cells according to the expression of BMAC surrogate markers (gated as shown in the upper panels of **Figure 10B**), and isolated RNA from sorted cells for *Aire* transcript detection. Real-Time PCR confirmed *Aire* expression in the sorted WT BMACs (**Figure 11A**).

Next, I conducted single cell sorting of WT BMACs and assessed the expression of *Aire* and TRA genes by single cell end-point PCR. *Aire* transcript was detected in single BMACs, whereas no samples of single or bulk-sorted total BM cells showed detectable *Aire* expression (**Figure 11B**). Both Aire-dependent (*Ins2*, *Csna* and *Csng*) and Aire-independent TRAs (*Csnb*, *Gad67*, *Tlbp*, *Expi* and *Crp*)[88] were detected in single or pooled BMACs, but not in bulk-sorted total BM cells (**Figure 11C**), although largely at lower expression levels than in mTECs. These data demonstrate that BMACs ectopically express a repertoire of TRAs in WT mice, which include both Aire-dependent and Aire-independent genes.

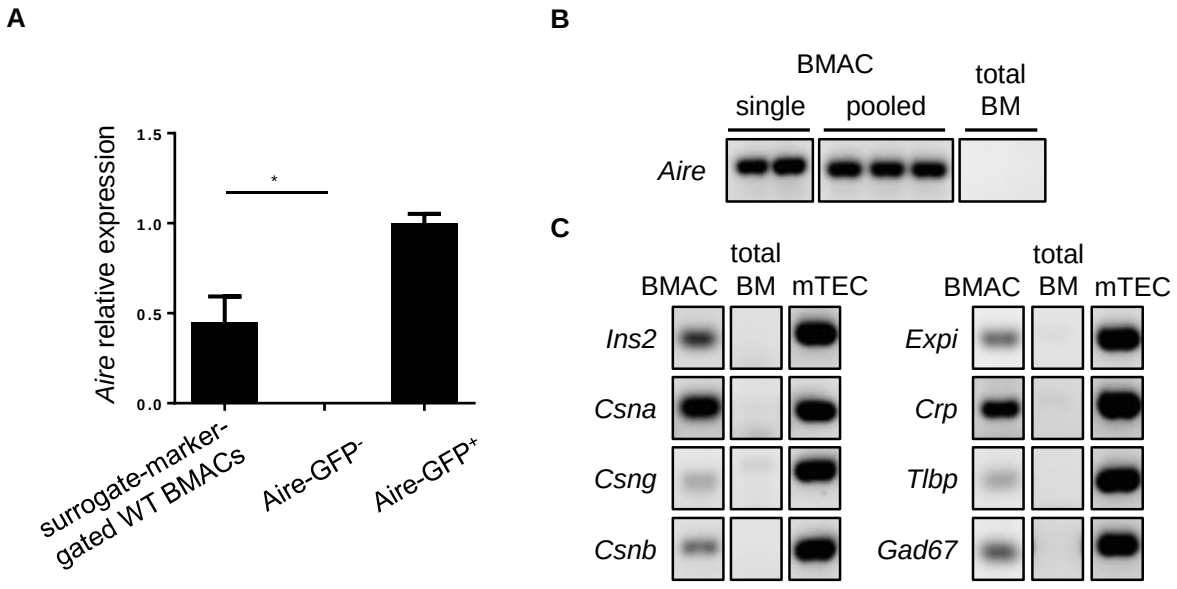


**Figure 11. Aire and TRA genes were expressed in BMACs of WT mice. (A)** Real-Time PCR analysis of Aire transcript expression (normalized to β-actin) in sorted Aire-GFP+ BMACs and Aire-GFP- BM cells from Adig mice, as well as BMACs from WT mice sorted according to the gating strategy shown in Figure 9. *, $P < 0.05$ (Student's t-test). Error bars indicate SEM. **(B and C)** Representative data of end-point PCR analysis of Aire and selected Aire-dependent (Ins2, Csna and Csng) or Aire-independent (Csnb, Expi, Crp, Tlbp and Gad67) TRA genes in sorted single or pooled BMACs, total BM cells or mTECs from WT mice.

### 3.3.3 Gating human BMACs using surrogate BMAC markers

In order to confirm whether the gating strategy using surrogate BMAC markers can be applied to human, single cell suspension of BM aspirate from patients with colorectal cancer was prepared and subjected to flow cytometric analysis for AIRE detection. As shown in **Figure 12A** and **12B**, gating on human BM cells revealed 59.0±11.9% overlap with $AIRE^+$ cells, substantially higher than gating with EpCAM and MHC-II only (5.5±4.7%, preliminary data). BM cells gated with surrogate BMAC markers also showed significantly higher mean fluorescence intensity (MFI) of AIRE than bulk BM cells (**Figure 12C**). These data demonstrated that the gating strategy using surrogate BMAC surface markers allows sorting BMACs with high purity from both WT murine and human BM cells, without fixation which disrupts RNA quality. It merits further study to delineate the scope of diversity of the TRA genes expressed by BMACs in human.

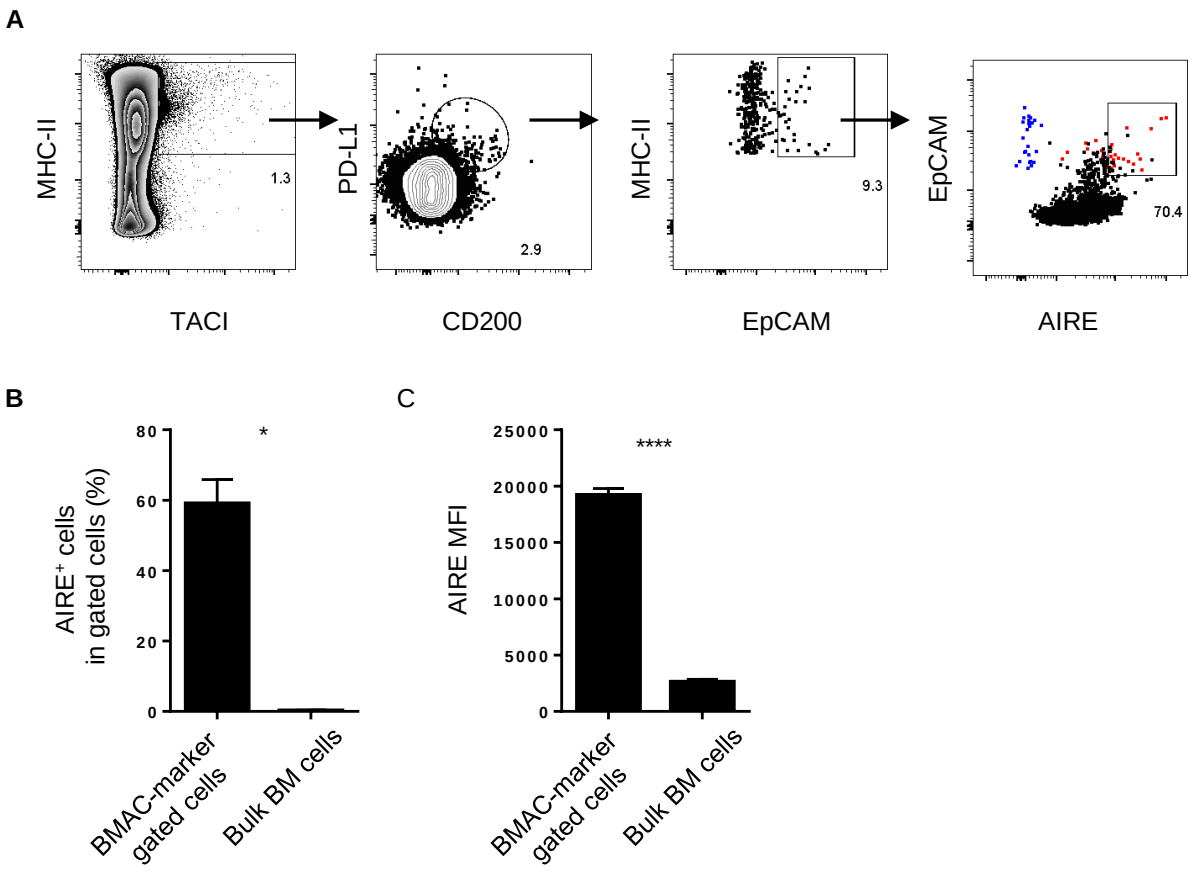


**Figure 12. Gating human BMACs using surrogate BMAC markers. (A)** Gating strategy of human BMACs using the surrogate BMAC markers. Cells gated with surrogate BMAC markers are shown in red (anti-AIRE) or blue (isotype control). Total bulk BM cells stained with anti-AIRE antibody are shown in black. **(B)** Percentage of AIRE$^+$ cells in bulk BM cells or cells gated with surrogate markers. *, $P < 0.05$. **(C)** Mean fluorescent intensity (MFI) of AIRE in bulk BM cells or cells gated with surrogate markers. ****, $P < 0.0001$ (Student's t-test). Error bars indicate SEM.

## 3.4 Analyses of immunological functions of BMACs

### 3.4.1 Co-localization of BMACs and CD4$^+$ T cells in BM

The fact that BMACs express MHC-II implies that they might present antigens to CD4$^+$ T cells in the BM. And therefore I assessed the col-localization of BMACs and CD4$^+$ T cells. As shown in **Figure 13**, in the BM parenchyma BMACs resided in the vicinity of CD4$^+$ T cell clusters,

indicating an *in situ* interaction between BMACs and CD4$^+$ T cells. Close contact between BMACs and clusters of CD8$^+$ T cells or CD19$^+$ B cells was not observed (**Figure 13**).

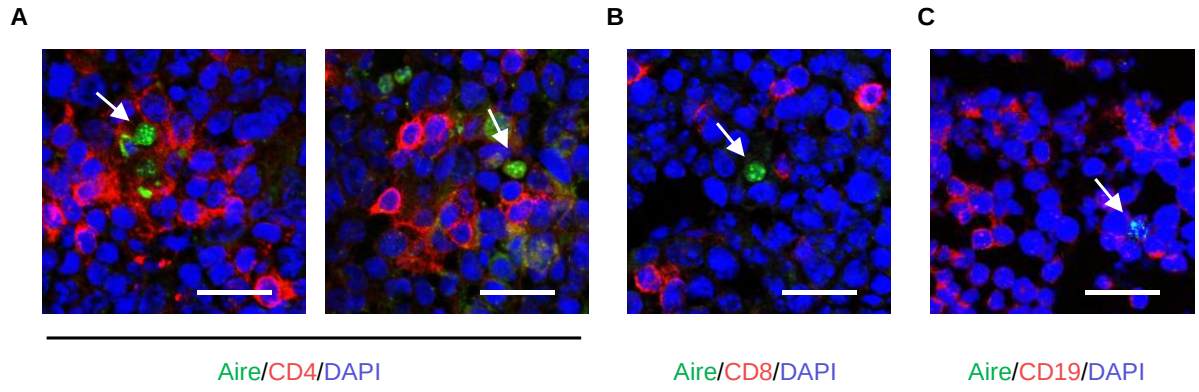


**Figure 13. Co-localization of BMACs and CD4$^+$ T cells in BM.** Immunofluorescence of Aire with CD4 **(A)**, CD8 **(B)** or CD19 **(C)** on BM tissue of WT mice. Arrows indicate BMACs. Scale bar indicates 15 μm.

### 3.4.2 BMACs present Aire-dependent antigens to CD4$^+$ T cells

In order to validate the function of BMACs in terms of antigen presentation, I next employed the Aire-HCO transgenic mouse system, in which a model antigen (hemagglutinin, HA) and a reporter protein surface marker (human CD2, hCD2) are expressed under the control of the Aire promoter[9, 12]. After sorting according to hCD2 expression (**Figure 14A**), BMACs from Aire-HCO mice were co-cultured with A5 T-hybridoma cells. A5 T-hybridoma cells express a TCR specific for HA peptide:I-E$^d$ complex, and carry a GFP expression cassette driven by the IL-2 promoter and NF-AT binding sites[100] reporting stimulation of the TCR. As shown in **Figure 14B** and **14C**, BMACs presented the Aire-regulated HA antigen and induced GFP expression in A5 hybridoma cells in a dose-dependent manner. Although mTECs and thymic B cells were equipped with higher capacities of antigen presentation, potentially due to their abundant expression of MHC-II[9], BMACs presented antigens more efficiently compared to splenic

eTACs. These results indicate that BMACs are competent APCs, and can present Aire-regulated antigens to CD4$^+$ T cells.

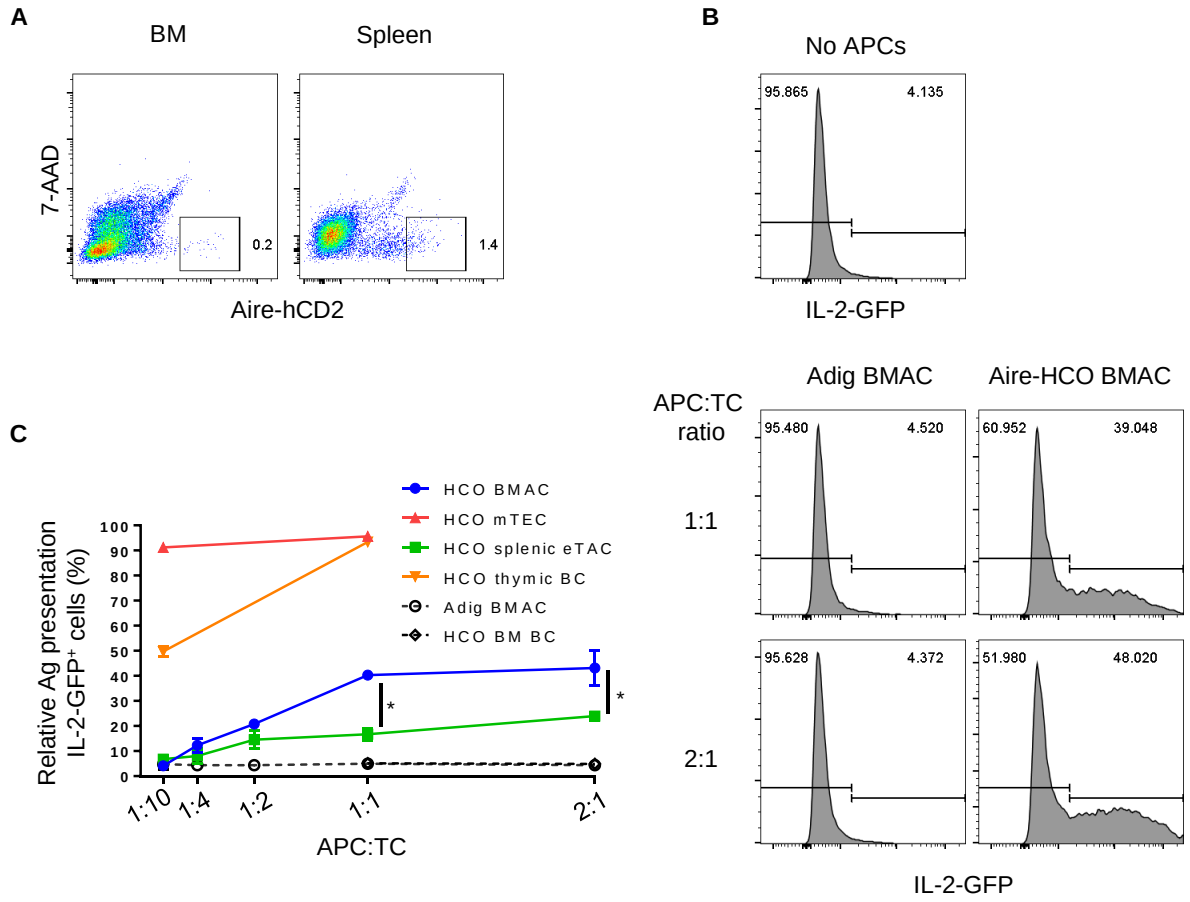


**Figure 14. BMACs present Aire-dependent antigens to CD4$^+$ T cells. (A)** Sorting strategy of Aire-HCO BMACs according to hCD2 expression. Number indicates percentage of gated cells among total BM cells. **(B)** Representative data of activation-dependent GFP expression in A5 T-hybridoma cells after co-culture with BMACs at indicated APC:TC ratios. Numbers indicate percentages of gated IL-2-GFP$^+$ cells among CD4$^+$ T-hybridoma cells. **(C)** Presentation of HA antigen to A5 T-hybridoma cells by various subsets of APCs from Aire-HCO or Adig mice at different APC:TC ratios. Percentages of NFAT-induced GFP$^+$ cells are shown. Results were pooled from two independent experiments (n ≥ 3). Numbers indicate percentages of gated cells among CD4$^+$ T-hybridoma cells. **, $P < 0.01$; ***, $P < 0.001$ (Student's t-test). Error bars indicate SEM.

### 3.4.3 BMACs selectively express genes associated with Treg induction

To further evaluate the impact of BMACs on $CD4^+$ T cells through cognate interaction, we examined the expression of receptors on BMACs that provide essential signals for T cell activation or differentiation. As depicted in **Figure 15**, BMACs strongly expressed the inhibitory checkpoint molecule PD-L1 compared to other APC subsets in the BM, while only a small fraction of BMACs express low level of PD-L2. In addition, BMACs showed intermediate levels of CD80 and CD86 expression, suggesting a mixed potential of promoting T cell tolerance and activation.

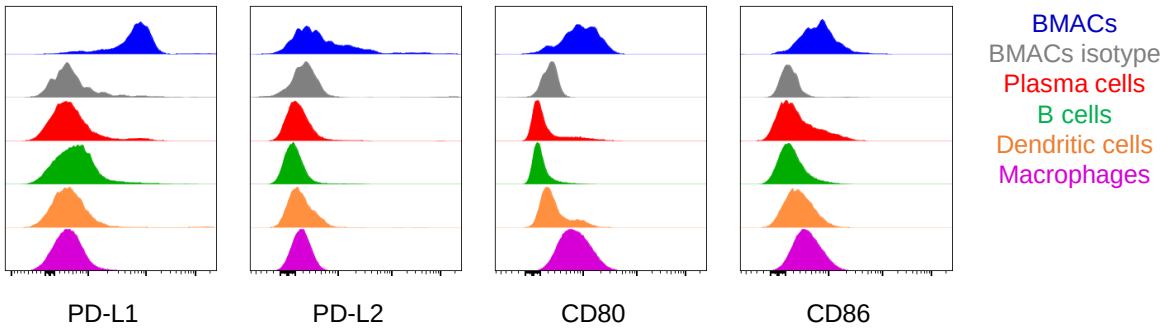


**Figure 15. BMACs express inhibitory receptor PD-L1 and co-stimulatory molecules CD80 and CD86.** Flow cytometric analysis of CD80, CD86, PD-L1 and PD-L2 expression on Aire-$GFP^+$ BMACs and various APC subsets ($B220^-CD138^+$ plasma cells, $B220^+CD138^-$ B cells, $CD11c^+$ DCs, $F4/80^+$ macrophages) from the BM of Adig mice. Representative data are shown (n = 3).

To gain further insight into the role of BMACs as APCs in directing the activation and/or differentiation $CD4^+$ T cells, I compared the gene expression profile of Aire-$GFP^+$MHC-$II^+EpCAM^+$ BMACs to BM $IgM^+CD138^+$ plasma cells of Adig mice. Gene expression array analysis revealed that, in addition to significantly higher *Aire* expression, BMACs displayed a distinct gene expression profile compared to $IgM^+$ plasma cells (**Figure 16A** and **16B**). Notably, BMACs expressed substantially lower levels of *CD22* (**Figure 16B**), suggesting that BMACs

are at the terminally differentiated stage of plasma cell development, which resembles IL-10- and IL-35-producing regulatory plasma cells reported in a previous study[94].

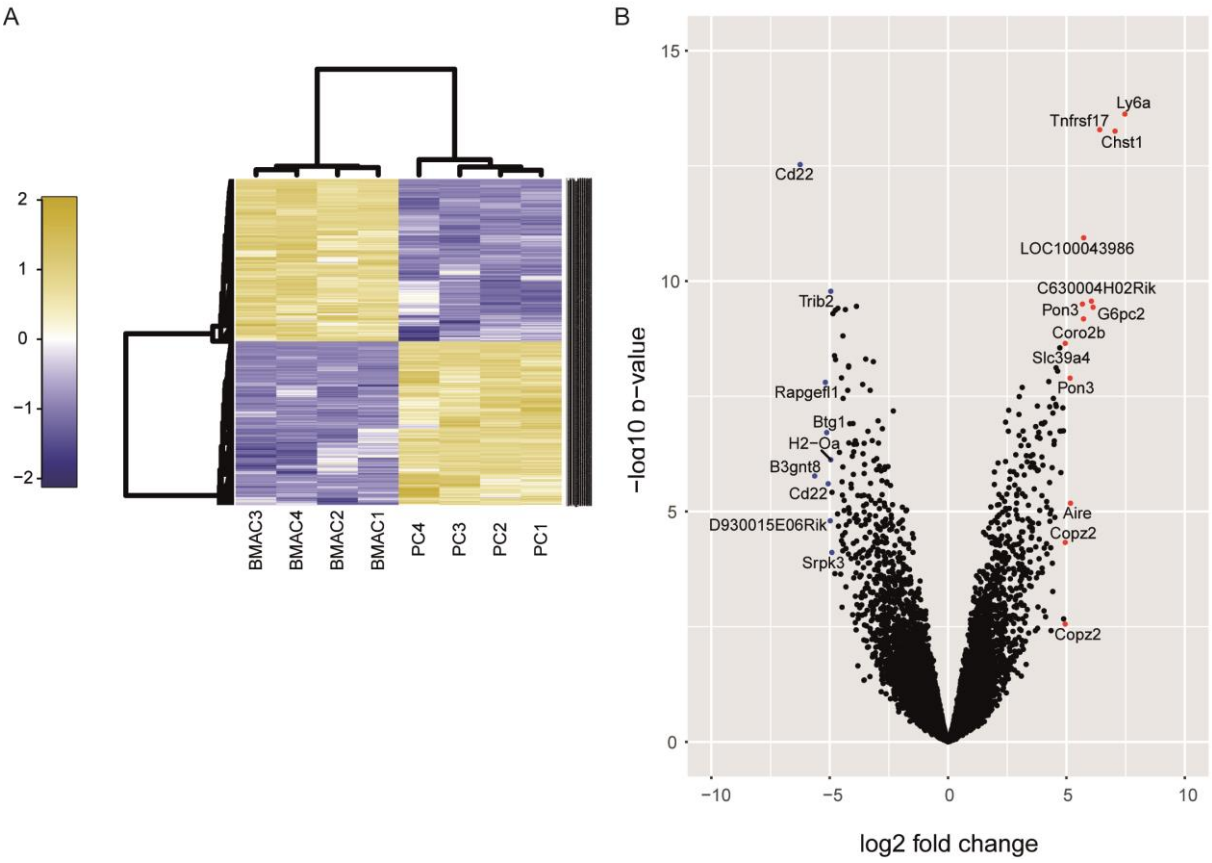


**Figure 16. Distinct gene expression profiles of BMACs and IgM$^+$CD138$^+$ plasma cells. (A)** Heat map of differentially expressed genes (adjusted *p*-value < 0.05) in BMACs compared to IgM$^+$CD138$^+$ plasma cells (PC). **(B)** Volcano plot of genes analyzed (BMAC vs PC), with labels of the genes which had a significant fold change > 30 (red) or < -30 (blue).

As depicted in **Figure 17A**, BMACs selectively expressed genes, which are known to induce Treg generation or conversion, or to induce suppressive functions of Treg cells. For example, BMACs differentially expressed genes for retinoic acid synthesis (*Aldh2* and *Rbp7*)[101], as well as *CD155* (also known as *Pvr*), which stimulates Treg upon ligation with TIGIT and subsequently enhances Treg-mediated suppression of cytotoxic T cell responses[102]. BMACs

also showed a modest increase of *Semaphorin-4a* (*Sema4a*) expression, suggesting that they can promote the stability of Treg cells[103]. Expression of *Tgfb1* in BMACs was significantly lower than that in $IgM^+$ plasma cells, which implies that other sources of TGFβ in BM might be involved in the BMAC-dependent Treg induction, if at all[104]. Interestingly, BMACs showed substantial expression of *IL-10* and *Ebi3*, however, *p35* (also known as *IL-12a*) was not detectable, indicating that (at least) under non-inflammatory conditions, BMACs employ distinct tolerogenic machineries than a recently described subset of regulatory plasma cells which mediate immune tolerance via IL-35 production[94]. Of note, BMACs expressed *p19* (also known as *IL-23a*), which forms IL-39 together with Ebi3, albeit the function of IL-39 on Treg cells is yet unclear. Tim-1 (also known as Havcr1) is essential for IL-10-producing regulatory B cells[105-107], and its transcript was expressed in BMACs, though not significantly higher than that in $IgM^+$ plasma cells. Importantly, among the genes that were associated with tolerance induction, we observed an enrichment of genes associated with Treg induction, instead of genes related to general T-cell tolerance through ligating inhibitory receptors, as most of the ligands known for inhibitory receptors were downregulated (**Figure 17A**). Similarly, BMACs themselves did not exploit the tolerogenic mechanisms mediated by Treg cells. Notably, BMACs showed high *LAG-3* expression, which has been reported on B cells after their activation by T cells[108], suggesting a feedback activation from T cells upon cognate interaction.

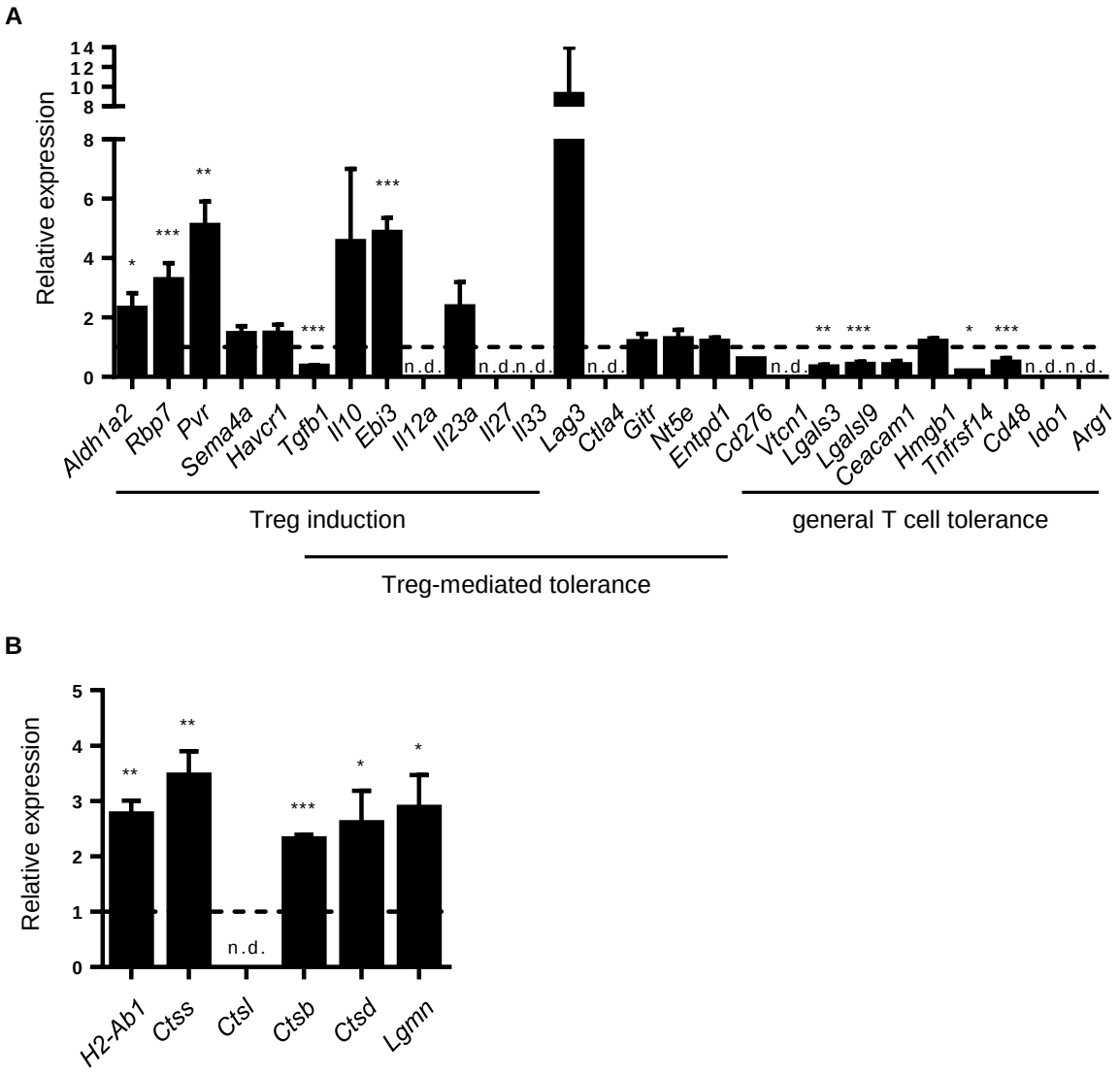


**Figure 17. BMACs selectively express genes associated with Treg induction.** Relative mRNA expression of genes associated with immune tolerance or with MHC-II antigen presentation in Aire-GFP+ BMACs compared to $IgM^+CD138^+$ plasma cells of Adig mice by gene expression array analysis (mean ± SEM). n.d., not detected. *, $P < 0.05$; **, $P < 0.01$; ***, $P < 0.001$.

In line with the capacity of antigen presentation, BMACs expressed higher amounts of MHC-II and lysosomal proteases such as *asparaginyl endopeptidase* (*Lgmn*) and *cathepsins* that are essential for peptide processing and loading to MHC-II[109] (**Figure 17B**). We did not detect *Cathepsin L*, the critical endopeptidase for $CD4^+$ T cell positive selection by cortical thymic epithelial cells. This finding reflects the ability of BMACs to present antigens to $CD4^+$ T cells,

despite their plasma cell feature and Blimp-1 expression[110]. This is consistent with a previous study showing that plasma cells are able to regulate $CD4^+$ T cell function by antigen presentation via MHC-II[111]. Together, our results demonstrated that BMACs are equipped with multiple tolerance-associated machineries that are selective for inducing Treg cells.

### 3.4.4 BMACs induce the conversion of naïve $CD4^+$ T cells into Treg cells *in vitro*

We next exploited naïve $CD4^+$ T cells from HA-TCR transgenic mice[12] to assess the outcome of the engagement of cognate $CD4^+$ T cells to BMACs expressing Aire-regulated antigens. The HA-TCR mice were crossed with *RAG2*$^{-/-}$ mice to ensure that all T cells were HA-specific. Naïve $CD4^+$ T cells were isolated from spleen of HA-TCR ($CD45.2^+$) or WT Balb/c ($CD45.1^+$) mice, followed by CD25-depletion (**Figure 18A**). The isolated naïve $CD4^+$ T cells were then co-cultured with BMACs sorted from Aire-HCO and Adig mice. CD45 congenic markers were used to distinguish the T cells from different sources (**Figure 18B**). After co-culture for 5 days, 67% of HA-specific $CD4^+$ T cells proliferated after co-culture with HA-expressing BMACs, while no proliferation was observed for HA-specific $CD4^+$ T cells co-cultured with Adig BMACs, nor for polyclonal $CD4^+$ T cells with both HA-expressing and WT BMACs (**Figure 18C**). Most importantly, the majority of HA-specific $CD4^+$ T cells expressed CD25, and more than one third of the T cells upregulated Foxp3 expression after encountering HA-expressing BMACs, indicating that BMACs induced a conversion of naïve $CD4^+$ T cells to Treg cells (**Figure 18D**). In contrast, only less than 10% of their polyclonal counterpart showed CD25 upregulation. This induction was antigen-dependent, as BMACs from Adig mice did not induce the expression of CD25 and Foxp3 on HA-specific $CD4^+$ T cells.

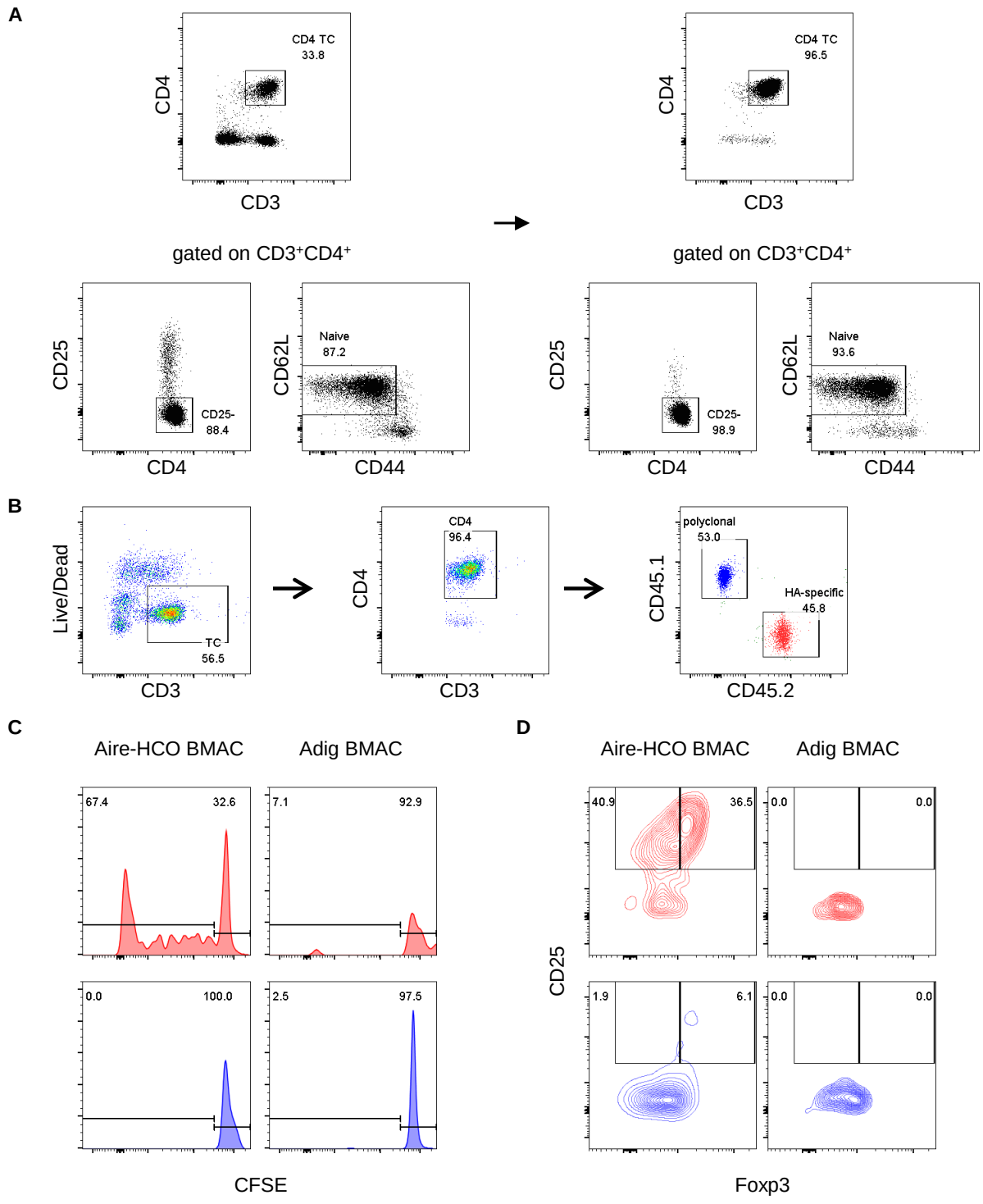


**Figure 18. BMACs induce the conversion of naïve CD4$^+$ T cells into Treg cells *in vitro*. (A)** Purity of naïve CD4$^+$ T cells before and after CD4$^+$ T cell isolation and CD25-depletion. **(B)** Gating strategy to distinguish HA-specific and polyclonal WT CD4$^+$ T cells. **(C)** Percentages of CFSE$^{low}$ proliferated cells among HA-specific and polyclonal WT CD4$^+$ T cells after 5-day co-culture at 1:1 ratio with BMACs from Aire-HCO or WT mice. **(D)** Frequencies of CD25$^+$Foxp3$^+$ cells among CD4$^+$ cells after co-culture of naïve HA-specific (red) or polyclonal (blue) CD4$^+$ T cells with BMACs from Aire-HCO or Adig mice. Representative data are shown (n = 3).

### 3.4.5 Naïve CD4$^+$ T cells are converted to Treg cells by BMACs *in vivo*

To further assess the impact of BMACs on naïve CD4$^+$ T cells *in vivo*, we transferred CD25-depleted naïve HA-specific CD4$^+$ T cells along with polyclonal naïve CD4$^+$ T cells into WT BM chimera mice, which were reconstituted with BM cells from Aire-HCO or WT mice 8 weeks prior to naïve T cell transfer (**Figure 19**). In the BM chimera mice, Aire-HA was expressed only in hematopoietic cells, thus avoiding the influence of HA expression by non-hematopoietic stromal cells.

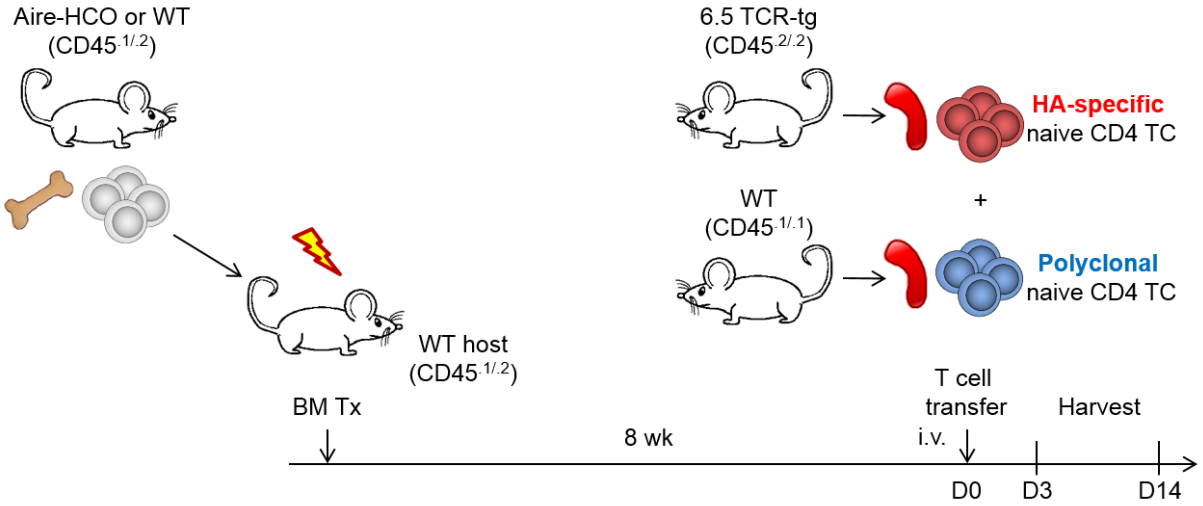


**Figure 19. Experimental scheme of *in vivo* Treg induction.** WT BM recipient mice were irradiated (4.5 Gy) twice with a 3-hour interval, and transplanted i.v. with donor BM cells from Aire-HCO or WT mice. After 8 weeks of reconstitution, naïve HA-specific CD4$^+$ T cells from 6.5 HA-TCR-transgenic (tg) mice or polyconal CD4$^+$ T cells from WT mice were transferred intravenously into the recipient mice. Donor cells were analyzed 3 days and 14 days post T cell transfer.

On day 3 post-transfer, HA-specific donor T cells showed robust proliferation in both the BM and spleen of Aire-HCO hosts. A comparable degree of proliferation of donor HA-specific T cells was neither observed in WT hosts, nor in both Aire-HCO and WT hosts for polyclonal T

cells, indicating that the expansion of the donor T cells was antigen-dependent (**Figure 20A**). Of note, a substantial proportion of non-divided donor T cells was also found in BM, demonstrating the migration of naïve T cells into the BM, as previously reported[78]. Two weeks after T cell transfer, the frequencies of HA-specific T cells remained more than two-fold of the polyclonal T cells in the BM, whereas in the spleen, less HA-specific T cells were detected than polyclonal ones (**Figure 20B** and **20C**). These results indicate that, while the autoreactive T cells are prone to diminishing upon encountering their cognate antigens presented by splenic eTACs[64], they acquire a survival advantage in the BM when engaging BMACs that present the same cognate antigens.

In accordance, a much higher proportion of HA-specific T cells were converted into $CD25^{+}Foxp3^{+}$ Treg cells in the BM (34.0±6.5%) than in the spleen (10.9±5.7%), as depicted in **Figure 21**. The same effect was not observed in polyclonal T cells in Aire-HCO hosts, nor in HA-specific T cells in WT hosts, indicating that the conversion of Treg cells depends on the cognate antigens presented by BMACs. These data demonstrate that BMACs can induce the conversion of naïve T cells that recognize Aire-regulated antigens into Treg cells *in vivo*.

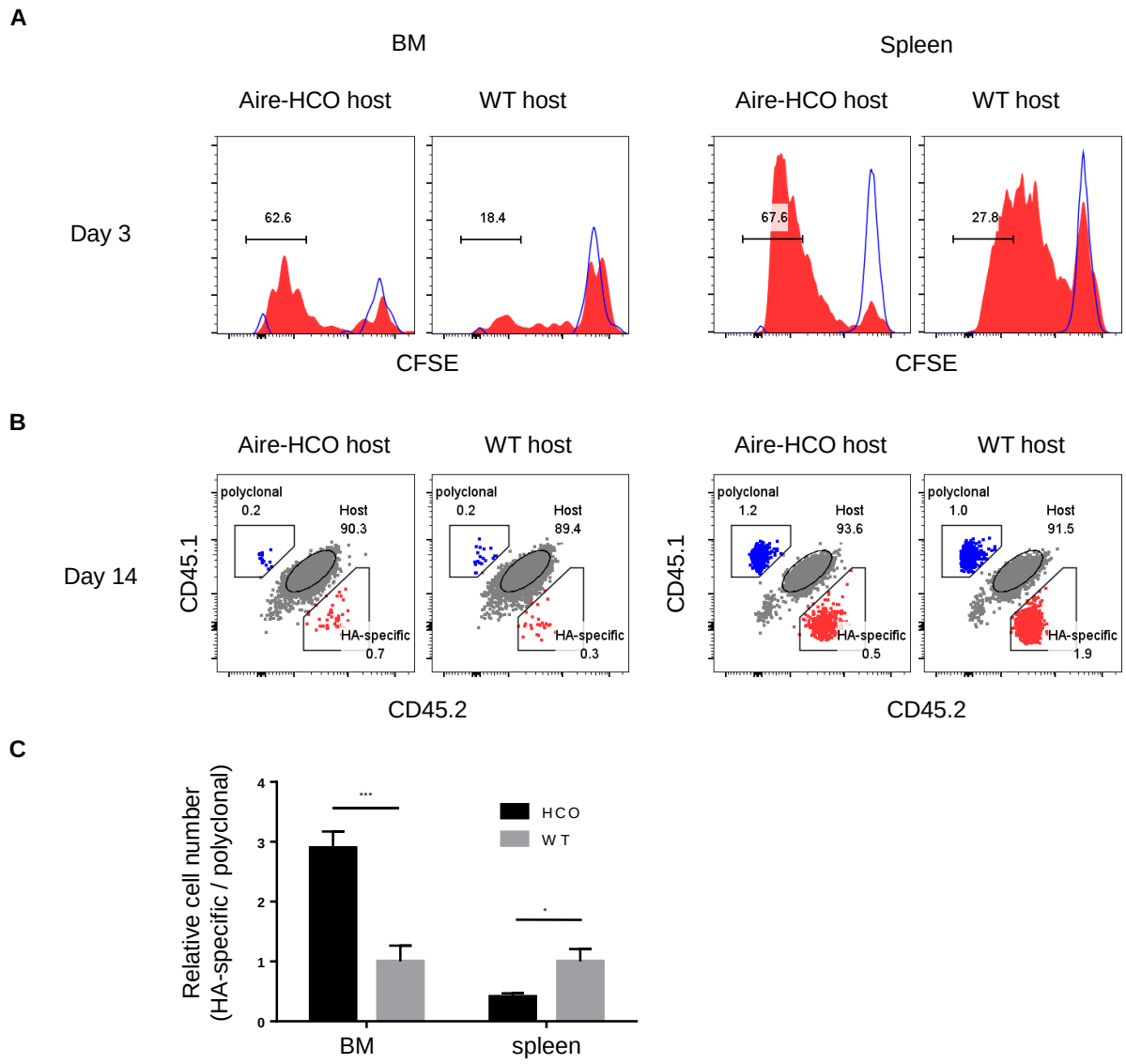


**Figure 20. Autoreactive T cells acquired survival advantage in the BM after encountering BMACs. (A)** Proliferation of CD45.2$^+$ HA-specific CD4+ T cells (red) and CD45.1$^+$ polyclonal CD4$^+$ T cells (blue) in the CD45.1$^+$CD45.2$^+$ hosts on day 3 post-transfer. Representative data are shown (n = 4). Numbers indicate percentages of gated cells among HA-specific donor CD4$^+$ T cells. **(B)** Percentages of CD45.2$^+$ HA-specific CD4$^+$ T cells (red) and CD45.1$^+$ polyclonal CD4$^+$ T cells (blue) in the BM of CD45.1$^+$CD45.2$^+$ hosts on day 14 post-transfer. Representative data are shown (n = 4). Numbers indicate percentages of gated cells among CD4+ T cells. **(C)** Ratio of HA-specific/polyclonal CD4$^+$ T cells in the BM or spleen of Aire-HCO or WT hosts on day 14 post-transfer (n = 4). *, $P < 0.05$; ***, $P < 0.001$ (Student's *t*-test). Error bars indicate SEM.

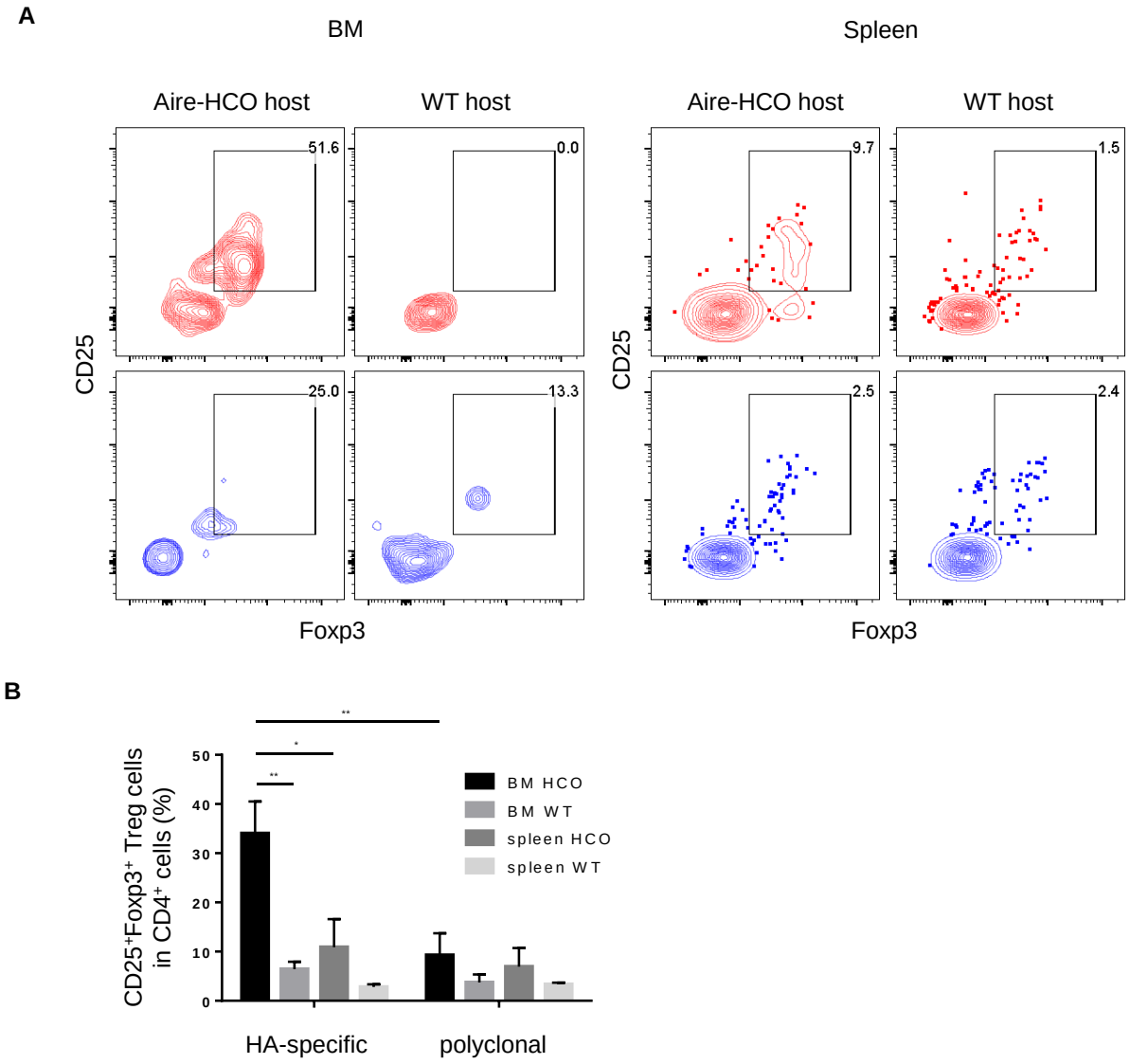


**Figure 21. Naïve CD4⁺ T cells are converted to Treg cells by BMACs *in vivo*.** (A) Frequencies of CD25⁺Foxp3⁺ Treg cells of CD45.2⁺ HA-specific CD4⁺ T cells (red) and CD45.1⁺ polyclonal CD4⁺ T cells (blue) in the BM of CD45.1⁺CD45.2⁺ host on day 14 post-transfer. Representative data are shown (n = 4). (B) Percentages of CD25⁺Foxp3⁺ Treg cells of CD45.2⁺ HA-specific CD4⁺ T cells and CD45.1⁺ polyclonal CD4⁺ T cells in the BM or spleen of CD45.1⁺CD45.2⁺ hosts on day 14 post-transfer (n = 4). Numbers indicate percentages of gated cells among CD45.2⁺ HA-specific CD4⁺ T cells or CD45.1⁺ polyclonal CD4⁺ T cells. *, $P < 0.05$; **, $P < 0.01$; (Student's *t*-test). Error bars indicate SEM.

### 3.4.6 Cytotoxic T cells are suppressed in the presence of BMAC-induced Treg cells

We sought to determine whether the BMAC-induced Treg cells are functional in terms of immune suppression. In Aire-HCO hosts, we observed that the BMAC-induced Treg cells

significantly upregulated the expression of CTLA-4 and LAP, but not of LAG-3, compared to the ones in WT hosts (**Figure 22**), indicating an activated and functional status of these Treg cells after recognizing the cognate antigens presented by BMACs[112-114]. Such activation status was found only for minor fractions of eTAC-induced Treg cells in the spleen (**Figure 22**).

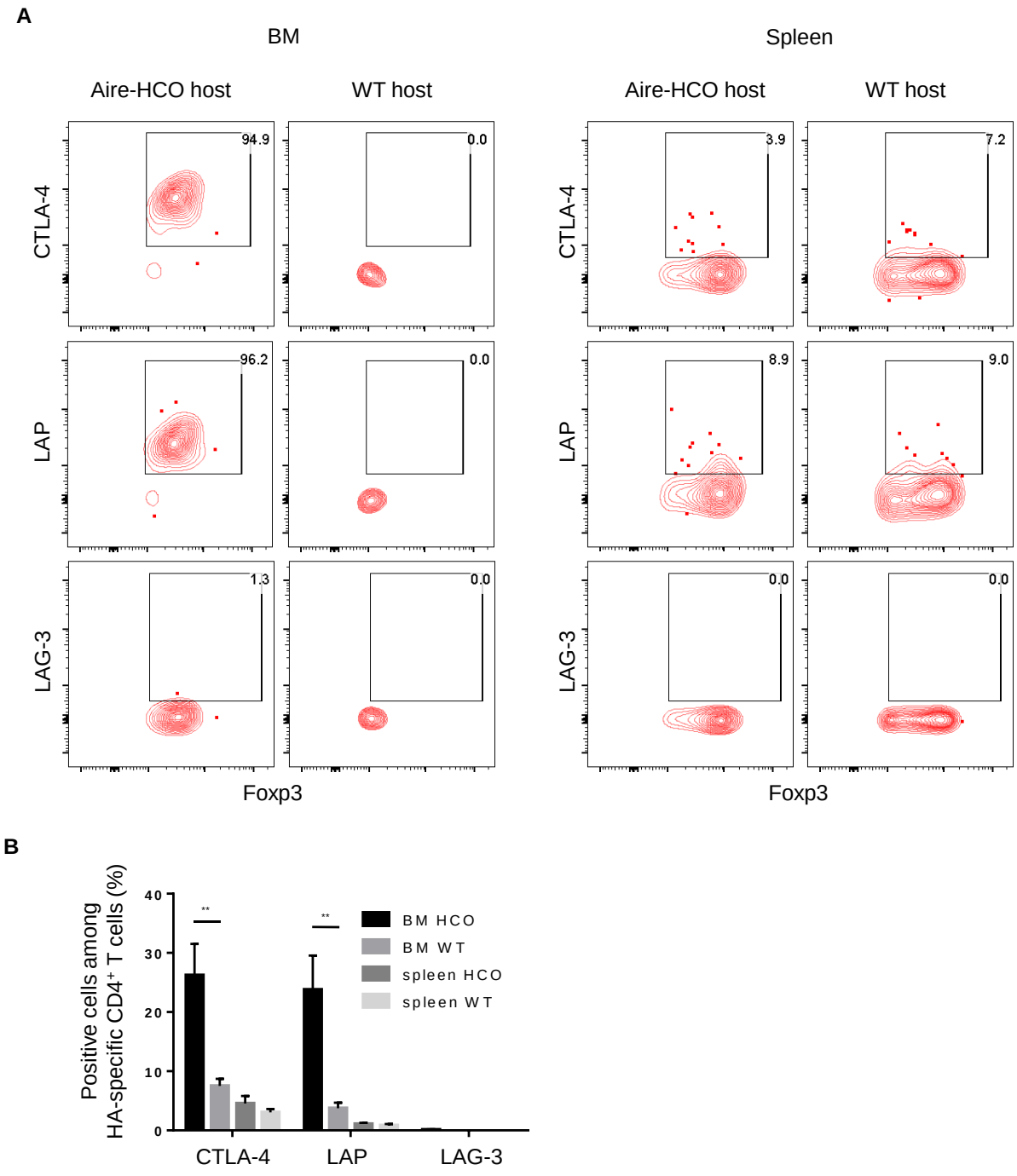


**Figure 22. BMAC-induced Treg showed activated phenotype. (A)** Frequencies of CTLA-4$^+$, LAP$^+$ and LAG-3$^+$ cells among HA-specific CD25$^+$Foxp3$^+$ Treg cells in the BM of Aire-HCO or WT hosts on

day 14 post-transfer (n = 4). **(B)** Percentages of cells expressing CTLA-4, LAP, or LAG-3 among HA-specific $CD4^+$ T cells in BM or spleen on day 14 post-transfer (n = 4). **, $P < 0.01$; (Student's *t*-test). Error bars indicate SEM.

We next assessed, whether BMAC-induced Treg cells are capable to regulate cytotoxic T cell responses *in vivo*. After naïve HA-specific $CD4^+$ T cells were converted into Treg cells in Aire-HCO hosts, we injected HA peptide-pulsed $CFSE^{high}$ and non-pulsed $CFSE^{low}$ target cells, together with or without cytotoxic HA-specific effector T cells isolated from the BM and spleen of WT mice immunized with HA peptide (**Figure 23**). One day after the transfer of target cells and cytotoxic effector T cells, we analyzed the frequencies of remaining $B220^+$ CFSE-labeled cells in the BM or spleen of Aire-HCO and WT hosts. As depicted in **Figure 24**, compared to WT hosts, HA-specific cytotoxicity in the BM was reduced in the Aire-HCO hosts, in which HA-specific $CD4^+$ T cells were converted into Treg cells. No significant suppressive effect was observed in the spleen, reflecting the activation status of the induced Treg cells (**Figure 22**). Taken together, these data indicate that BMAC-induced Treg cells are activated and functionally competent.

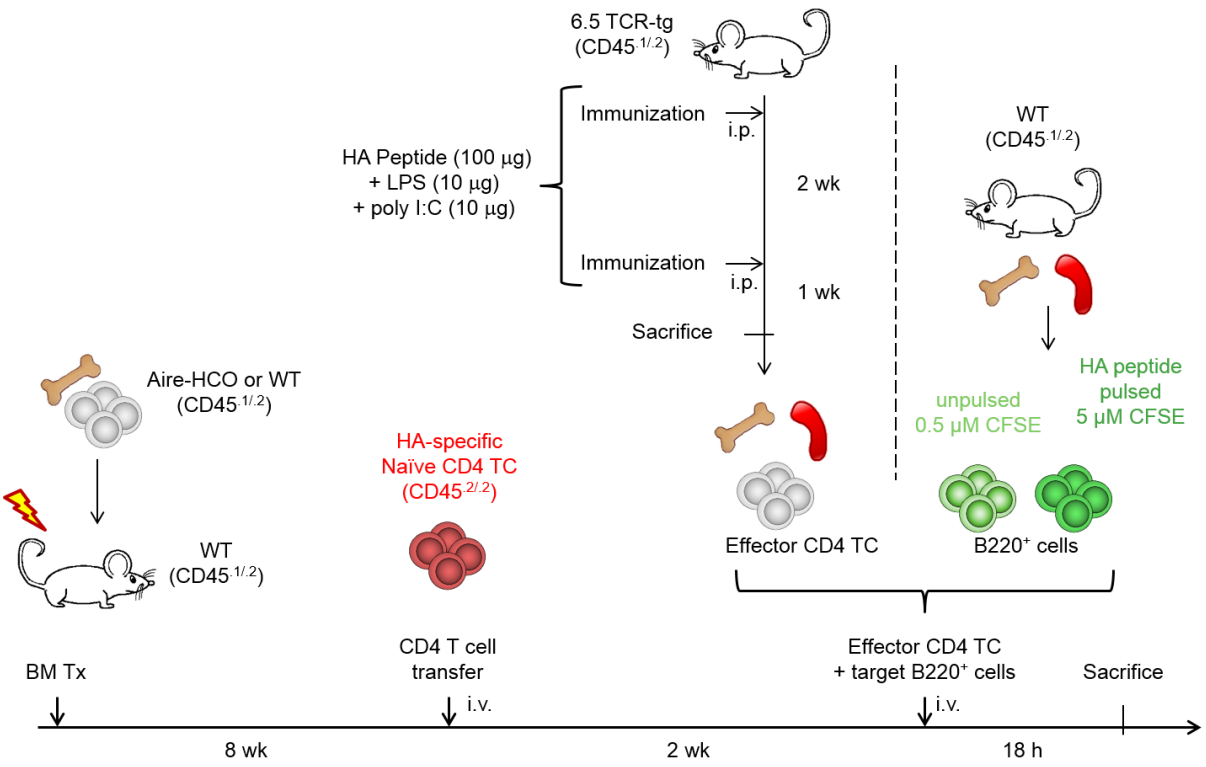


**Figure 23. Experimental scheme of *in vivo* cytotoxicity suppression**. WT BM recipient mice were irradiated (4.5 Gy) twice with a 3-hour interval, and transplanted i.v. with donor BM cells from Aire-HCO or WT mice. After 8 weeks of reconstitution, naïve HA-specific $CD4^+$ T cells from 6.5TCR-transgenic (tg) mice or polyconal $CD4^+$ T cells from WT mice were transferred intravenously into the recipient mice. Two weeks after naïve T cell transfer, HA peptide-pulsed $CFSE^{high}$ and non-pulsed $CFSE^{low}$ target cells were injected i.v., together with or without cytotoxic HA-specific effector T cells isolated from the BM and spleen of WT mice immunized with HA peptide. Percentages of target cells were analyzed 1 day after target cell transfer.

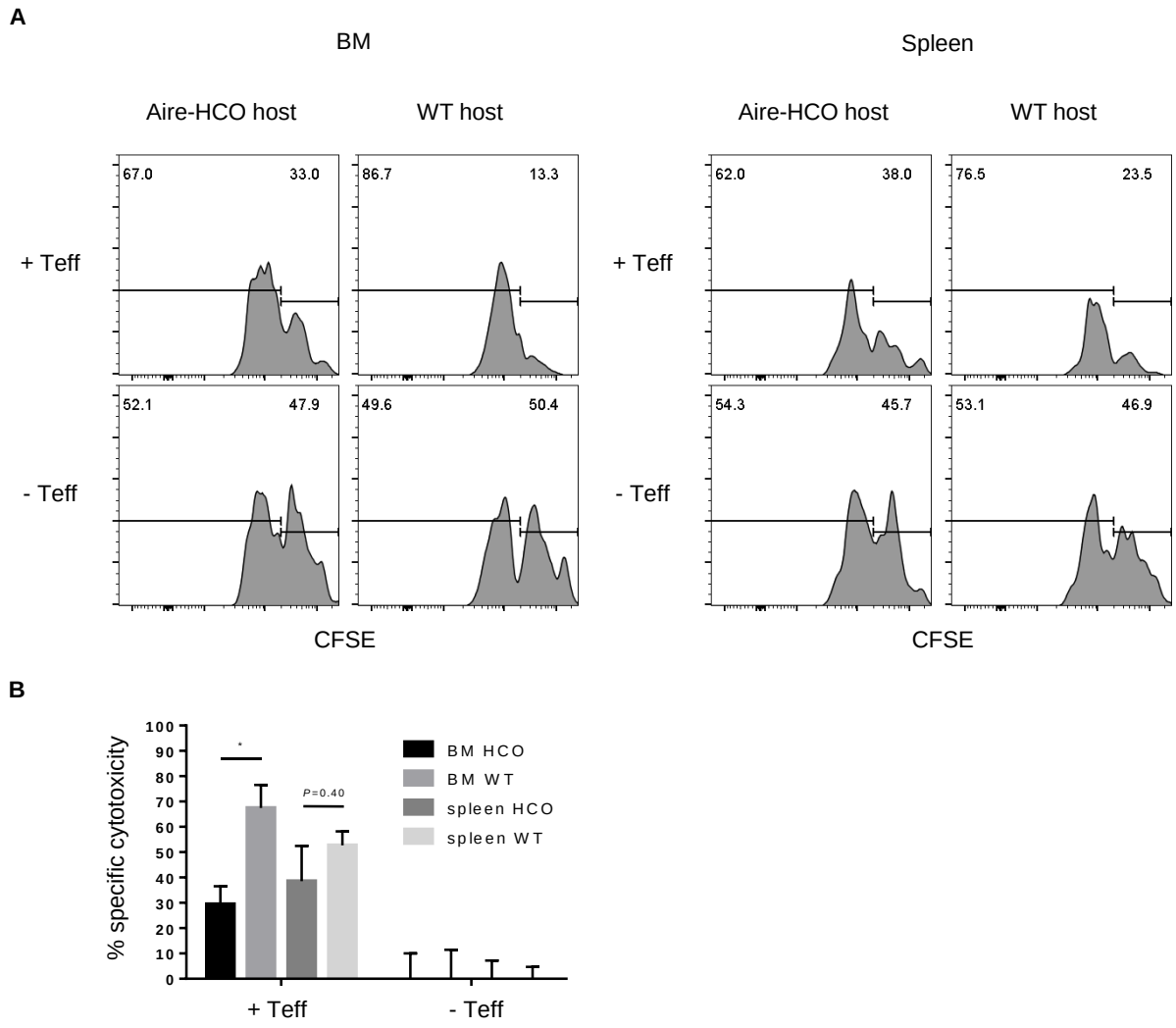


**Figure 24. T cell cytotoxicity was suppressed in the presence of cognate BMAC-induced Treg cells.** (A) Frequencies of B220+CFSEhigh and $B220^{+}CFSE^{low}$ target cells (18 h post transfer) in the BM or spleen of Aire-HCO or WT hosts with or without co-transfer of effector T cells. The Numbers indicate percentages of gated $B220^{+}$ cells. Representative data are shown (n = 3). (B) Percentages of specific cytotoxicity in the BM or spleen of Aire-HCO or WT hosts (n=3). *, $P < 0.05$ (Student's *t*-test). Error bars indicate SEM.

# 4. Discussion

The BM is a known major reservoir of Treg cells[80] and as such a major site for the regulation and maintenance of local and systemic tolerance. While extensive recirculation of Treg from and to the BM has been described, a potential contribution of BM intrinsic mechanisms to generate a repertoire of self-reactive Treg has not been addressed so far. Our study revealed a novel subset of BM cells which expressed Aire and TRAs ectopically, and was able to present Aire-regulated antigens to naïve $CD4^+$ T cells via MHC-II, leading to the conversion into $CD25^+Foxp3^+$ Treg cells. This finding provides insight into the regulation of active T cell tolerance: under physiological conditions, both immigrant and *in situ*-generated autoreactive Treg cells may contribute to the diverse Treg repertoire in the BM. These regulator cells assist the homeostasis of hematopoiesis by modulating the differentiation of hematopoietic stem cells and providing immune-privileged niches[82, 84]. At the onset of inflammation in the periphery, these autoreactive Treg cells, upon activation, migrate from the BM to inflammatory sites and regulate local inflammation[67, 80, 87]. The TRAs expressed by BMACs included self-antigens associated to autoimmune diseases and cancers, indicating that BMACs can induce Treg cells that are specific to these self-antigens and important for controlling autoimmune diseases and for promoting tumor growth.

## 4.1 Distinct phenotypic features and tolerogenic immunological functions of BMACs compared to other hematopoietic Aire-expressing cells

Recent evidence showed that self-representation in the peripheral lymphoid tissues contributes to the maintenance of T cells tolerance[54-56]. Lymph node stromal cells such as fibroblastic reticular cells and lymphatic endothelial cells express TRAs. They are able to shape the clonality of autoreactive $CD8^+$ T cells via direct presentation[57-60] and induce anergy of autoreactive $CD4^+$ T cells in cooperation with DCs which acquire the antigens from lymph node

stromal cells[61, 62]. While Lymph node stromal cells support Treg cells homeostasis, a role in Treg induction has not been described for these subsets[63].

eTACs were the first hematopoietic cell-derived APCs reported to express TRAs and Aire in the peripheral lymphoid organs[64, 65]. They share some phenotypic markers with BMACs such as CD45, EpCAM and MHC-II expression, but display a conventional DC-like morphology and express CD11c and Zbtb46[65], which according to our flow cytometric and microarray analyses are both not expressed by BMACs. Self-antigens expressed by eTACs induce deletion of diabetes-inducing autoreactive $CD8^+$ T cells and prevent disease onset in Adig mice bred on a non-obese diabetic (NOD) background[64]. Importantly, eTACs also induce anergy of autoreactive $CD4^+$ T cells[65]. Of note, a fraction of naïve autoreactive $CD4^+$ T cells upregulated Foxp3 in spleen and lymph nodes after encountering eTACs, however, these peripherally induced Treg cells do not account for the prevention of diabetes in the NOD SCID hosts, as the depletion of eTAC-induced Treg cells do not affect the eTAC-mediated protection from diabetes onset, and these cells fail to actively suppress naïve autoreactive $CD4^+$ T cells after co-transfer into the hosts[65]. The tolerogenic capacity of eTACs lies in inactivating $CD4^+$ T cells through the absence of costimulatory molecules. In keeping with this finding, we observed that the Treg cells induced by splenic eTACs in our model showed a lowly activated state and modest suppression capacity. In contrast, BMACs express CD80 and CD86, and the majority of the $CD25^+Foxp3^+$ Treg cells induced by BMACs upregulated CTLA-4 and LAP, and cytotoxic T cell responses in BM were significantly reduced in the presence of BMAC-induced Treg cells. It is noteworthy that HA-specific donor $CD4^+$ T cells in the spleen diminished compared to their polyclonal counterparts 2 weeks after transfer, even though they initially proliferated (our data not shown). This is similar to the deletional effect of eTACs on cognate $CD8^+$ T cells. In contrast, BMAC-induced Treg cells maintained high frequencies for at least 2 weeks. These findings suggest that BMACs and splenic eTACs exploit different tolerogenic

mechanisms to control autoreactive $CD4^+$ T cells. Thus, we conclude that BMACs are a phenotypically and functionally distinct subset of Aire-expressing antigen presenting cells.

## 4.2 Subsets in B cell lineage for T cell central and peripheral tolerance

BMACs displayed a $CD19^{low}CD138^+B220^-Blimp\text{-}1^+$ plasma cell phenotype, which indicates that B cells are not only involved in promoting negative selection of T cells in thymus[9, 10], but also in the maintenance of peripheral T cell tolerance in the BM. In Adig mice, approximately half of thymic B cells are Aire-$GFP^+$ (that is about 0.05% of total thymic cells). In hind bones of 6-12 weeks old mice, BMACs take up comparable proportion (0.01%-0.04%) of total BM cells. Despite the scarceness of these cell subsets, they contribute to central and peripheral T cell tolerance, respectively. In thymus, licensing of B cells by CD4 single-positive thymocytes via CD40 signaling initiates the complex program including proliferation, upregulation of Aire, MHC-II, and CD80 expression, and pGE. In contrast, BMACs had lower levels of CD80 and MHC-II expression, which reflects the lower antigen presentation capacity. Moreover, isotype analyses have revealed that Aire-expressing thymic B cells contain $IgM^+IgD^+$ and $IgM^+IgD^-$ cells, as well as $IgM^-IgD^-$ cells which undergo class switch after CD40-licensing[9]. Unlike in thymic B cells, no expression of isotype IgD, IgG1, IgG2a and IgG2b was detected in BMACs, while the majority of BMACs were surface $IgM^+$, indicating that class switch is not coupled with Aire expression in BMACs.

The licensing of thymic B cells requires the cognate interaction via peptide:MHC-II and TCR between B cells and cognate $CD4^+$ T cells, which provide CD40 signal to initiate the program of Aire, MHC-II and ectopic TRA expression. BMACs express MHC-II and the machinery for antigen presentation despite showing characteristics of plasma cells and Blimp-1 expression, and they are able to present Aire-regulated antigens to $CD4^+$ T cells. However, whether the interaction with $CD4^+$ T cells is essential for BMACs to express Aire should be further assessed. In addition, the effect of CD40 signaling on Aire expression in BMACs merits further study.

The fact that BM memory T cells interact with B cells through the CD40L/CD40 axis[115] renders this signaling pathway a potential driving force of Aire expression in BMACs.

## 4.3 Common features of BMACs and regulatory B cells (Breg cells)

Apart from being the potential prerequisite of Aire expression, cognate interaction between BMACs and T cells might also be the key to initiate the molecular program of Treg induction, as having been reported for regulator B (Breg) cells[116, 117]. Indeed, BMACs substantially expressed *LAG-3*, which has been shown as a marker for B cell activation induced by T cells[108]. It merits further investigation to determine whether the Treg cell-inducing mechanisms (*IL-10*, *CD155*, and retinoic acid) are all necessary or redundant for BMACs to convert naïve T cells to Treg cells. IL-10 produced by Breg cells is important for the induction of Treg cells as the frequency of the latter decreases in mice with B cell-restricted *IL-10* deficiency[118, 119]. Breg-mediated induction of Treg cells depends on cognate interaction between the two parts, since CD80, CD86[120] and MHC-II[121] are indispensable for this induction. The phenotype of BMACs ($CD138^+Blimp\text{-}1^+IgM^+MHC\text{-}II^+$) resembles the phenotype of regulatory plasma cells which can suppress experimental autoimmune encephalitis and inhibit anti-bacterial immunity through IL-10[94, 122, 123] and IL-35[94]. It is noteworthy that BMACs downregulated *CD22* expression, indicating a more terminally differentiated status, similar to the fact that IL-10 and IL-35-producing regulatory plasma cells are more enriched in $CD138^{hi}CD22^-$ subset than in $CD138^+CD22^+$ population[94]. However, BMAC-mediated Treg induction under physiological condition is independent on IL-35, as BMACs did not express *p35* (*IL-12a*, a subunit of IL-35), and the frequency of Treg cells is not affected in naïve mice lacking B cell-produced IL-35[94]. Nevertheless, we do not eliminate the notion that BMACs can upregulate p35 and utilize IL-35 as an auxiliary tolerogenic mediator under inflammatory condition, such as infection or onset of autoimmune diseases.

## 4.4 Peripherally derived Treg cells (pTreg) induced by BMACs maintain self-tolerance

Peripherally derived Treg (pTreg) cells are originally identified in the mucosa, such as gut and lung[124, 125]. These mucosal sites are in constant exposure to commensal bacteria and harmless foreign antigens, and the pTreg cells are indispensable to maintain the immune tolerance towards harmless foreign antigens, and thus avoiding the unnecessary inflammation. In mesenteric lymph nodes, $CD103^+$ DCs present the antigens acquired from the gut to cognate $CD4^+$ T cells and induce the development of pTreg cells[126]. The induction of pTreg cells by $CD103^+$ DCs in mesenteric lymph nodes is dependent on TGF-β and retinoic acid. Like tTreg cells, pTreg cells also manifest epigenetic marks of "natural" Treg cells, including demethylation of the *Foxp3* conserved non-coding sequence 2 (CNS2, also called Treg-specific demethylated region, TSDR)[127-132], *Ctla4*, *Tnfrsf18* and *Il2ra*[133, 134]. In contrast, *in vitro*-induced Treg (iTreg) cells have methylated TSDR, and thus the expression of Foxp3 in iTreg cells is rather unstable[128, 131]. However, pTreg cells can be distinguished from tTreg cells by the lack of Helios[135, 136] and Nrp1[137, 138] expression. The BMAC-induced Treg cells are generated in the BM (and thus by definition belong to pTreg cells), and further examination of their DNA methylation status and expression of Helios and Nrp1 is required to confirm their identity.

Apart from playing crucial roles in immune tolerance towards microbiota and harmless mucosal antigens, pTreg cells are also important in controlling autoimmune diseases such as multiple sclerosis[139-141] and type I diabetes[142]. In experimental autoimmune encephalomyelitis (EAE, a mouse model of multiple sclerosis), $CD8^+CD11c^+DEC205^+BTLA^{hi}$ DCs can induce pTreg cells through engaging HVEM on T cells[143]. Upon engagement of BLTA on DCs, HVEM signaling promotes Foxp3 expression and induces the conversion of pTreg cells. As BMACs express *CNP* and *Col5a1* that are associated with multiple sclerosis and rheumatoid arthritis,

respectively, it is plausible that BMAC-induced Treg cells are able to prevent the onset of these autoimmune diseases, which should be confirmed with further studies.

It is noteworthy that BMACs over-express genes necessary for retinoic acid production compared to $IgM^+$ plasma cells. However, expression of *Tgfb* and *BTLA* in BMACs is lower than that in plasma cells, suggesting the induction of Treg cells by BMACs is governed by mechanisms distinct from mesenteric $CD103^+$ or $CD205^+BTLA^{hi}$ DCs.

## 4.5 Potential tumor-supporting role of BMAC-induced Treg cells

Under physiological condition, Treg cells are enriched in the bone marrow, while in cancer patients the tumor-reactive Treg cells in the bone marrow are selectively activated, and then emigrate to the peripheral tumor tissue[86, 87]. It is currently unclear how the activation of these tumor-reactive Treg cells is induced. Since the tumor cells do not express MHC-II and are therefore incapable of presenting antigens to Treg cells, the source of TAAs and the identity of APCs, which can present the tumor-associated antigens (TAAs) to Treg cells via MHC-II, remain elusive.

We have now identified BMACs as one subset of the APCs (if more than one) capable to ectopically express TRAs and induce the conversion of naïve $CD4^+$ T cells to Treg cells through direct presentation of the self-antigens. The TRAs expressed by BMACs cover a broad spectrum of self-antigens, including several TAAs such as *Mage-d1* and *Mage-e1*. It is foreseeable that naïve $CD4^+$ T cells specific to TAAs that escape central tolerance in the thymus can be converted to Treg cells in the BM by BMACs. These newly generated Treg cells can potentially migrate to the periphery and suppress anti-tumor immunity and facilitate tumor-growth. It remains to be determined whether BMACs are able to induce endogenous TAA-specific Treg cells. And whether BMACs promote tumor growth through the induction of those TAA-specific Treg cells also needs further investigation.

Moreover, BM is a preferential site of metastasis in several different solid tumors, such as breast

and prostate cancer[144-146]. After epithelial-mesenchymal transition and extravasation, disseminated cancer cells travel through circulation and intravasate into BM. They interact with stromal cells and immune cells in BM and subsequently colonize within the organ. The niche of colonization for disseminated cancer cells is tolerogenic[147, 148]. It is critical to evaluate whether the tolerogenic niches consist of BMACs and induced Treg cells. As BM Treg cells have been reported to provide immune privileged niches for hematopoietic stem cells, TAA-specific Treg cells induced by BMACs might also create a tolerogenic microenvironment, which favors the colonization of disseminated cancer cells.

Furthermore, transient abrogation of central tolerance towards tumor has been shown to enhance anti-tumor immunity[149]. By blocking RANK signaling and thus mTEC maturation, Khan and colleagues are able to create a transient window where they can induce anti-tumor immune responses against tumor via immunization with tumor antigens. Given the potential of BMACs in promoting tolerance towards tumor growth and metastasis, the depletion of BMACs might benefit the immune responses against tumor and thus could provide new insight into cancer immunotherapy.

# 5. Conclusion

Immune tolerance towards self-antigens is essential to avoid the onset of autoimmune diseases. BM Treg cells are key players in self-tolerance that actively suppress immune responses and create a tolerogenic microenvironment for the fine regulation of hematopoiesis. Although BM has hitherto been viewed as a preferential site for the recirculation of tTreg cells, little is known about its role in the generation of pTreg cells. Here, our results unravel a direct conversion of naïve $CD4^+$ T cells into functional, self-antigen reactive Treg cells in the periphery by a BM-resident population of $Aire^+$ cells capable of ectopic TRA expression and presentation. This mechanism contributes to the formation of the repertoire of Treg cells in the BM that mediates local and systemic peripheral tolerance towards Aire-dependent self-antigens. As the self-antigens expressed by BMACs include antigens involved in autoimmune diseases, the Treg cells induced by BMACs might play a crucial role in the prevention of autoimmunity. On the other hand, BMACs also express tumor-associated self-antigens, which can lead to the induction of tumor-specific Treg cells that suppress anti-tumor immune responses. Therefore, promoting or repressing the activity of BMACs could be a potential therapeutic approach for the treatment of autoimmune diseases or cancer, respectively. In summary, these findings provide further insight into the induction and maintenance of peripheral immune tolerance in the BM.

# 6. References


1. Castellino, F. & Germain, R.N. Cooperation between CD4+ and CD8+ T cells: when, where, and how. *Annu Rev Immunol* **24**, 519-540 (2006).

2. Crotty, S. Follicular helper CD4 T cells (TFH). *Annu Rev Immunol* **29**, 621-663 (2011).

3. La Gruta, N.L., Gras, S., Daley, S.R., Thomas, P.G. & Rossjohn, J. Understanding the drivers of MHC restriction of T cell receptors. *Nat Rev Immunol* (2018).

4. Kyewski, B. & Klein, L. A central role for central tolerance. *Annu Rev Immunol* **24**, 571-606 (2006).

5. Klein, L., Hinterberger, M., Wirnsberger, G. & Kyewski, B. Antigen presentation in the thymus for positive selection and central tolerance induction. *Nat Rev Immunol* **9**, 833-844 (2009).

6. Klein, L., Kyewski, B., Allen, P.M. & Hogquist, K.A. Positive and negative selection of the T cell repertoire: what thymocytes see (and don't see). *Nat Rev Immunol* **14**, 377-391 (2014).

7. Derbinski, J., Schulte, A., Kyewski, B. & Klein, L. Promiscuous gene expression in medullary thymic epithelial cells mirrors the peripheral self. *Nat Immunol* **2**, 1032-1039 (2001).

8. Kyewski, B. & Derbinski, J. Self-representation in the thymus: an extended view. *Nat Rev Immunol* **4**, 688-698 (2004).

9. Yamano, T. *et al.* Thymic B Cells Are Licensed to Present Self Antigens for Central T Cell Tolerance Induction. *Immunity* **42**, 1048-1061 (2015).

10. Yamano, T., Steinert, M. & Klein, L. Thymic B Cells and Central T Cell Tolerance. *Front Immunol* **6**, 376 (2015).

11. Perry, J.S.A. *et al.* Distinct contributions of Aire and antigen-presenting-cell subsets to the generation of self-tolerance in the thymus. *Immunity* **41**, 414-426 (2014).

12. Aschenbrenner, K. *et al.* Selection of Foxp3+ regulatory T cells specific for self antigen expressed and presented by Aire+ medullary thymic epithelial cells. *Nat Immunol* **8**, 351-358 (2007).

13. Klein, L. & Jovanovic, K. Regulatory T cell lineage commitment in the thymus. *Semin Immunol* **23**, 401-409 (2011).

14. Hsieh, C.S., Lee, H.M. & Lio, C.W. Selection of regulatory T cells in the thymus. *Nat Rev Immunol* **12**, 157-167 (2012).

15. Lei, Y. *et al.* Aire-dependent production of XCL1 mediates medullary accumulation of thymic dendritic cells and contributes to regulatory T cell development. *J Exp Med* **208**, 383-394 (2011).

16. Wirnsberger, G., Hinterberger, M. & Klein, L. Regulatory T-cell differentiation versus clonal deletion of autoreactive thymocytes. *Immunol Cell Biol* **89**, 45-53 (2011).

17. Leventhal, D.S. *et al.* Dendritic Cells Coordinate the Development and Homeostasis of Organ-Specific Regulatory T Cells. *Immunity* **44**, 847-859 (2016).

18. Kyewski, B. & Feuerer, M. Love is in the Aire: mTECs share their assets. *Immunity* **41**, 343-345 (2014).

19. Anderson, M.S. *et al.* Projection of an immunological self shadow within the thymus by the aire protein. *Science* **298**, 1395-1401 (2002).

20. Mathis, D. & Benoist, C. Aire. *Annu Rev Immunol* **27**, 287-312 (2009).

21. Finnish-German, A.C. An autoimmune disease, APECED, caused by mutations in a novel gene featuring two PHD-type zinc-finger domains. *Nat Genet* **17**, 399-403 (1997).

22. Nagamine, K. *et al.* Positional cloning of the APECED gene. *Nat Genet* **17**, 393-398 (1997).

23. Malchow, S. *et al.* Aire-dependent thymic development of tumor-associated regulatory T cells. *Science* **339**, 1219-1224 (2013).

24. Malchow, S. *et al.* Aire Enforces Immune Tolerance by Directing Autoreactive T Cells into the Regulatory T Cell Lineage. *Immunity* **44**, 1102-1113 (2016).

25. Meredith, M., Zemmour, D., Mathis, D. & Benoist, C. Aire controls gene expression in the thymic epithelium with ordered stochasticity. *Nat Immunol* **16**, 942-949 (2015).

26. Derbinski, J., Pinto, S., Rosch, S., Hexel, K. & Kyewski, B. Promiscuous gene expression patterns in single medullary thymic epithelial cells argue for a stochastic mechanism. *Proc Natl Acad Sci U S A* **105**, 657-662 (2008).

27. Villasenor, J., Besse, W., Benoist, C. & Mathis, D. Ectopic expression of peripheral-tissue antigens in the thymic epithelium: probabilistic, monoallelic, misinitiated. *Proc Natl Acad Sci U S A* **105**, 15854-15859 (2008).

28. Pinto, S. *et al.* Overlapping gene coexpression patterns in human medullary thymic epithelial cells generate self-antigen diversity. *Proc Natl Acad Sci U S A* **110**, E3497-3505 (2013).

29. Brennecke, P. *et al.* Single-cell transcriptome analysis reveals coordinated ectopic gene-expression patterns in medullary thymic epithelial cells. *Nat Immunol* **16**, 933-941 (2015).

30. Anderson, M.S. & Su, M.A. AIRE expands: new roles in immune tolerance and beyond. *Nat Rev Immunol* **16**, 247-258 (2016).

31. Pitkanen, J. *et al.* The autoimmune regulator protein has transcriptional transactivating properties and interacts with the common coactivator CREB-binding protein. *J Biol Chem* **275**, 16802-16809 (2000).

32. Su, M.A. *et al.* Mechanisms of an autoimmunity syndrome in mice caused by a dominant mutation in Aire. *J Clin Invest* **118**, 1712-1726 (2008).

33. Oftedal, B.E. *et al.* Dominant Mutations in the Autoimmune Regulator AIRE Are Associated with Common Organ-Specific Autoimmune Diseases. *Immunity* **42**, 1185-1196 (2015).

34. Koh, A.S. *et al.* Aire employs a histone-binding module to mediate immunological tolerance, linking chromatin regulation with organ-specific autoimmunity. *Proc Natl Acad Sci U S A* **105**, 15878-15883 (2008).

35. Org, T. *et al.* The autoimmune regulator PHD finger binds to non-methylated histone H3K4 to activate gene expression. *EMBO Rep* **9**, 370-376 (2008).

36. Waterfield, M. *et al.* The transcriptional regulator Aire coopts the repressive ATF7ip-MBD1 complex for the induction of immunotolerance. *Nat Immunol* **15**, 258-265 (2014).

37. Zumer, K., Low, A.K., Jiang, H., Saksela, K. & Peterlin, B.M. Unmodified histone H3K4 and DNA-dependent protein kinase recruit autoimmune regulator to target genes. *Mol Cell Biol* **32**, 1354-1362 (2012).

38. Giraud, M. *et al.* Aire unleashes stalled RNA polymerase to induce ectopic gene expression in thymic epithelial cells. *Proc Natl Acad Sci U S A* **109**, 535-540 (2012).

39. Oven, I. *et al.* AIRE recruits P-TEFb for transcriptional elongation of target genes in medullary thymic epithelial cells. *Mol Cell Biol* **27**, 8815-8823 (2007).

40. Giraud, M. *et al.* An RNAi screen for Aire cofactors reveals a role for Hnrnpl in polymerase release and Aire-activated ectopic transcription. *Proc Natl Acad Sci U S A* **111**, 1491-1496 (2014).

41. Yoshida, H. *et al.* Brd4 bridges the transcriptional regulators, Aire and P-TEFb, to promote elongation of peripheral-tissue antigen transcripts in thymic stromal cells. *Proc Natl Acad Sci U S A* **112**, E4448-4457 (2015).

42. Metzger, T.C. *et al.* Lineage tracing and cell ablation identify a post-Aire-expressing thymic epithelial cell population. *Cell Rep* **5**, 166-179 (2013).

43. Haljasorg, U. *et al.* A highly conserved NF-kappaB-responsive enhancer is critical for thymic expression of Aire in mice. *Eur J Immunol* **45**, 3246-3256 (2015).

44. LaFlam, T.N. *et al.* Identification of a novel cis-regulatory element essential for immune tolerance. *J Exp Med* **212**, 1993-2002 (2015).

45. Yanagihara, T. *et al.* Intronic regulation of Aire expression by Jmjd6 for self-tolerance induction in the thymus. *Nat Commun* **6**, 8820 (2015).

46. Chuprin, A. *et al.* The deacetylase Sirt1 is an essential regulator of Aire-mediated induction of central immunological tolerance. *Nat Immunol* **16**, 737-745 (2015).

47. Saare, M., Rebane, A., Rajashekar, B., Vilo, J. & Peterson, P. Autoimmune regulator is acetylated by transcription coactivator CBP/p300. *Exp Cell Res* **318**, 1767-1778 (2012).

48. Liiv, I. *et al.* DNA-PK contributes to the phosphorylation of AIRE: importance in transcriptional activity. *Biochim Biophys Acta* **1783**, 74-83 (2008).

49. Rattay, K. *et al.* Homeodomain-interacting protein kinase 2, a novel autoimmune regulator interaction partner, modulates promiscuous gene expression in medullary thymic epithelial cells. *J Immunol* **194**, 921-928 (2015).

50. von Andrian, U.H. & Mempel, T.R. Homing and cellular traffic in lymph nodes. *Nat Rev Immunol* **3**, 867-878 (2003).

51. Obst, R. The Timing of T Cell Priming and Cycling. *Front Immunol* **6**, 563 (2015).

52. Walker, L.S. & Abbas, A.K. The enemy within: keeping self-reactive T cells at bay in the periphery. *Nat Rev Immunol* **2**, 11-19 (2002).

53. Mueller, D.L. Mechanisms maintaining peripheral tolerance. *Nat Immunol* **11**, 21-27 (2010).

54. Rouhani, S.J., Eccles, J.D., Tewalt, E.F. & Engelhard, V.H. Regulation of T-cell Tolerance by Lymphatic Endothelial Cells. *J Clin Cell Immunol* **5** (2014).

55. Brown, F.D. & Turley, S.J. Fibroblastic reticular cells: organization and regulation of the T lymphocyte life cycle. *J Immunol* **194**, 1389-1394 (2015).

56. Humbert, M., Hugues, S. & Dubrot, J. Shaping of Peripheral T Cell Responses by Lymphatic Endothelial Cells. *Front Immunol* **7**, 684 (2016).

57. Lee, J.W. *et al.* Peripheral antigen display by lymph node stroma promotes T cell tolerance to intestinal self. *Nat Immunol* **8**, 181-190 (2007).

58. Fletcher, A.L. *et al.* Lymph node fibroblastic reticular cells directly present peripheral tissue antigen under steady-state and inflammatory conditions. *J Exp Med* **207**, 689-697 (2010).

59. Cohen, J.N. *et al.* Lymph node-resident lymphatic endothelial cells mediate peripheral tolerance via Aire-independent direct antigen presentation. *J Exp Med* **207**, 681-688 (2010).

60. Nichols, L.A. *et al.* Deletional self-tolerance to a melanocyte/melanoma antigen derived from tyrosinase is mediated by a radio-resistant cell in peripheral and mesenteric lymph nodes. *J Immunol* **179**, 993-1003 (2007).

61. Rouhani, S.J. *et al.* Roles of lymphatic endothelial cells expressing peripheral tissue antigens in CD4 T-cell tolerance induction. *Nat Commun* **6**, 6771 (2015).

62. Dubrot, J. *et al.* Lymph node stromal cells acquire peptide-MHCII complexes from dendritic cells and induce antigen-specific CD4(+) T cell tolerance. *J Exp Med* **211**, 1153-1166 (2014).

63. Baptista, A.P. *et al.* Lymph node stromal cells constrain immunity via MHC class II self-antigen presentation. *Elife* **3** (2014).

64. Gardner, J.M. *et al.* Deletional tolerance mediated by extrathymic Aire-expressing cells. *Science* **321**, 843-847 (2008).

65. Gardner, J.M. *et al.* Extrathymic Aire-expressing cells are a distinct bone marrow-derived population that induce functional inactivation of CD4(+) T cells. *Immunity* **39**, 560-572 (2013).

66. Mercier, F.E., Ragu, C. & Scadden, D.T. The bone marrow at the crossroads of blood and immunity. *Nat Rev Immunol* **12**, 49-60 (2011).

67. Zhao, E. *et al.* Bone marrow and the control of immunity. *Cell Mol Immunol* **9**, 11-19 (2012).

68. Koni, P.A. *et al.* Conditional vascular cell adhesion molecule 1 deletion in mice: impaired lymphocyte migration to bone marrow. *J Exp Med* **193**, 741-754 (2001).

69. Tokoyoda, K., Hauser, A.E., Nakayama, T. & Radbruch, A. Organization of immunological memory by bone marrow stroma. *Nat Rev Immunol* **10**, 193-200 (2010).

70. Di Rosa, F. Two Niches in the Bone Marrow: A Hypothesis on Life-long T Cell Memory. *Trends Immunol* **37**, 503-512 (2016).

71. Choi, C. *et al.* Enrichment of functional CD8 memory T cells specific for MUC1 in bone marrow of patients with multiple myeloma. *Blood* **105**, 2132-2134 (2005).

72. Muller-Berghaus, J. *et al.* Melanoma-reactive T cells in the bone marrow of melanoma patients: association with disease stage and disease duration. *Cancer Res* **66**, 5997-6001 (2006).

73. Feuerer, M. *et al.* Therapy of human tumors in NOD/SCID mice with patient-derived reactivated memory T cells from bone marrow. *Nat Med* **7**, 452-458 (2001).

74. Beckhove, P. *et al.* Specifically activated memory T cell subsets from cancer patients recognize and reject xenotransplanted autologous tumors. *J Clin Invest* **114**, 67-76 (2004).

75. Schuetz, F. *et al.* Treatment of advanced metastasized breast cancer with bone marrow-derived tumour-reactive memory T cells: a pilot clinical study. *Cancer Immunol Immunother* **58**, 887-900 (2009).

76. Domschke, C. *et al.* Long-term survival after adoptive bone marrow T cell therapy of advanced metastasized breast cancer: follow-up analysis of a clinical pilot trial. *Cancer Immunol Immunother* **62**, 1053-1060 (2013).

77. Tripp, R.A., Topham, D.J., Watson, S.R. & Doherty, P.C. Bone marrow can function as a lymphoid organ during a primary immune response under conditions of disrupted lymphocyte trafficking. *J Immunol* **158**, 3716-3720 (1997).

78. Feuerer, M. *et al.* Bone marrow as a priming site for T-cell responses to blood-borne antigen. *Nat Med* **9**, 1151-1157 (2003).

79. Schirrmacher, V. *et al.* T-cell priming in bone marrow: the potential for long-lasting protective anti-tumor immunity. *Trends Mol Med* **9**, 526-534 (2003).

80. Zou, L. *et al.* Bone marrow is a reservoir for CD4+CD25+ regulatory T cells that traffic through CXCL12/CXCR4 signals. *Cancer Res* **64**, 8451-8455 (2004).

81. Wei, S., Kryczek, I. & Zou, W. Regulatory T-cell compartmentalization and trafficking. *Blood* **108**, 426-431 (2006).

82. Fujisaki, J. *et al.* In vivo imaging of Treg cells providing immune privilege to the haematopoietic stem-cell niche. *Nature* **474**, 216-219 (2011).

83. Pierini, A. *et al.* Foxp3(+) regulatory T cells maintain the bone marrow microenvironment for B cell lymphopoiesis. *Nat Commun* **8**, 15068 (2017).

84. Urbieta, M. *et al.* Hematopoietic progenitor cell regulation by CD4+CD25+ T cells. *Blood* **115**, 4934-4943 (2010).

85. Le Texier, L., Lineburg, K.E. & MacDonald, K.P. Harnessing bone marrow resident regulatory T cells to improve allogeneic stem cell transplant outcomes. *Int J Hematol* **105**, 153-161 (2017).

86. Schmidt, H.H. *et al.* HLA Class II tetramers reveal tissue-specific regulatory T cells that suppress T-cell responses in breast carcinoma patients. *Oncoimmunology* **2**, e24962 (2013).

87. Rathinasamy, A. *et al.* Tumor specific regulatory T cells in the bone marrow of breast cancer patients selectively upregulate the emigration receptor S1P1. *Cancer Immunol Immunother* (2017).

88. Derbinski, J. *et al.* Promiscuous gene expression in thymic epithelial cells is regulated at multiple levels. *J Exp Med* **202**, 33-45 (2005).

89. Hubert, F.X. *et al.* Aire-deficient C57BL/6 mice mimicking the common human 13-base pair deletion mutation present with only a mild autoimmune phenotype. *J Immunol* **182**, 3902-3918 (2009).

90. Guzvic, M. *et al.* Combined genome and transcriptome analysis of single disseminated cancer cells from bone marrow of prostate cancer patients reveals unexpected transcriptomes. *Cancer Res* **74**, 7383-7394 (2014).

91. Quah, B.J., Warren, H.S. & Parish, C.R. Monitoring lymphocyte proliferation in vitro and in vivo with the intracellular fluorescent dye carboxyfluorescein diacetate succinimidyl ester. *Nat Protoc* **2**, 2049-2056 (2007).

92. Nutt, S.L., Hodgkin, P.D., Tarlinton, D.M. & Corcoran, L.M. The generation of antibody-secreting plasma cells. *Nat Rev Immunol* **15**, 160-171 (2015).

93. Minnich, M. *et al.* Multifunctional role of the transcription factor Blimp-1 in coordinating plasma cell differentiation. *Nat Immunol* **17**, 331-343 (2016).

94. Shen, P. *et al.* IL-35-producing B cells are critical regulators of immunity during autoimmune and infectious diseases. *Nature* **507**, 366-370 (2014).

95. Blanc, P. *et al.* Mature IgM-expressing plasma cells sense antigen and develop competence for cytokine production upon antigenic challenge. *Nat Commun* **7**, 13600 (2016).

96. Miller, J.J. & Cole, L.J. The radiation resistance of long-lived lymphocytes and plasma cells in mouse and rat lymph nodes. *J Immunol* **98**, 982-990 (1967).

97. Shinkai, Y. *et al.* RAG-2-deficient mice lack mature lymphocytes owing to inability to initiate V(D)J rearrangement. *Cell* **68**, 855-867 (1992).

98. O'Neill, L.A., Golenbock, D. & Bowie, A.G. The history of Toll-like receptors - redefining innate immunity. *Nat Rev Immunol* **13**, 453-460 (2013).

99. Rossi, S.W. *et al.* RANK signals from CD4(+)3(-) inducer cells regulate development of Aire-expressing epithelial cells in the thymic medulla. *J Exp Med* **204**, 1267-1272 (2007).

100. Bot, A., Bot, S., Antohi, S., Karjalainen, K. & Bona, C. Kinetics of generation and persistence on membrane class II molecules of a viral peptide expressed on foreign and self proteins. *Journal of Immunology* **157**, 3436-3442 (1996).

101. Benson, M.J., Pino-Lagos, K., Rosemblatt, M. & Noelle, R.J. All-trans retinoic acid mediates enhanced T reg cell growth, differentiation, and gut homing in the face of high levels of co-stimulation. *J Exp Med* **204**, 1765-1774 (2007).

102. Joller, N. *et al.* Treg cells expressing the coinhibitory molecule TIGIT selectively inhibit proinflammatory Th1 and Th17 cell responses. *Immunity* **40**, 569-581 (2014).

103. Delgoffe, G.M. *et al.* Stability and function of regulatory T cells is maintained by a neuropilin-1-semaphorin-4a axis. *Nature* **501**, 252-256 (2013).

104. Janssens, K., ten Dijke, P., Janssens, S. & Van Hul, W. Transforming growth factor-beta1 to the bone. *Endocr Rev* **26**, 743-774 (2005).

105. Xiao, S. *et al.* Defect in regulatory B-cell function and development of systemic autoimmunity in T-cell Ig mucin 1 (Tim-1) mucin domain-mutant mice. *Proc Natl Acad Sci U S A* **109**, 12105-12110 (2012).

106. Xiao, S., Brooks, C.R., Sobel, R.A. & Kuchroo, V.K. Tim-1 is essential for induction and maintenance of IL-10 in regulatory B cells and their regulation of tissue inflammation. *J Immunol* **194**, 1602-1608 (2015).

107. Yeung, M.Y. *et al.* TIM-1 signaling is required for maintenance and induction of regulatory B cells. *Am J Transplant* **15**, 942-953 (2015).

108. Kisielow, M., Kisielow, J., Capoferri-Sollami, G. & Karjalainen, K. Expression of lymphocyte activation gene 3 (LAG-3) on B cells is induced by T cells. *Eur J Immunol* **35**, 2081-2088 (2005).

109. Roche, P.A. & Furuta, K. The ins and outs of MHC class II-mediated antigen processing and presentation. *Nat Rev Immunol* **15**, 203-216 (2015).

110. Piskurich, J.F. *et al.* BLIMP-I mediates extinction of major histocompatibility class II transactivator expression in plasma cells. *Nat Immunol* **1**, 526-532 (2000).

111. Pelletier, N. *et al.* Plasma cells negatively regulate the follicular helper T cell program. *Nat Immunol* **11**, 1110-1118 (2010).

112. Vignali, D.A., Collison, L.W. & Workman, C.J. How regulatory T cells work. *Nat Rev Immunol* **8**, 523-532 (2008).

113. Sakaguchi, S., Wing, K., Onishi, Y., Prieto-Martin, P. & Yamaguchi, T. Regulatory T cells: how do they suppress immune responses? *Int Immunol* **21**, 1105-1111 (2009).

114. Johnston, C.J., Smyth, D.J., Dresser, D.W. & Maizels, R.M. TGF-beta in tolerance, development and regulation of immunity. *Cell Immunol* **299**, 14-22 (2016).

115. Li, Y. *et al.* B cells and T cells are critical for the preservation of bone homeostasis and attainment of peak bone mass in vivo. *Blood* **109**, 3839-3848 (2007).

116. Rosser, E.C. & Mauri, C. Regulatory B cells: origin, phenotype, and function. *Immunity* **42**, 607-612 (2015).

117. Shen, P. & Fillatreau, S. Antibody-independent functions of B cells: a focus on cytokines. *Nat Rev Immunol* **15**, 441-451 (2015).

118. Carter, N.A. *et al.* Mice lacking endogenous IL-10-producing regulatory B cells develop exacerbated disease and present with an increased frequency of Th1/Th17 but a decrease in regulatory T cells. *J Immunol* **186**, 5569-5579 (2011).

119. Carter, N.A., Rosser, E.C. & Mauri, C. Interleukin-10 produced by B cells is crucial for the suppression of Th17/Th1 responses, induction of T regulatory type 1 cells and reduction of collagen-induced arthritis. *Arthritis Res Ther* **14**, R32 (2012).

120. Mann, M.K., Maresz, K., Shriver, L.P., Tan, Y. & Dittel, B.N. B cell regulation of CD4+CD25+ T regulatory cells and IL-10 via B7 is essential for recovery from experimental autoimmune encephalomyelitis. *J Immunol* **178**, 3447-3456 (2007).

121. Yoshizaki, A. *et al.* Regulatory B cells control T-cell autoimmunity through IL-21-dependent cognate interactions. *Nature* **491**, 264-268 (2012).

122. Neves, P. *et al.* Signaling via the MyD88 adaptor protein in B cells suppresses protective immunity during Salmonella typhimurium infection. *Immunity* **33**, 777-790 (2010).

123. Matsumoto, M. *et al.* Interleukin-10-producing plasmablasts exert regulatory function in autoimmune inflammation. *Immunity* **41**, 1040-1051 (2014).

124. Mucida, D. *et al.* Oral tolerance in the absence of naturally occurring Tregs. *J Clin Invest* **115**, 1923-1933 (2005).

125. de Lafaille, M.A.C. *et al.* Adaptive Foxp3(+) regulatory T cell-dependent and -independent control of allergic inflammation. *Immunity* **29**, 114-126 (2008).

126. Coombes, J.L. *et al.* A functionally specialized population of mucosal CD103+ DCs induces Foxp3+ regulatory T cells via a TGF-beta and retinoic acid-dependent mechanism. *J Exp Med* **204**, 1757-1764 (2007).

127. Floess, S. *et al.* Epigenetic control of the foxp3 locus in regulatory T cells. *PLoS Biol* **5**, e38 (2007).

128. Polansky, J.K. *et al.* DNA methylation controls Foxp3 gene expression. *Eur J Immunol* **38**, 1654-1663 (2008).

129. Huehn, J., Polansky, J.K. & Hamann, A. Epigenetic control of FOXP3 expression: the key to a stable regulatory T-cell lineage? *Nat Rev Immunol* **9**, 83-89 (2009).

130. Zheng, Y. *et al.* Role of conserved non-coding DNA elements in the Foxp3 gene in regulatory T-cell fate. *Nature* **463**, 808-812 (2010).

131. Morikawa, H. & Sakaguchi, S. Genetic and epigenetic basis of Treg cell development and function: from a FoxP3-centered view to an epigenome-defined view of natural Treg cells. *Immunol Rev* **259**, 192-205 (2014).

132. Josefowicz, S.Z., Lu, L.F. & Rudensky, A.Y. Regulatory T cells: mechanisms of differentiation and function. *Annu Rev Immunol* **30**, 531-564 (2012).

133. Ohkura, N. *et al.* T cell receptor stimulation-induced epigenetic changes and Foxp3 expression are independent and complementary events required for Treg cell development. *Immunity* **37**, 785-799 (2012).

134. Delacher, M. *et al.* Genome-wide DNA-methylation landscape defines specialization of regulatory T cells in tissues. *Nat Immunol* **18**, 1160-1172 (2017).

135. Thornton, A.M. *et al.* Expression of Helios, an Ikaros transcription factor family member, differentiates thymic-derived from peripherally induced Foxp3+ T regulatory cells. *J Immunol* **184**, 3433-3441 (2010).

136. Shevach, E.M. & Thornton, A.M. tTregs, pTregs, and iTregs: similarities and differences. *Immunol Rev* **259**, 88-102 (2014).

137. Sarris, M., Andersen, K.G., Randow, F., Mayr, L. & Betz, A.G. Neuropilin-1 expression on regulatory T cells enhances their interactions with dendritic cells during antigen recognition. *Immunity* **28**, 402-413 (2008).

138. Bilate, A.M. & Lafaille, J.J. Induced CD4+Foxp3+ regulatory T cells in immune tolerance. *Annu Rev Immunol* **30**, 733-758 (2012).

139. Henderson, J.G., Opejin, A., Jones, A., Gross, C. & Hawiger, D. CD5 instructs extrathymic regulatory T cell development in response to self and tolerizing antigens. *Immunity* **42**, 471-483 (2015).

140. Jones, A. *et al.* Peripherally Induced Tolerance Depends on Peripheral Regulatory T Cells That Require Hopx To Inhibit Intrinsic IL-2 Expression. *J Immunol* **195**, 1489-1497 (2015).

141. Jones, A. & Hawiger, D. Peripherally Induced Regulatory T Cells: Recruited Protectors of the Central Nervous System against Autoimmune Neuroinflammation. *Front Immunol* **8**, 532 (2017).

142. Schuster, C., Jonas, F., Zhao, F. & Kissler, S. Peripherally induced regulatory T cells contribute to the control of autoimmune diabetes in the NOD mouse model. *Eur J Immunol* (2018).

143. Jones, A. *et al.* Immunomodulatory Functions of BTLA and HVEM Govern Induction of Extrathymic Regulatory T Cells and Tolerance by Dendritic Cells. *Immunity* **45**, 1066-1077 (2016).

144. Husemann, Y. *et al.* Systemic spread is an early step in breast cancer. *Cancer Cell* **13**, 58-68 (2008).

145. Shiozawa, Y., Eber, M.R., Berry, J.E. & Taichman, R.S. Bone marrow as a metastatic niche for disseminated tumor cells from solid tumors. *Bonekey Rep* **4**, 689 (2015).

146. Hosseini, H. *et al.* Early dissemination seeds metastasis in breast cancer. *Nature* (2016).

147. Koh, B.I. & Kang, Y. The pro-metastatic role of bone marrow-derived cells: a focus on MSCs and regulatory T cells. *EMBO Rep* **13**, 412-422 (2012).

148. Wang, H. *et al.* The osteogenic niche promotes early-stage bone colonization of disseminated breast cancer cells. *Cancer Cell* **27**, 193-210 (2015).

149. Khan, I.S. *et al.* Enhancement of an anti-tumor immune response by transient blockade of central T cell tolerance. *J Exp Med* **211**, 761-768 (2014).

# 7. Abbreviations

| | |
|---|---|
| 7-AAD | 7-Amino-actinomycin D |
| ACK | ammonium-chloride-potassium |
| Adig | Aire-driven IGRP-GFP |
| Aire | autoimmune regulator |
| Aldh2 | aldehyde dehydrogenase 2 family (mitochondrial) |
| APC | allophycocyanin |
| APC | antigen presenting cell |
| BC | B cell |
| BM | bone marrow |
| BMAC | bone marrow Aire-expressing cell |
| CD | cluster of differentiation |
| cDNA | complementary DNA |
| CFSE | carboxyfluorescein diacetate succinimidyl ester |
| CpG ODN | CpG oligodeoxynucleotide |
| Crp | C-reactive protein |
| Csna | casein alpha |
| Csnb | casein beta |
| Csng | casein gamma |
| cTEC | cortical thymic epithelial cell |
| CTLA-4 | cytotoxic T-lymphocyte associated protein 4 |
| Cy | cyanin |

| | |
|---|---|
| DC | dendritic cell |
| ddH2O | double-distilled water |
| DMEM | Dulbecco's Modified Eagle Media |
| DNA | deoxyribonucleic acid |
| DNase | deoxyribonuclease |
| dNTP | deoxynucleotide triphosphate |
| Ebi3 | Epstein-Barr virus induced 3 |
| EDTA | ethylenediaminetetraacetic acid |
| EpCAM | epithelial cell adhesion molecule |
| eTAC | extra-thymic Aire-expressing cell |
| Expi | extracellular proteinase inhibitor |
| FACS | fluorescence-activated cell sorting |
| FBS | fetal bovine serum |
| FC | fold change |
| Foxp3 | forkhead box P3 |
| g | gram(s) |
| *g* | standard gravity |
| Gad67 | glutamate decarboxylase 67 |
| GFP | green fluorescence protein |
| h | hour(s) |
| HA | hemagglutinin |

| | |
|---|---|
| HEPES | 4-(2-hydroxyethyl)-1-piperazineethanesulfonic acid |
| Ig | immunoglobulin |
| IGRP | islet-specific glucose-6-phosphatase–related protein |
| IL | interleukin |
| Ins2 | insulin II |
| KO | knock out |
| l | liter |
| LAG-3 | lymphocyte-activation gene 3 |
| LAP | latency associated peptide |
| LPS | lipopolysaccharide |
| M | molar |
| MACS | magnetic-activated cell sorting |
| MFI | mean fluorescence intensity |
| MHC | major histocompatibility complex |
| min | minute(s) |
| MNC | mononuclear cell |
| mRNA | messenger RNA |
| mTEC | medullary thymic epithelial cells |
| NF-κB | nuclear factor kappa-light-chain-enhancer of activated B cells |
| OVA | ovalbumin |
| PBMC | peripheral blood mononuclear cell |
| PBS | phosphate-buffered saline |
| PCR | polymerase chain reaction |
| PD-L1 | programmed death ligand 1 |
| PD-L2 | programmed death ligand 2 |
| PE | phycoerythrin |
| PerCP | peridinin-Chlorophyll-protein |
| pGE | promiscuous gene expression |
| pH | potentia hydrogenii |
| polyI:C | polyinosinic-polycytidylic acid |
| RAG2 | recombination activating gene 2 |
| RANK | receptor activator of NF-κB |
| Rbp7 | retinol binding protein 7 |
| RNA | ribonucleic acid |
| rpm | revolutions per minute |
| RPMI | Roswell Park Memorial Institute medium |
| SD | standard deviation |
| SEM | standard error of the mean |
| TAA | tumor-associated antigen |
| TC | T cell |
| TCR | T cell receptor |
| TGFβ1 | transforming growth factor beta 1 |
| Tim-1 | T-cell immunoglobulin mucin receptor 1 |
| Tlbp | testis lipid-binding protein |
| TRA | tissue-restricted antigen |
| Treg cells | regulatory T cells |
| tRNA | transfer RNA |
| WT | wild type |

# 8. Acknowledgments

There were ups and downs along the road in this unforgettable PhD life. Sometimes it can be so frustrating, but the darkest hour comes before the dawn. If we don't give up, we will get there eventually. However, I know for a fact that if it weren't for the support from so many people around me, I wouldn't have made it through. At the end of this long journey (although time passes by so fast and it doesn't feel like 5 years at all), I'd like to thank everyone who has helped me in all aspects on this spectacular part of my life.

First of all, I'd like to express my gratitude to my supervisor Prof. Philipp Beckhove. He gave me not only freedom to explore, but also valuable suggestions and guidance when I felt lost. He also provided me the opportunities to apply for a research grant and to attend conferences where I could present my project in front of hundreds. All these experiences I gained over these years from his training inspired my independent and critical thinking. I am very lucky to have joined his lab, which has become my second family in Germany.

I want to give my deepest thanks to everyone in this big family of Beckhove Lab: Slava literally took care of every single thing, from lab organization to insightful scientific suggestions. This lab wouldn't be the same without her. Maria has always brought me passion and motivation on our work. She has come up with many good ideas and discussing with her was very inspiring. Till has always been of great help when I was in trouble, not just in the lab but also in my daily life. Antonio has brought great fun and joy to the lab, and he is also a good listener whom I can share my thought with. Vale and Ayse are my great partners in the PhD office and always bring laughter in the room. Heiko has helped me a lot when I was struggling with all the German language problems. Anchana and Kathi have given me many great advises. Birgitta, Jasmin M., Karin, Eva and Janine are the best technicians and have always got my back when there were too many experiments to do. Sabine T. and Sabine R. are the greatest administration team. With

their support we can fully focus on our work. I'd like to give my special thanks to Franzi, Felix N. and Michelle for their contribution on this project and technical set-up. Many thanks to my former colleagues in Heidelberg, Hans-Henning, Noemi, Jasmin Q, Nisit, Yinze, Mudita, Lit, Lora, Ludmila, Simone and Mariana. My special appreciation goes to Felix K. who established animal models and paved the way for this project.

I'd like to give my gratitude to all my collaborators. They gave me priceless comments and I've always learned a lot after talking to them. Sheena and Tomo helped me a lot on performing experiments, as well as critical suggestions on the direction of the project. Siao-Han spent so much time analyzing the transcriptome data, and she is my best teacher on bioinformatics. Thanks to Mio for processing all the single cells, Prof. Christoph Klein, Prof. Ludger Klein and Prof. Benedikt Brors for their input on the manuscript of the project, and Prof. Karsten Mahnke for suggestion in my TAC meetings. I want to give my deepest gratitude to Prof. Bruno Keywski. This project was co-supervised by him and Philipp. It has developed successfully due to his contribution. I wish he could have seen how this project has grown today.

I want to thank my friends outside the lab, Calvin, Siao-Han, Ya-Yun, Ling-Shih, Li-Ling, Roxy, Kun-Hui, Lance, Ming-Han, Xingchen, Yih-Shiuan, Victor, Chia-Lin and Kuan-Ming. They have made my life in both Heidelberg and Regensburg full of joy and laughter. With them I never felt homesick.

Nevertheless, nothing is more precious from the love of my family. Thank you, mom and dad. Thank you, my brother. No matter what I do, you'd always give me your support and freedom to keep moving forward. Even though you are almost 10,000 kilometers away, it feels like you are standing right by my side. Thank you for your unconditional love.

Lastly, I want to give my exclusive gratitude to Hung-En. You are always there for me. When I needed to work on the weekends, you've travelled so far without a second thought to keep me

company and take care of everything for me. Every time when nothing seems to work, it is your hug that gives me strength to carry on. Laughter or tears, I appreciate every moment with you. Thank you for being part of my life. It is magnificent, because of you.